

**DESIGN OF A STATIC FREQUENCY CONVERTER  
SUITABLE FOR AIRCRAFT POWER SYSTEMS**

**AUTHOR: AHMAD RAHAL**

**SUBMITTED FOR THE AWARD OF  
MASTER OF ENGINEERING**

**SUPERVISOR: Aengus Murray Ph.D**

**School of Electronic Engineering  
Dublin City University**

**DECEMBER 1991**

**The contents of this thesis are based on my own research**

## DECLARATION

I hereby declare that this dissertation is entirely of my own work and has not been submitted as an exercise to any other university.

A handwritten signature in cursive script, appearing to read 'Ahmad', is written over a solid horizontal line.

Ahmad Rahal

## Table of contents

<b>Acknowledgments</b> .....	<b>i</b>
<b>Abstract</b> .....	<b>ii</b>
<b>List of figures</b> .....	<b>iii</b>
<b>List of tables</b> .....	<b>vi</b>
<b>List of plates</b> .....	<b>vii</b>
<b>Chapter 1 Introduction</b> .....	<b>1</b>
<b>Chapter 2 Aircraft generating systems</b> .....	<b>5</b>
2-1 Introduction .....	5
2-2 Types of power .....	6
2-2 Aircraft generators .....	6
2-3-1 AC Aircraft generators .....	8
2-3-2 High-output aircraft generators .....	9
2-4 Cooling of aircraft generators .....	9
2-5 Batteries .....	11
2-6 Aircraft bus arrangements .....	12
2-7 Power system requirements .....	14
2-8 Constant frequency systems .....	15
<b>Chapter 3 VSCF Aircraft generating systems</b> .....	<b>17</b>
3-1 Introduction .....	17

3-2 Constant-speed conventional system .....	18
3-2-1 Introduction .....	18
3-2-2 Constant-speed drive (CSD) .....	20
3-3 cycloconverters .....	23
3-4 DC-Link VSCF scheme .....	25
3-5 DC-Link versus cycloconverter .....	27
<b>Chapter 4 Static frequency converter .....</b>	<b>29</b>
4-1 Introduction .....	29
4-2 Switch-mode DC-TO-AC inverter .....	30
4-3 Three-phase PWM inverter .....	32
4-4 PWM in three-phase voltage-source inverters .....	34
4-5 Selection of the amplitude modulation ratio $m_a$ .....	37
4-5-1 For $m_a \leq 1.0$ .....	37
4-5-2 For $m_a \geq 1.0$ .....	39
4-6 Selection of the switching frequency and the frequency modulation ratio $m_f$ .....	39
4-6-1 Small frequency modulation ratio .....	39
4-6-2 Large frequency modulation ratio .....	40
4-7 Pulse width modulation (PWM) techniques .....	40
4-7-1 Natural sampled PWM .....	41
4-7-2 Regular sampled PWM .....	44
4-7-3 Optimised PWM .....	46

<b>Chapter 5 Three-phase PWM inverter design .....</b>	<b>48</b>
5-1 Power circuit design .....	50
5-1-1 Choice of switching devices .....	50
5-1-2 Heat-sink design .....	57
5-1-3 Snubber circuit design .....	59
5-1-3-1 Choice of snubber resistor .....	60
5-1-3-2 Choice of snubber capacitor .....	62
5-1-4 Gate drive circuit design .....	63
5-1-5 Isolation circuit design .....	68
5-1-5-1 Transformer isolation .....	68
5-1-5-2 Opto-coupler isolation .....	70
5-1-6 Isolated power supply design .....	72
5-1-7 Blanking time circuit design .....	72
5-1-8 Breadboard construction .....	78
5-2 PWM control circuit design .....	80
5-2-1 Sine and square wave generation circuit .....	82
5-2-2 Filter circuit .....	83
5-2-3 Three-phase sinusoidal wave generation circuit .....	85
5-2-4 Triangular waveform generation circuit .....	91
5-2-5 Comparator circuit .....	95
<b>Chapter 6 power harmonic filter .....</b>	<b>99</b>
6-1 Introduction .....	99

6-2 Analysis of the inverter output voltage (filter input) .....	100
6-3 Analysis of the filter output voltage .....	105
6-4 Filter design .....	109
6-4-1 Filter capacitors .....	110
6-4-2 Power inductor design .....	111
6-4-2-1 Select the core material .....	111
6-4-2-2 Select the minimum-sized magnet wire .....	112
6-4-2-3 Select the minimum-sized core .....	114
6-4-2-4 Determine the number of turns .....	115
6-4-2-5 Design calculations .....	115
6-4-2-5-1 The minimum-sized magnet wire calculation .....	116
6-4-2-5-2 The $W_a$ product calculation .....	116
6-4-2-5-2-1 Calculation of core height .....	117
6-4-2-5-2-2 Calculation the inside diameter of the core .....	118
6-4-2-5-2-3 Calculation of the outside diameter $O_D$ of the core .....	118
6-4-2-5-2-4 Calculation of the magnetic path length .....	119
6-4-2-5-3 Calculation of the number of turns .....	120
<b>Chapter 7 Experimental results and conclusion .....</b>	<b>122</b>
7-1 Low voltage test .....	122
7-1-1 Inverter output .....	123
7-1-2 Filter output voltage .....	124
7-2 High voltage test .....	127

7-3 Conclusion .....	129
7-4 Recommendation .....	130
<b>References .....</b>	<b>132</b>
<b>Appendix A</b>	
<b>Appendix B</b>	
<b>Appendix C</b>	
<b>Appendix D</b>	
<b>Appendix E</b>	

## ACKNOWLEDGEMENTS

*I would like to express my deepest gratitude to my supervisor **Dr. Aengus Murray** for his guidance throughout the period of research and for his help in many other aspects.*

*My thanks goes to all the staff and my fellow research students in the school of electronic engineering for making it a very pleasant place to work in.*

*I am indebted to the **Scientific Studies and Research Center (SSRC)** in **Syrian Arab Republic** for its sponsorship and guidance.*

*I wish to thank my supervisors at home **Dr. A. Qusai Kayali** and **Dr. Mohammed Abou Samra** for their guidance and advice.*

*A special thank-you to be extended to my brother **Dr. Salah Rahal** and his wife **Dr. Feryal Haj Hassan** for their advice, stimulating and valuable discussions we had through the letters.*

*I am deeply indebted to **my wife and children** for their patience and appreciation during my research career. I am also indebted to **my parents and to my brothers and sisters** for their support and encouragement.*



## ABSTRACT

Aircraft electrical systems use a three-phase, 400 HZ, AC Bus supplied by engine driven generators.

In an effort to simplify and improve the production of AC power for aircraft and to eliminate the need for hydromechanical constant-speed drive (CSD), a number of systems have been devised for producing 400 HZ three-phase electric power using electronic circuitry. This has been made possible by some of the major advances in solid-state technology developed in recent years.

One of these systems is a DC-Link converter, which has a variable input frequency but a constant output frequency. This offer a viable alternative to the CSD as means of providing a constant frequency power supply from an aircraft generator. The ease of replacement and repair, the reduction in servicing needs, and the ability to locate the components of the electrical systems through the aircraft all combine to bring about a considerable reduction in the maintenance time required.

This thesis discusses aircraft generating systems, variable speed constant frequency systems (VSCF) and the principle of the static frequency converter. The operation and design of a 1 KVA three-phase PWM inverter and its associated control circuitry to produce 400 HZ AC is described in detail. Finally a design of a power harmonic filter is given.

## LIST OF FIGURES

<u>FIGURE</u>		<u>PAGE</u>
2.1	Typical modern technology aircraft two-channel bus configuration .....	12
2.2	Loop distribution .....	13
2.3	Network distribution .....	14
3.1	Constant drive system .....	19
3.2	An integrated-drive generator .....	20
3.3	Principle of constant speed drive unit .....	22
3.4	Cycloconverter VSCF system .....	23
3.5	Three-phase cycloconverter .....	24
3.6	Cycloconverter input/output waveform .....	24
3.7	DC-Link VSCF system .....	26
4.1	Static frequency converter .....	30
4.2	Three-phase inverter .....	33
4.3	Three-phase PWM waveforms .....	35
4.4	Block diagram of analogue method of generating natural sampled PWM .....	43
4.5	Natural sampled PWM .....	43

4.6	Symmetric and asymmetric regular sampled PWM .....	45
5.1	Block diagram of the three-phase PWM inverter .....	51
5.2	One-phase of three-phase PWM inverter with tapped inductors to prevent shorting Q1 and Q2 .....	54
5.3	One-phase of three-phase PWM inverter with schottky and freewheeling diodes to prevent shorting Q1 and Q2 .	56
5.4	One-phase of three-phase PWM inverter with snubber circuits .....	61
5.5	MOSFET equivalent circuit .....	64
5.6	Gate drive circuit for one-phase of the PWM inverter ....	66
5.7	Transformer-isolated gate drive .....	69
5.8	Isolation circuit for one-phase of the PWM inverter .....	71
5.9	Four isolated power supplies .....	73
5.10	Blanking time circuit for phase-A of three-phase PWM inverter .....	76
5.11	Control signals for upper/lower inverter switches with blanking and dead times .....	77
5.12	Block circuit diagram of three-phase PWM control circuit .....	81
5.13	Sine and square waveform generating circuit .....	84
5.14	Filter circuit .....	86

5.15	Three-phase sine wave generating circuit .....	88
5.16	Vector diagram of the thee-phase waveform .....	87
5.17	Triangular waveform generating circuit .....	93
5.18	Comparator circuit .....	96
6.1	Harmonic voltages as function of frequencies .....	104
6.2	Frequency response of single low-pass LC filter .....	106
6.3	Frequency response of two-pole low-pass LC filter .....	107
6.4	Frequency response of three-pole low-pass LC filter .....	108
6.5	Three-pole low-pass LC filter circuit .....	109
6.6	Cross-sectional of the core .....	121
7.1	Inverter output voltage of a single phase .....	125
7.2	Harmonic spectrum of the inverter output voltage at 2 dB/DIV .....	125
7.3	Filter output voltage waveform of a single phase .....	126
7.4	Harmonic spectrum of the filter output voltage at 2 dB/DIV .....	126
7.5	Inverter output voltage of a single phase at 100 V .....	128

## LIST OF TABLES

<u>TABLE</u>		<u>PAGE</u>
1.1	Aircraft generating system comparisons.....	3
6.1	Generalized harmonics of $V_o$ for a large $m_f$ $(V_o)_n/(V_d/2)$ is tabulated as a function of $m_a$ .....	102
6.2	Summary of the designed core of the inductor.....	121

## LIST OF PLATES

<u>PLATE</u>		<u>PAGE</u>
5.1	Photograph of the power supply (from inside) .....	74
5.2	Photograph of one-phase power circuit of the PWM inverter .....	79
5.3	Photograph of the actual PC board of the sine/square, filter and three-phase sinusoidal wave generation circuits .....	90
5.4	Photograph of the actual PC board of the triangular waveform generation circuit .....	94
5.5	Photograph of the actual PC board of the comparator circuit and blanking circuit .....	97
5.6	Photograph of the three-phase PWM inverter (power and control circuits together in one box) .....	98

# CHAPTER 1

## INTRODUCTION

Aircraft electrical systems use a three-phase, 400 HZ, AC bus supplied by engine driven generators. Constant frequency power generation is required even though the aircraft engine speed can vary over a wide range. This results in voltage magnitude and frequency changes of the generator output. In order to provide constant speed generator operation it is common practice to use a hydromechanical constant speed drive (CSD) to couple the output of the engine to the input of the generator. This system is very expensive, complex and must be located close to the engine.

However, recently, developments in both power electronics and microprocessor technology have led to the electrical variable speed constant frequency (VSCF) systems becoming a viable alternative to the CSD.

The VSCF electrical systems are proving to be far more flexible in contrast to CSD mechanical system, which must be located close to the engine. As essential components, these former systems can be distributed throughout the aircraft. In addition, maintenance and replacement of these VSCF systems are far easier compared with the CSD system.

The VSCF electrical systems can be classified as follows:

1. A cycloconverter VSCF systems. These were the first type of VSCF electrical systems developed and successfully applied due to the availability of the basic power switching device (SCR). These systems electronically directly converts the variable input frequency power to a fixed frequency output power.
2. A DC-Link VSCF electrical systems. These systems have become practical in recent years for aircraft with the availability of high voltage, high-power transistors. In these systems the variable frequency generator output is rectified to provide an intermediate DC power link. This power is then inverted to a fixed AC output by means of a three-phase PWM inverter, the three-phase PWM inverter is the most critical item in the DC-Link VSCF electrical system.

Both the cycloconverter and the DC-Link VSCF electrical system have specific advantages over the constant speed drive (CSD). By replacing the mechanical/hydraulic CSD with a solid state power converter, the reliability of the generating system is improved. Also, since the DC-Link VSCF system output frequency is crystal controlled, the output frequency variations inherent with CSD drives are eliminated. Table 1.1 compares the different types of VSCF electrical systems with respect to weight, efficiency, and operating temperatures.



**Table 1.1 Aircraft Generating System Comparisons**

	<u>IDG/CSD</u>	<u>CYCLOCONVERTER</u>	<u>DC-LINK</u>
Input Oil Temperature	150°C	80°C	120°C
Limitation			
Efficiency (30/40 KVA)	66.4%	71.4%	76.3%
Weight (30/40 KVA)	79 lbs	77 lbs	82 lbs

This thesis discusses aircraft power generators and describes in detail of the design of a DC-Link converter. The principal aim of this study is to design a three-phase PWM inverter and its associated control circuitry to produce 400 HZ, 1 KVA AC power suitable for use in aircraft electrical systems.

**In chapter two**, two types of aircraft electric power are outlined and brief discussion of the aircraft generators are presented. In addition, three methods of cooling of these generators are given.

**In chapter three**, brief descriptions of three types of VSCF aircraft generating systems are described. Some of the attributes and trade-offs for each system are listed. Several critical design parameters having a direct bearing on the selection of the best system for a given application are mentioned. Also a comparison

between the DC-Link and cycloconverter VSCF systems is given.

**In chapter four**, the basic concept and analysis of the switch-mode DC to AC inverter are presented. The selection of the amplitude modulation ratio and the switching frequency ratio were presented. Also the various switching techniques associated with pulse width modulation are reviewed.

**In chapter five**, the procedure for design the power and control circuits of the three-phase PWM inverter is described in details. This inverter able to generate 1 KVA, 115 V ac, 400 HZ. The choice of the power components, gate drive circuit, isolation circuit and snubber circuit for the power circuit are discussed in details. The design of the PWM control circuit to generate the control signals is described.

**In chapter six**, the design procedure for the power harmonic filter is outlined. The purpose of the filter is to eliminate the harmonic components from the inverter output.

**In chapter seven**, an experimental results for the inverter output voltage waveforms are illustrated, followed by conclusions.

# CHAPTER 2

## AIRCRAFT GENERATING SYSTEMS

### 2-1 INTRODUCTION

All modern aircraft and spacecraft are very largely dependent upon electrical power for communications, navigation and control. Typical electrical loads in aircraft include identification lights, landing lights, instrument lights, heaters, retractable landing gear, wing flaps, engine cowl flaps, radio, navigation equipment and so on. The main electrical supply for the aircraft is provided by generators coupled to the engine, and power is also supplied by batteries which act as a back-up system.

Aircraft electric power requirements have expanded with the advancement in technology of modern aircraft systems. Flight control and other computers demand the delivery of reliable, uninterruptible power. The introduction of low-bleed engines to increase reliability, maintainability, and damage tolerance capabilities has resulted in reduced pneumatic power availability. This, along with the replacement of hydraulic systems and accessories with electric equipment, has led to the requirement for larger electric generating systems.

## **2-2 TYPES OF POWER**

Since the late 1940s, the dominant method of generating and distributing electric power on aircraft has been, and is in the process of being, 400 HZ three-phase 115 V ac. This type of power is suitable for transmission throughout the aircraft without excessive penalties for feeder weight.

It is suitable for motor loads and transformation and rectification to other voltage levels for avionics loads. Its nature and quality are specified by Mil-std-704 as well as generating system specifications such as Mil-G-21480.

On most aircraft, electric power is also available as 28 Vdc. This type of power is compatible with batteries and can be easily paralleled. It is therefore used for critical loads. It is generally produced by transformer rectifier units from 400 HZ power. It is specified by Mil-std-704, but higher quality levels may be desired for specific applications.

## **2-3 AIRCRAFT GENERATORS**

Electric generators have been used for many years to produce electric power for a multitude of purposes.

The generator has been developed to a very high level of dependability and efficiency, especially for aircraft use. Ever since the first aircraft to use any kind of electric equipment was launched, the electrical loads on aircraft and other flying devices have increased. Today modern jet airliners are equipped with many different electric systems, each requiring a substantial amount of electric energy.

To supply the power for their electric systems, these aircraft are equipped with generating equipment, such as, dc generators in old aircraft and ac generator in recent aircraft.

Aircraft generators differ considerably from generators for other purpose, such as those built for automobiles or for stationary power plants [1]. The main difference is that aircraft generators have a much higher power-weight ratio than the other types.

Several factors contribute to the efficiency and light weight of the aircraft generator; the enamels, varnishes, and insulating materials being highly heat-resistant.

Hence, the aircraft generator can operate at a high temperature and carry a maximum load.

Generators are classified according to the type of current they supply, their capacity, or power output, type of windings, number of phases, internal connections and frequency. Large aircraft like jet airliners employ three-phase ac power systems rated at 117/208 V, with a frequency of 400 HZ. Compared with a 28 V dc system, an ac system can develop several times as much power for the same weight, hence it is a great advantage in large aircraft to use the ac systems. So now most recent aircraft use ac generators.

### 2-3-1 AC Aircraft generators

AC generators, often called alternators, were not used extensively in aircraft until the late 1950s. Since that time, the ac generator has become the principle source of electric power in almost all types of aircraft. On jet airliners and military aircraft, the ac system supplies almost all the electric power required for the aircraft. Where dc is needed rectifiers are used. AC power systems provide a maximum amount of power for the weight of electric equipment.

For light aircraft, ac generators are used, and rectifiers are used to provide dc for the operating systems.

There are three principle advantages in the use of alternating current for electric-power systems [2] :

1. The voltage of ac power may be changed at will by means of transformers. This makes it possible to transmit power at a high voltage with low current, thus reducing the size and weight of wire required.
2. Alternating current can be produced in a three-phase system, thus making it possible to use motors of less weight for the same amount of power developed.
3. AC machinery, such as alternators, do not require the use of commutators; hence, service and upkeep are greatly reduced.

AC generators or alternators are manufactured in many sizes to meet the requirements of electric systems for different types of aircraft. These generators

are three-phase, 115 V ac, 400 HZ and with different output power depending on the size of aircraft.

### **2-3-2 High-Output Aircraft Generators**

High-output brushless generators were developed for the purpose of eliminating some of the problems of ac generators which employ slip rings and brushes to carry exciter current to the rotating field. This was made possible by the development of the silicon rectifier.

Among the advantages of a brushless generator are the following [2]:

1. Lower maintenance cost, since there is no brush or slip-ring wear.
2. High stability and consistency of output, because variations of resistance and conductivity at the brushes and slip rings are eliminated.
3. Better performance at high altitude, because arcing at the brushes is eliminated.

## **2-4 COOLING OF AIRCRAFT GENERATORS**

Air cooling, the first method used for aircraft generators, brings the coolant into intimate contact with the heat sources, but it has severe limitations [3]: Air has low specific heat, and it also has low density and therefore a low heat-transfer coefficient; both factors result in a high temperature differential between coolant and heat sources. Moreover, in supersonic aircraft the ram effect (compression of air in the cooling-air intake) produces such high inlet air temperatures that air

cooling is impractical.

Oil cooling, the second method used for aircraft generators. The generators were cooled by circulating oil through passages to carry their heat to heat exchangers, where it was transferred to the fuel (or to the air at low aircraft speeds). Oil was selected for the coolant because it was readily available from the constant-speed drive (a mechanical drive commonly used to provide constant generator speed, and thus constant ac frequency, from the varying aircraft engine speed).

The first practical oil-cooled aircraft generator systems are still in service on B-58 aircraft.

Spray oil cooling, the third method used for aircraft generators. It is the best method of cooling, which combines the best cooling features of the two previous methods. Coolant oil is sprayed on windings and other parts of generator to bring the coolant into direct contact with the sources of heat (as in air cooling), and the oil's good heat capacity and heat transfer capability result in low temperature rise between coolant and heat source. Thus, the concept is valuable for all applications where constant-speed drives are required not just for supersonic aircraft. This method is still using with the new IDG generators. Besides great weight reduction, spray oil cooling in new integrated drive generator system will enhance reliability and lengthen overhaul intervals.



## **2-5 BATTERIES**

A battery is device which converts chemical energy into electrical energy and is made up of a number of cells.

In almost all aircraft electric systems a battery has the following principle functions:

1. To help maintain the dc system under transient conditions. The starting of large dc motor-driven accessories, such as inverters and pumps, requires high input current which would lower the busbar voltage momentarily unless the battery was available to assume a share of the load.
2. To supply power for short term heavy loads when generator or ground power is not available, eg. internal starting of an engine.
3. Under emergency conditions, a battery is intended to supply limited amounts of power. Under these conditions the battery could be the sole remaining source of power to operate essential flight instruments, radio communication equipment, etc., for as long as the capacity of the battery allows.

The batteries selected for use in aircraft employ secondary cells, where the secondary cell can have a life of numerous discharge actions, followed by the action of re-conversions more commonly known as charging. These batteries are normally either of the lead-acid or nickel-cadmium type.

Depending on the size of aircraft and on the power requirements for the operation of essential services under emergency conditions, a single battery or several batteries may be provided. When several batteries are employed they are,

most often, connected in parallel although in some types of aircraft a series connection is used.

## 2-6 AIRCRAFT BUS ARRANGEMENTS

A typical state-of-the-art electric power generating system bus architecture is shown in figure 2.1. In the past, multiple electric power generating system channels were paralleled to reduce the impact of high magnitude load switching and provide greater fault clearing capability [4]. In modern transport aircraft with larger single rating generators, the trend has been to use a split bus or split-parallel bus.

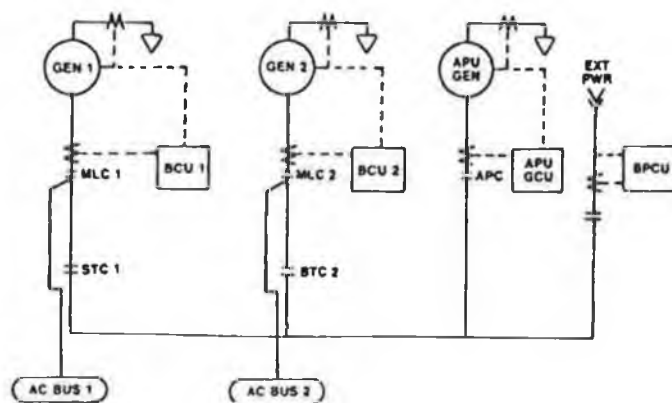


Figure 2.1 Typical modern technology aircraft  
two-channel bus configuration

The diagram shown in figure 2.1 describes the primary distribution system for an aircraft. The AC busses shown would actually be substations or load centres for secondary distribution networks which carry the electric power to the user loads.

Present aircraft systems also use radial networks. The next generation aircraft have greater requirements for fault tolerance and mission reliability will require more complex architectures. This includes various types of parallel or loop circuits or even more complicated network or grid forms [5,6]. Examples of these are shown in figures 2.2 and 2.3.

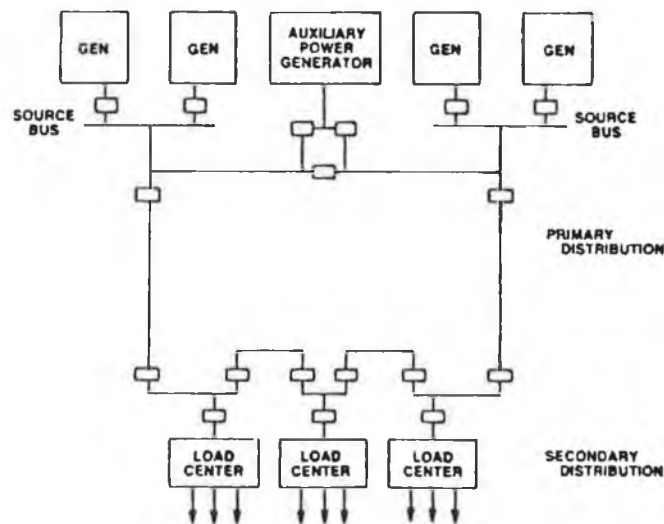


Figure 2.2 Loop distribution

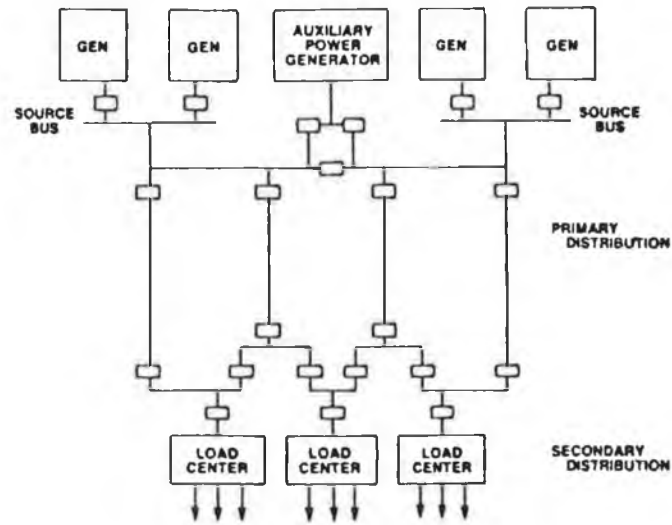


Figure 2.3 Network distribution

## 2-7 POWER SYSTEM REQUIREMENTS

Aircraft electric power systems, channel rating requirements are rising from the 40 to 100 KVA range to the several-hundred KVA range. This places increased demands on system efficiency, thermal management, and distribution components to reduce adverse affects on aircraft performance.

As the system rating rise, the nature of the loads is also changing. Direct-driven motors are becoming a smaller portion of the total load, and dc loads becoming dominant. These new loads include digital electronics, special military equipment, and inverter-driven speed-controlled motors for environmental control

systems, actuators, and fuel pumps. These loads require conversion from the distribution power-type to the usage power-type. Additional aircraft electric power requirements include increasingly redundant sources to supply flight-critical loads. Uninterruptible power is a related requirement that can be addressed with techniques such as no break power transfer [5].

## **2-8 CONSTANT FREQUENCY SYSTEMS**

One of the problems which had been a major stumbling block to the most effective use of ac generators was the problem of controlling frequency to permit several generators to operate in parallel. Parallel operation is, of course, of the highest importance in system reliability, and the frequency must be constant within fairly narrow limits. The frequency of an ac generator depends on the speed of the generator, so in an ac power system it is usually necessary to maintain a fairly constant speed in the ac generator. In order to provide constant-speed generator operation in ac electric systems, it was common practice to use a constant-speed generator drive.

In an effort to simplify and improve the production of ac power for aircraft and to get away from the need for a hydromechanical constant-speed drive. A number of systems have been devised for producing 400 HZ three-phase electric power through electronic circuitry. This has been achieved by the great advances

in solid-state technology developed in recent years. The principles by which this has been accomplished will be explained in the next chapter.

# CHAPTER 3

## VSCF AIRCRAFT GENERATING SYSTEMS

### 3-1 INTRODUCTION

Constant frequency power generation is required against the prime mover speed fluctuations. The speed variation of an aircraft engine is considerably large depending on the aircraft states (take-off, steady-state, landing). The speed variation results in voltage magnitude and frequency changes of the generator [7]. These are countered by a constant-speed drive (CSD) generating system.

The CSD generating system found onboard many aircraft comprises a 3-stage regulated synchronous generator, the output frequency of which is maintained constant by means of a hydromechanical CSD connecting it to the engine via a gearbox.

In the most recent version [8], a reduction in the weight of the system is brought about by a combination of the drive and the generator into a single unit, thereby providing the integrated drive generator (IDG). However, continuing developments in both power electronics and microprocessor technology have led to the variable-speed constant-frequency (VSCF) electrical systems [9,10] becoming a viable alternative to the CSD.

Recent advances in generator design, in particular the use of spray oil cooling [5], have increased considerably the power/weight ratio of both CSD/IDG

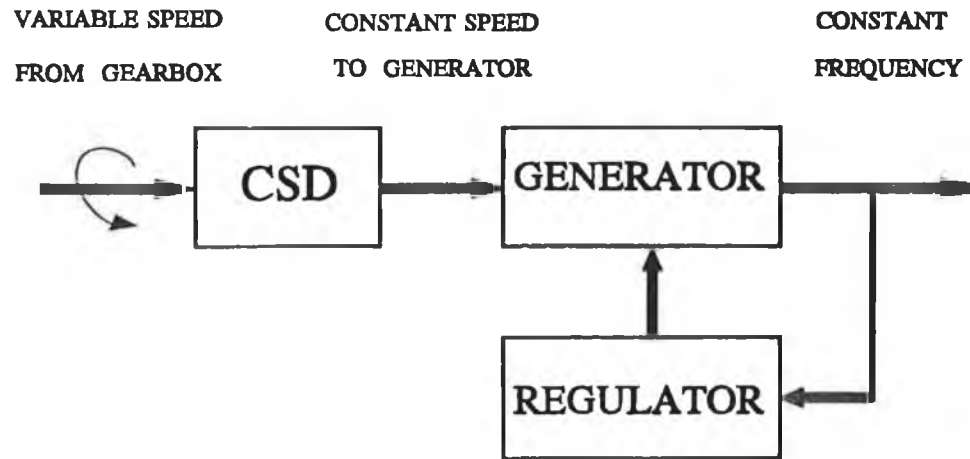


Figure 3.1 Constant drive system

The engine output is coupled through a gearbox to a mechanical/hydraulic constant speed drive (CSD). Variations in engine speed (typically 2:1 range ) are reduced at the constant speed drive output, thus the generator input speed is maintained at a constant value. A synchronous generator is used to maintain constant frequency output. Generator output voltage amplitude is controlled by a generator control unit (GCU).

More advanced CSD design incorporate the generator and constant speed drive into one package as shown in figure 3.2.



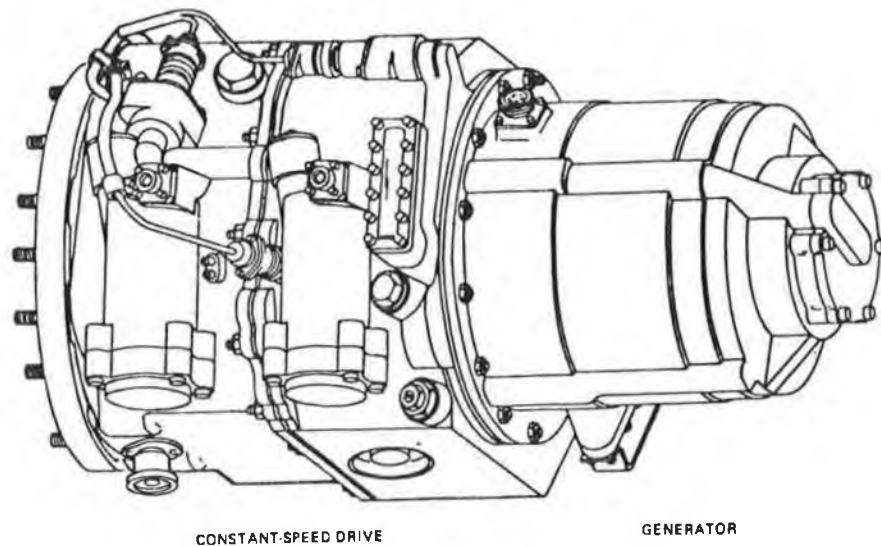


Figure 3.2 An integrated-drive generator

The complete unit is called an integrated-drive generator (IDG). The principle of operation for all CSDs is essentially the same, but these integrated drive generator (IDGs) systems have the advantage of a lower weight as compared to discrete CSD systems.

### 3-2-2 Constant-speed drive (CSD):

Constant-speed drive (CSD) is employed with each generator on each engine. The CSD has the ability to convert a variable engine speed to a constant rpm.

The complete CSD system consists of an axial-gear differential (AGD) whose output speed relative to input speed is controlled by a flyweight-type governor that controls a variable-delivery hydraulic pump. The pump supplies hydraulic pressure to a hydraulic motor which varies the ratio of input rpm to output rpm for the AGD in order to maintain an ac frequency of 400 HZ. The operation of the CSD may be understood by tracing the mechanical actions. Figure 3.2 shows a constant speed unit coupled to a generator, based on the Sundstrand design which is in use in several current types of turbojet-powered aircraft.

CSD employs a hydromechanical variable-ratio drive which in its basic form, consists of a variable- displacement swash plate type of hydraulic pump and constant displacement swash plate type of motor. The oil for system operation is supplied by charge pumps and governor systems fed from a reservoir which is pressurized by air tapped from the low-pressure compressor of the engine. Power from the engine is transmitted through an input shaft and gears, to a hydraulic cylinder block common to both pump and motor, and by the action of the internal hydraulic system, is finally transmitted to the motor and output gears and shaft coupled to the generator. The principle is illustrated very simply in figure 3.3.

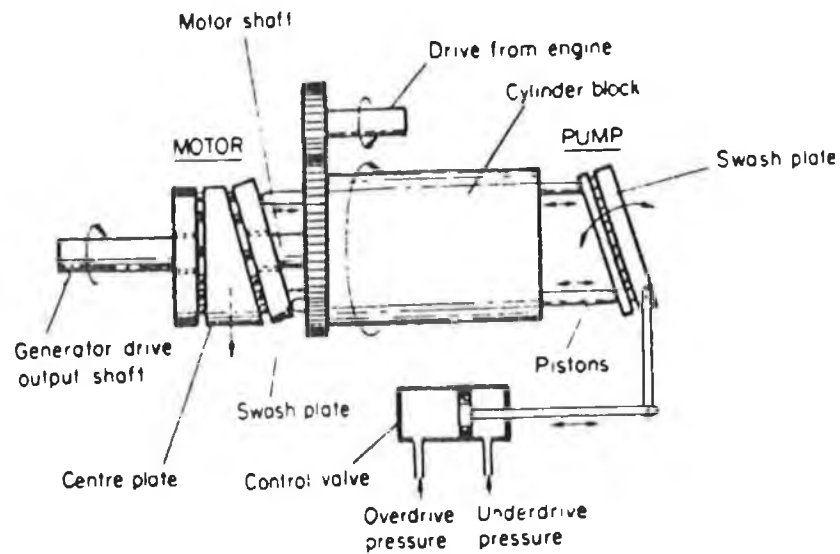


Figure 3.3 Principle of constant speed drive unit

When the engine output is exactly equal to the required generator speed, the oil pressure and flow within the hydraulic system are such that the motor is hydraulically locked to the cylinder block and they rotate together; thus, the whole transmission system acts as a fixed coupling. If however, there is a change in engine and input shaft speed, the governor system senses this and applies a greater or smaller pressure to the pump to vary the angle of its swash-plate. For example, if engine output is slower than the required generator speed, called an 'overdrive' condition, the pressure increases; conversely, in an 'underdrive' condition when engine output is faster, the pressure decreases.

### 3-3 CYCLOCONVERTERS

Cycloconverters-one approach to VSCD systems in shown in figure 3.4.

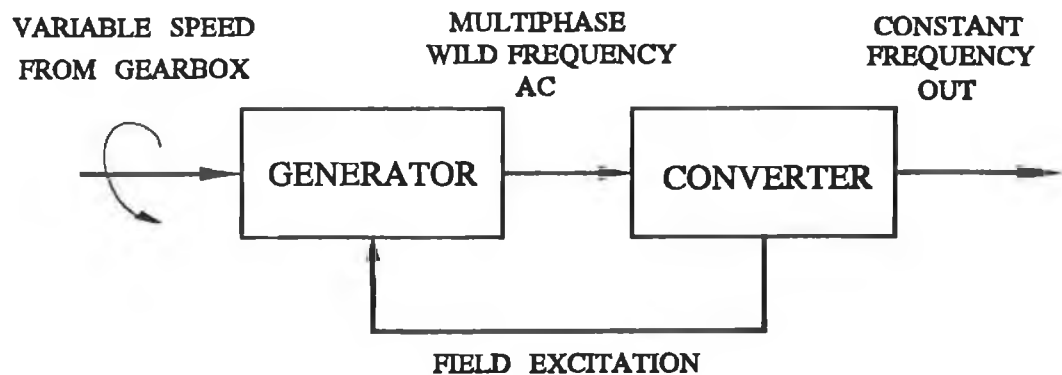


Figure 3.4 Cycloconverter VSCF

Cycloconverter system eliminates the constant speed mechanical/hydraulic drive and couples the engine gearbox directly to the generator. With variations in engine speed, the frequency of the generator output is proportionally changed. This varying generator frequency is converted to a constant output frequency of 400 HZ by means of an electronic converter. The converter uses solid-state switches, to select the proper input generator phase at each instant in time to synthesize a constant 400 HZ output. A basic cycloconverter circuit is shown in figure 3.5.

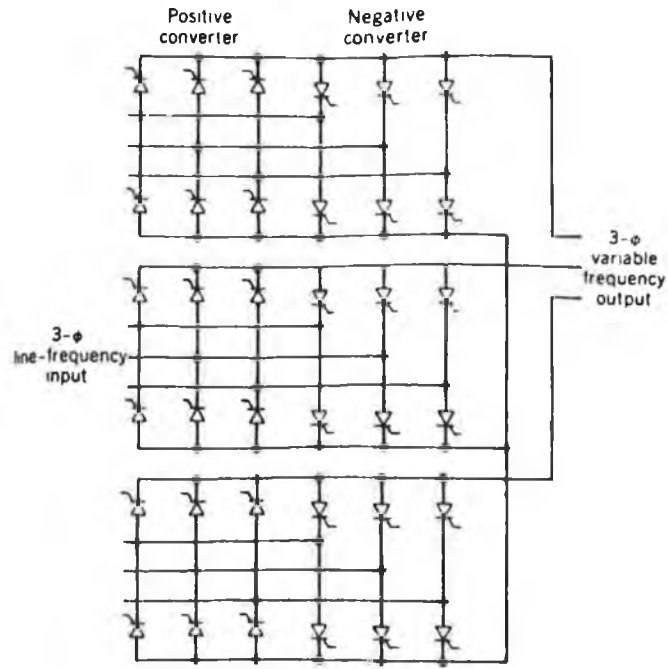


Figure 3.5 Three-phase cycloconverter

Each phase consists of two back-to-back connected line frequency thyristor converters. The delay angles of the two converters in each phase are cyclically controlled to yield a low-frequency sinusoidal output [12]. The input/output voltage relationship is shown in figure 3.6.

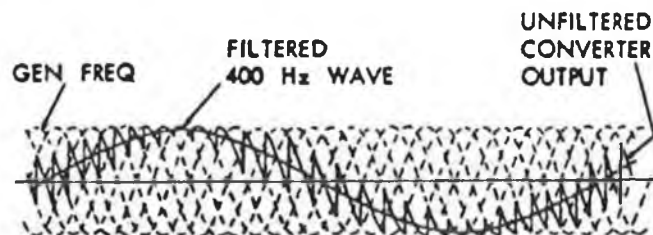


Figure 3.6 Cycloconverter input/output waveform

Cycloconverter system can be used in both low speed and very large horsepower applications, where the cycloconverter output is derived directly from the line frequency input without an intermediate dc link. The maximum output frequency is limited to about one-third of the input ac frequency to maintain an acceptable waveform with low harmonic content.

To date, the electronic switches used in cycloconverters have been silicon controlled rectifiers (SCR's), which limit the steady state operation oil temperature of the cycloconverter system to approximately 80 °C.

### **3-4 DC-LINK VARIABLE SPEED CONSTANT FREQUENCY SCHEME**

With the availability of high voltage, high-power transistors, DC-Link converters having a variable input frequency but a constant output frequency now provide a viable alternative to the constant-speed mechanical drive as a means of providing a constant frequency power supply from an aircraft generator.

The ease of replacement and repair, the reduction in servicing needs, and the ability to locate the components of the electrical system throughout the aircraft all combine to bring about a considerable reduction in the maintenance time which is required.

Figure 3.7 shows the block diagram of the DC-Link VSCF system. Basically, the system employ a generator whose variable speed and variable-frequency power would not be suitable for power needs in an aircraft

system; however, the variable-frequency power is converted to constant frequency power by means of solid-state circuitry, and this makes the power suitable for aircraft use.

The generator is driven directly by the engine, so its speed and output frequency will vary as engine speed varies. The variable three-phase power is fed to the full-wave diode rectifier, where it is converted to direct current and filtered. This direct current is fed to the conversion circuitry, to produce three-phase 400 HZ alternating current. The DC-link system may be physically separated or integrated into one package.

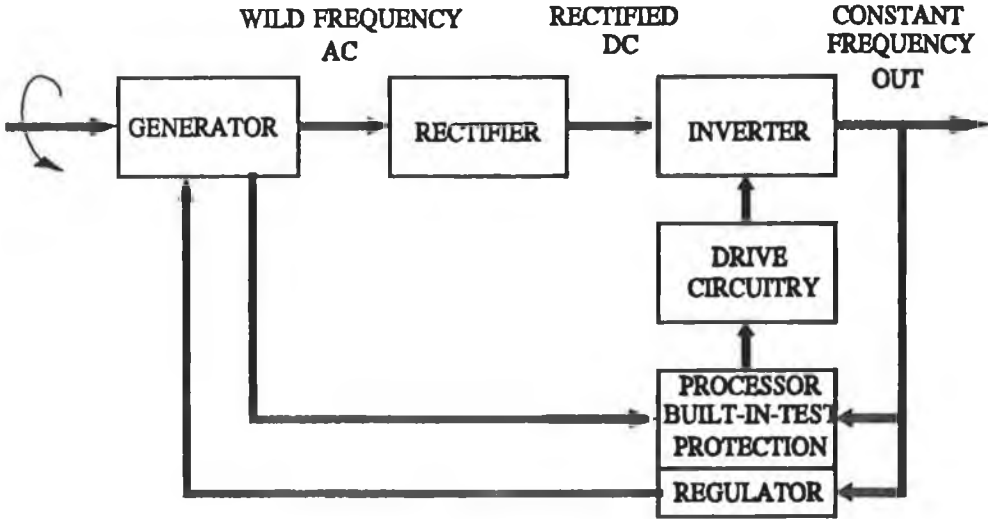


Figure 3.7 DC-Link VSCF System

### 3-5 DC-LINK VERSUS CYCLOCONVERTER

The basic difference between the dc-link approach and the cycloconverter are:

1. The dc-link system as the name implies, uses a dc voltage as the converter input, while the input is a multiphase in the case of the cycloconverter.
2. The electronic switches in the dc-link are transistors, while SCR are used in cycloconverter systems.
3. The switching control scheme in a dc-link can generally be simplified in comparison to a cycloconverter, since the dc-link system uses dc voltage as an input.
4. The dc-link system requires a minimum of six active switching devices and six commutating diodes, while the cycloconverter requires a minimum of thirty-six switching elements.
5. A higher temperature cooling oil can also be used in dc-link systems (120 °C), since transistors are used instead of SCR's.

Nevertheless, both dc-link and cycloconverter approach have specific advantages over the constant speed drive. By replacing the mechanical/hydraulic csd with a solid-state power converter, the reliability of the generating system is improved. Also, since the dc-link VSCF system output frequency is crystal controlled, the output frequency variations inherent with CSD drives are eliminated.



The most critical item in the dc-link is the inverter design and the power switching elements (transistors and commutating diodes ), where the power transistors will control all power flow to the load and the commutating diodes will connect in antiparallel with the power transistors, which are commutating diodes for reverse current flow.

# CHAPTER 4

## STATIC FREQUENCY CONVERTER

### 4-1 INTRODUCTION

This chapter gives the basic concepts of a static frequency converter which accepts a variable frequency power as the input and produces a constant frequency power as the output.

Figure 4.1 shows a block diagram of the principal elements of the static frequency converter.

The ac generator is driven directly by the engine, its speed and output frequency will vary as engine speed varies. The variable three-phase power from the generator is fed into the full-wave diode rectifier where it is converted to direct current. This is fed to the PWM inverter to produce three-phase, 400 HZ alternating current. The output voltage of this inverter is a square-wave of variable pulse width. This voltage is finally fed to a power harmonic filter which reduces the harmonic components to produce a sine wave output at the required frequency. The output voltage of the system is regulated using the AC generator voltage regulator.

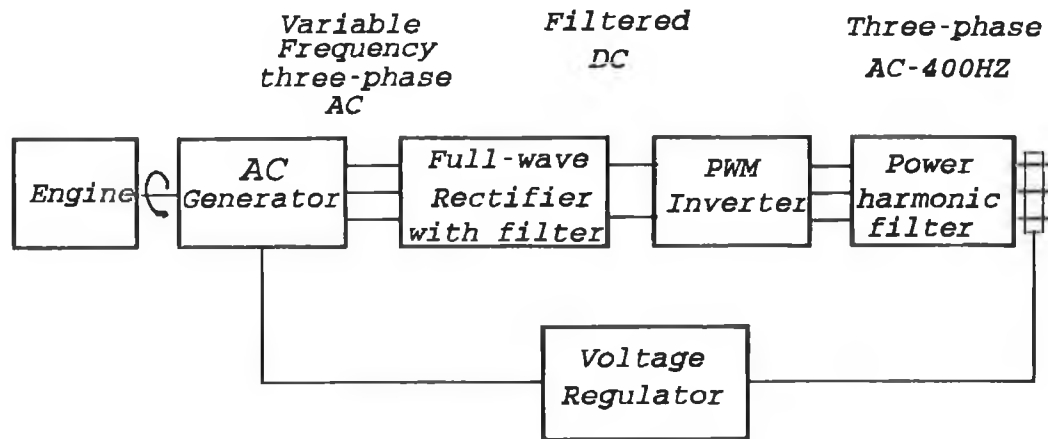


Figure 4.1 Static frequency converter

The PWM inverter is the essential part of the static frequency converter. This chapter will discuss the basic concepts of switch-mode dc-to-ac inverters. Particular emphasis will be placed on the PWM in three-phase voltage-source inverter. Next, the selection of both the amplitude ratio and the frequency ratio will be considered. Finally pulse width modulation techniques are reviewed.

## 4-2 SWITCH-MODE DC-TO-AC INVERTER

Switch-mode inverters are used to convert a dc input to ac output whose magnitude and frequency can both be controlled.

In general, there are two types of switch-mode dc-to-ac inverter [12,13,14], voltage-source inverters (VSI) and current-source inverters (CSI).

In this case a voltage source inverter is used since we require a voltage output.

The voltage-source inverters (VSI) can further divided into the two general categories:

1. Pulse-width modulated (PWM) inverters. In these inverters, the input dc voltage is essentially constant in magnitude. Therefore, the inverter must control both the magnitude and the frequency of the ac output voltage. This is achieved by pulse-width modulation (PWM) of the inverter switches.

The average output voltage of the inverter is varied by controlling the switch ON and OFF durations ( $t_{on}$  and  $t_{off}$ ) at a constant switching frequency.

The output frequency is varied by controlling the frequency of the modulating control signal at the desired frequency.

The principle applications for this kind of inverter are in uninterruptible power supplies and ac motor drives.

2. Square-wave inverters. In these inverters, the output ac voltage waveform is a square wave. The input dc voltage of these inverters must

be controlled in order to control the magnitude of the output ac voltage, and therefore the inverter has to control only the frequency of the output voltage.

We can further sub-divide PWM inverters into different types including:

1. Sinusoidal PWM.
2. Adaptive current control PWM.
3. Phase-shift PWM.

The type of inverter, used here, is a three-phase sinusoidal PWM inverter.

### **4-3 THREE-PHASE PWM INVERTER**

To provide a three-phase, 400 HZ AC electric power, a three-phase inverter is used. It consists of three legs, one for each phase, as shown in figure 4.2. Each inverter leg consists of two switches and their antiparallel diodes. These two switches are always operated alternatively, that is, when one is ON the other is OFF connecting the output to either  $+V_d/2$  or  $-V_d/2$ . The two switches must never be ON simultaneously to avoid short circuiting of the dc input. Therefore, both switches must be OFF for a short time interval (known as dead time).

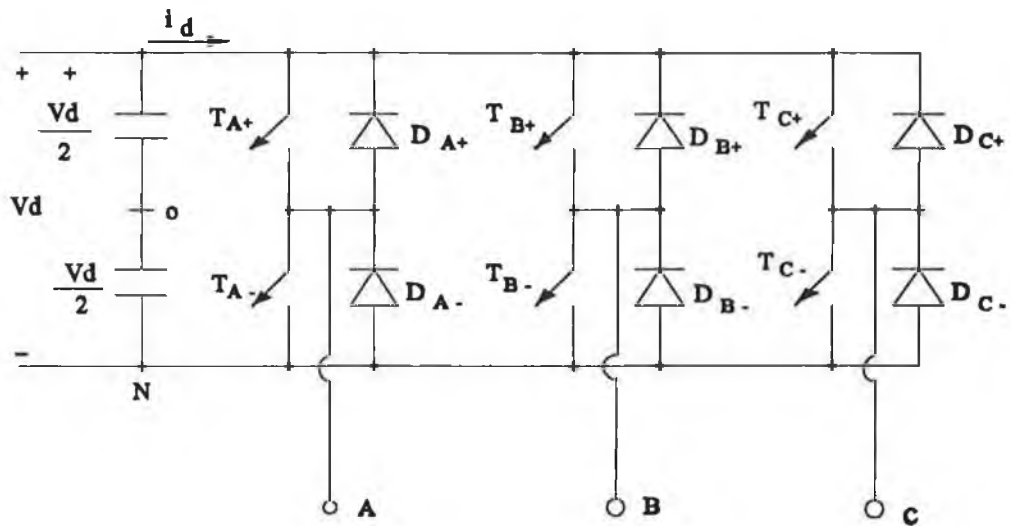


Figure 4.2 Three-phase inverter

The effect of dead time as presented [15] has shown that it affects the amplitude of the fundamental component as well as introducing low order harmonics.

The output waveform of the inverter is greatly influenced by harmonics which arise from many factors including the following:

1. Frequency ratio.
2. Load power factor.
3. Modulation factor of output voltage.
4. Commutation overlap effect.

It is possible to supply a three-phase load by means of three separate single phase inverters, where each inverter produces an output displaced  $120^\circ$  (of the fundamental frequency) with respect to each other. Though this arrangement may be preferable under certain conditions, it requires either a three-phase output transformer or separate access to each of three phases of the load.

#### **4-4 PWM IN THREE-PHASE VOLTAGE-SOURCE INVERTERS**

In a three-phase pulse-width modulated (PWM) inverter a triangular reference voltage waveform is compared with three sinusoidal control voltages, each  $120^\circ$  out of phase, where the objective is to control balanced three-phase output voltages in magnitude and frequency as shown in figure 4.3.

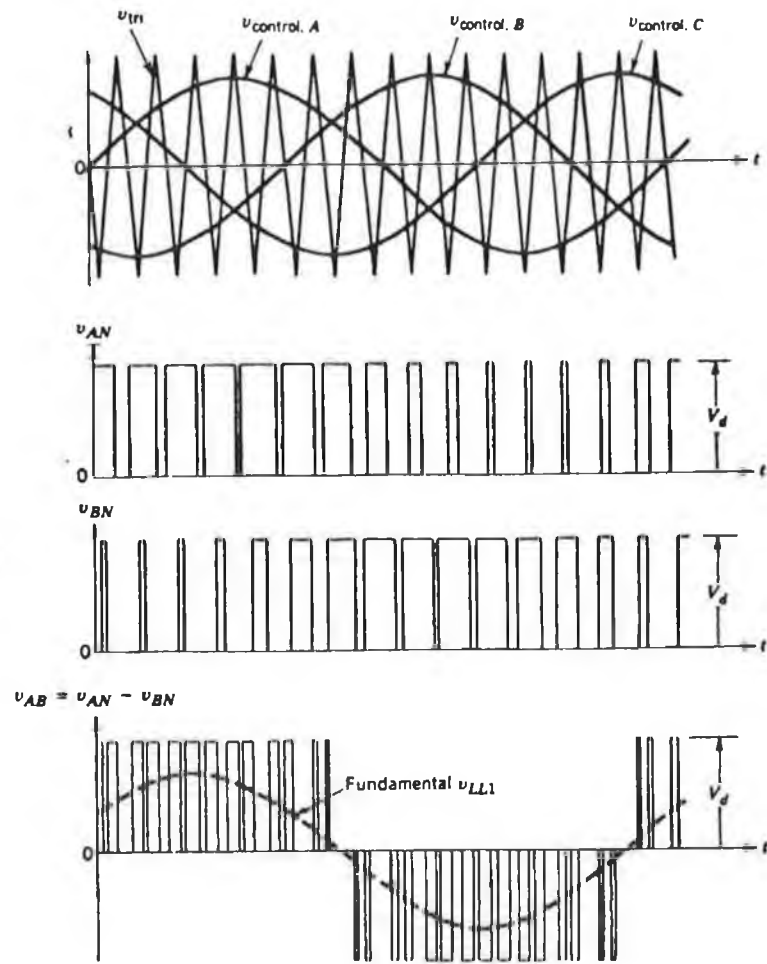


Figure 4.3 Three-phase PWM waveforms



It is necessary to define a few terms before discussing the PWM behaviour:

1. The control signal  $v_{\text{control}}$  which has a frequency  $f_1$  is used to modulate the switch duty ratio, which is the desired fundamental frequency of the inverter voltage output ( $f_1$  is also called the modulating frequency).
2. The triangular waveform  $v_{\text{tri}}$  at a switching frequency  $f_s$ , which establishes the frequency with which the inverter switches are switched ( $f_s$  is also called the carrier frequency).
3. The inverter output is not a perfect sine wave and contains voltage components at harmonic frequencies of  $f_1$ .
4. The amplitude modulation ratio  $m_a$  is defined as:

$$m_a = \frac{\hat{V}_{\text{control}}}{\hat{V}_{\text{tri}}} \quad (1)$$

Where  $\hat{V}_{\text{control}}$  is the peak amplitude of the control signal.

$\hat{V}_{\text{tri}}$  is the peak amplitude of the triangular signal which is generally kept constant.

5. The frequency modulation ratio  $m_f$  is defined as:

$$m_f = \frac{f_m}{f_1} \quad (2)$$

Where  $f_s$  is the carrier frequency.

$f_1$  is the modulating frequency.

In the three-phase inverter, only the harmonics in the line-to-line voltages are of concern. The harmonic at  $m_f$  and odd multiples are suppressed in the line-to-line voltage, if  $m_f$  is chosen to be an odd multiple of 3 (where the reason for choosing  $m_f$  to be an odd multiple of 3 is to eliminate even harmonics). Thus, some of the dominating harmonics in on the one-leg inverter can be eliminated from the line-to-line voltage of three-phase inverter.

## 4-5 SELECTION OF THE AMPLITUDE MODULATION

### RATIO $m_a$

There are two cases of modulation:

- When the amplitude modulation ratio  $m_a \leq 1.0$ .
- When the amplitude modulation ratio  $m_a > 1.0$ .

#### 4-5-1 For $m_a \leq 1.0$

There are three items of importance:

1. The peak amplitude of fundamental frequency component  $(V_{Ao})_1$  is  $m_a$

times of input voltage that is:

$$(V_{AO})_1 = m_a \cdot \frac{V_d}{2} \quad (3)$$

Where  $(V_{AO})_1$  is the fundamental frequency component.

$V_d/2$  is the input voltage.

$m_a$  is the amplitude modulation ratio.

2. The harmonics in the inverter output voltage waveform appear as sidebands, centred around the switching frequency and its multiples, that is, around harmonics  $m_f$ ,  $2m_f$ ,  $3m_f$ , and so on.

The harmonic amplitudes are independent of  $m_f$ , that when frequency modulation ratio  $m_f \geq 9$ .

3. Frequency modulation ratio  $m_f$  should be an odd integer, therefore, only odd harmonics are present and the even harmonics disappear from the waveform of output voltage.

Now we can say when  $m_a \leq 1.0$  the amplitude of the fundamental frequency component of the output voltage varies linearly with  $m_a$  corresponding to a sinusoidal PWM in the linear range and one of the drawbacks is that the maximum available amplitude of the fundamental frequency is not as we wish. PWM pushes the harmonics into a high frequency range around the switching frequency and its multiples.

#### **4-5-2 For $m_a > 1.0$**

To increase the amplitude of the fundamental frequency component in the output voltage,  $m_a$  is increased beyond 1.0. This kind of modulation is called over modulation, which causes the output voltage to contain many more harmonics in the sidebands as compared with the linear range (with  $m_a \leq 1.0$ ). In this case, the amplitude of the fundamental frequency component does not vary linearly with the amplitude modulation ratio  $m_a$ .

### **4-6 SELECTION OF THE SWITCHING FREQUENCY AND THE FREQUENCY MODULATION RATIO $m_f$**

Because of the relative ease in filtering harmonic voltages at high frequency, it is desirable to use as high a switching frequency as possible, except for one significant drawback; switching losses in the inverter switches increase proportionally with the switching frequency  $f_s$ .

There are two cases of frequency modulation ratio  $m_f$ :

- Small frequency modulation ratio  $m_f$  (  $m_f < 21$  ).
- Large frequency modulation ratio  $m_f$  (  $m_f > 21$  ).

#### **4-6-1 Small frequency modulation ratio $m_f$**

There are three items of importance:

1. At small values of  $m_f$ , the synchronous PWM must be used. The triangular waveform signal and the control signal should be synchronized with each other.
2. Frequency modulation ratio  $m_f$  should be an integer. as discussed previously.
3. Slopes of the control signal  $v_{\text{control}}$  and  $v_{\text{tri}}$  should be of the opposite polarity at the coincident zero crossings. This particularly important at very low values of  $m_f$ .

#### **4-6-2 Large frequency modulation ratio $m_f$**

At large values of  $m_f$ , the asynchronous PWM can be used because the amplitudes of subharmonics due to asynchronous PWM are small at large values of  $m_f$ .

The asynchronous PWM can be used where the frequency of the triangular waveform is kept constant, whereas the frequency of  $v_{\text{control}}$  varies, resulting in noninteger values of  $m_f$ .

### **4-7 PULSE WIDTH MODULATION TECHNIQUES**

The pulse width modulation (PWM) method can move unwanted frequency components to a higher frequency region [17]. Thus the output waveform of a

PWM inverter is generally improved by using a high ratio between the carrier frequency and the output fundamental frequency.

It is widely recognised that PWM inverters offer many advantages over other inverter types (square-wave and phase shift inverters) [18,20]. These advantages are usually gained at the expense of more complex control and power circuit configurations. However, in the future, the cost as well as the complexity of PWM inverters systems is likely to reduce due to continuing development in microprocessor technology and semiconductors.

In general, the PWM output is characterised by a constant amplitude pulse train, whose duration is related to the desired information to be transmitted, (as defined by the modulation or information wave), and the carrier or sampling system. It is possible to identify three basic switching schemes that are currently employed:

1. Natural sampled PWM.
2. Regular sampled PWM.
3. Optimised PWM.

#### **4-7-1 Natural sampled PWM**

Natural sampled PWM is generally associated with analogue implementations and represents the classical PWM switching strategy. The pulse widths are 'naturally' defined by the instantaneous intersections of the carrier and modulating functions.

The principle of generating a PWM pattern is illustrated in figure 4.4. A triangular carrier wave is compared with the sinusoidal modulating wave of lower frequency. The output of the comparator, figure 4.4 has a "high" level whenever the instantaneous value of the modulating wave exceeds the carrier wave level and a "low" level when the instantaneous value of the modulating wave is exceed by the carrier wave, resulting in a PWM waveform as shown in figure 4.5(b).

Since the switching edges of the width-modulated pulse is determined by the instantaneous intersection of two waves, the resulting pulse width is proportional to the amplitude of the sine wave at the instant where the intersection occurs.

The width of the naturally sampled PWM pulses can be defined using a transcendental equation of the following form [19]:

$$t_p = \frac{T}{2} \left[ 1 + \frac{m_a}{2} (\sin \omega_m t_1 + \sin \omega_m t_2) \right] \quad (4)$$

where

T represents the carrier period.

$m_a$  is the modulation ratio.

$\omega_m$  is the modulating frequency.

$t_1$  and  $t_2$  are the sampling instances.

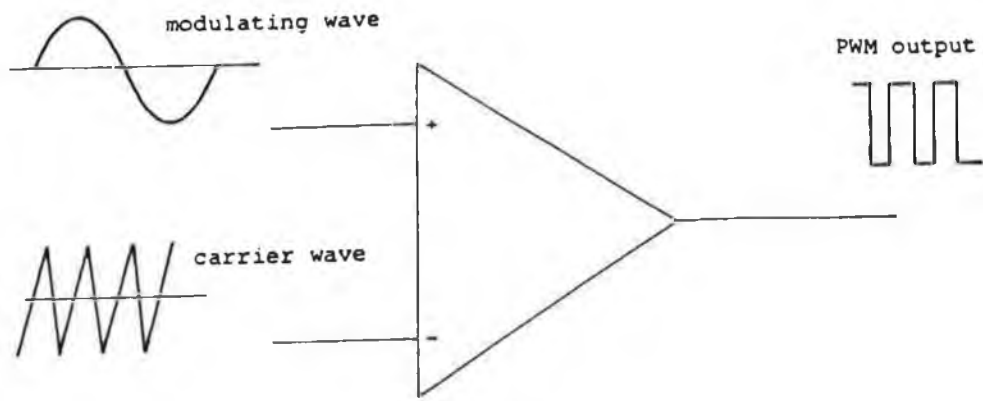


Fig. 4.4 Block diagram of analogue method of generating natural sampled PWM

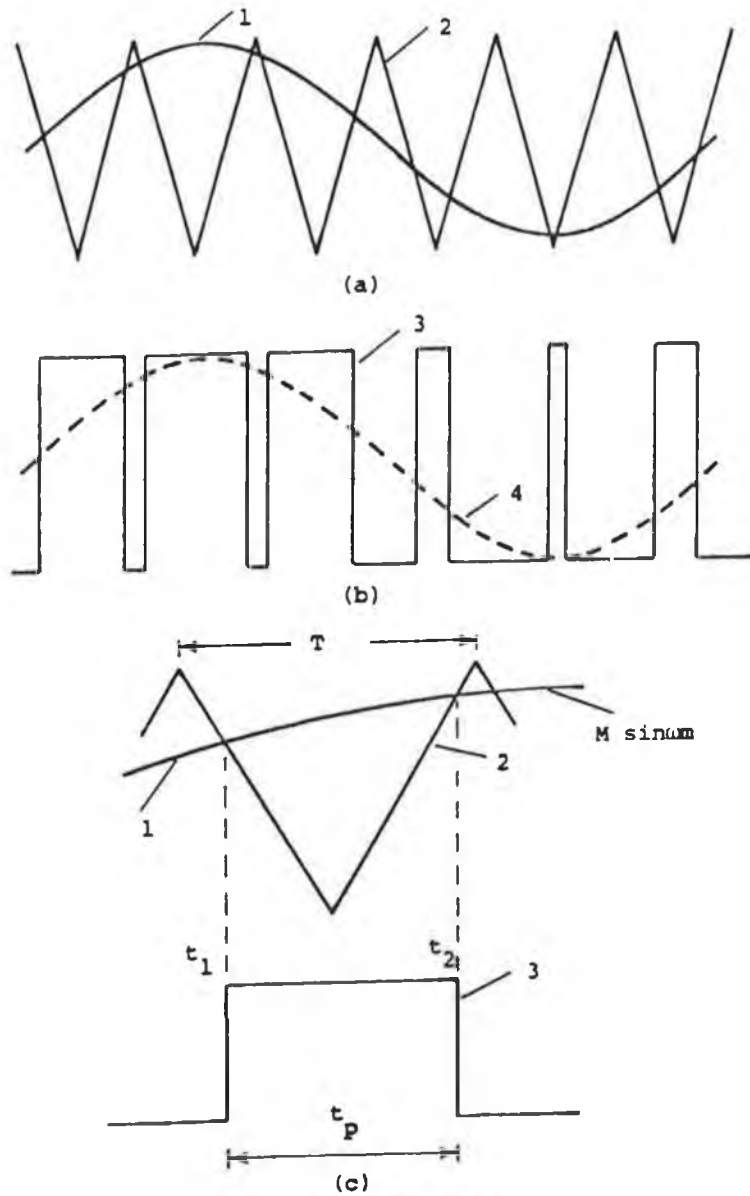


Fig. 4.5 Natural sampled PWM  
 (a) Sampling process, (b) output waveform, (c) detail of single pulse  
 1 modulating wave, 2 carrier wave, 3 PWM waveform,  
 4 fundamental of PWM waveform



#### 4-7-2 Regular sampled PWM

The use of regular sampled PWM inverter control was first proposed by Bowes [20]. He demonstrated that this sampling system, unlike natural sampled PWM, enables exact defining of the pulses and hence gives a considerable advantage in harmonic cancellation. Furthermore, regular sampled PWM improves the frequency spectra by reducing the lower-frequency harmonics and suppressing the subharmonics at non-integer frequency ratios. This results in significantly wider inverter output frequency ranges [20].

There are two types of regular sampled modulation, namely 'symmetric' and 'asymmetric'. In symmetric modulation, as illustrated in the upper part of figure 5.11, each pulse edge, with respect to regularly spaced pulse position, is the same. The width of a pulse may be defined in terms of the sampled values of the modulating wave taken at time  $t_1$ , thus:

$$t_p = \frac{T}{2} [1 + m_a \cdot \sin(\omega_m t_1)] \quad (5)$$

where  $t_1$  represents the sampling instance.

In asymmetric modulation each pulse edge is modulated by a different amount, as shown in the lower part of figure 4.6. In this case the leading and trailing edges of each pulse are determined using two different samples of the modulating wave, taken at time instants  $t_1$  and  $t_3$  respectively. The width of the resulting asymmetrically modulated pulse may be defined in terms of these sampling times thus:

$$t_p = \frac{T}{2} \left[ 1 + \frac{m_a}{2} [\sin(\omega_m t_1) + \sin(\omega_m t_3)] \right] \quad (6)$$

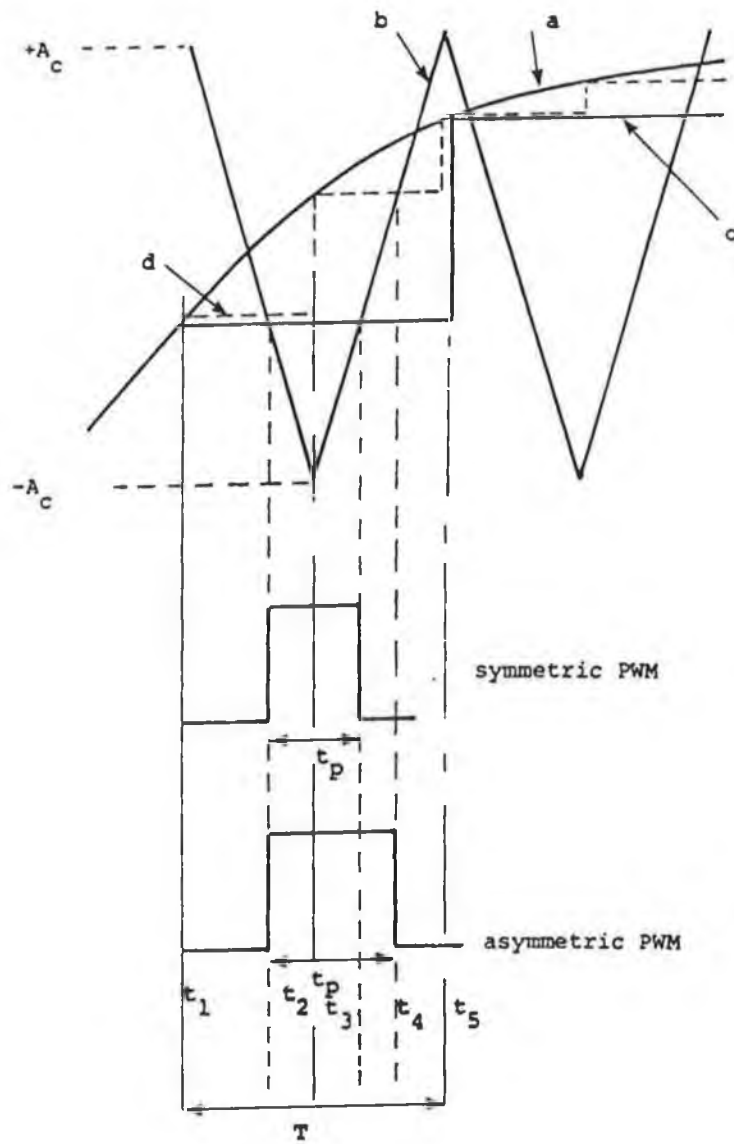


Fig. 4.6 Symmetric and asymmetric regular sampled PWM

- a modulating wave  $e = E_R \sin \omega_m t$
- b carrier wave
- c sample-hold modulating wave (symmetric PWM)
- d sample-hold modulating wave (asymmetric PWM)

### 4-7-3 Optimised PWM

Through recent developments in processor technology, optimised PWM strategies have become an attractive alternative to natural or regular PWM. These strategies are based on the optimisation of particular performance criteria, [21,22].

Invariably, optimised PWM forms part of a closed loop system and is required to adapt to the particular environment. There are two methods in which the optimisation strategy can be adapted, the switching calculations to be performed in real time, or the switching instances are calculated, and stored in memory, 'off line'.

The former system generally necessitates a great deal of processing power, since it is often required to solve a set of non-linear equations.

The latter is based on a system with a well defined set of input stimulation and through the optimisation algorithms, a sufficient set of waveforms are stored in memory. Generally, the size of this memory will be large to provide the required level of system integrity.

It is possible to constrain the degree of memory and processing overheads by appropriate interpolation techniques. However, each method of the optimized PWM techniques is associated with the difficult task of computing specific PWM switching instants to optimize a particular objective function. This difficulty is particularly encountered at lower-output frequency range due to the necessity of a large number of PWM switching instants.

This section has reviewed the techniques of PWM applicable to inverters; naturally sampled PWM is used in this design because of its simplicity.

# CHAPTER 5

## THREE-PHASE PWM INVERTER DESIGN

In this chapter, the design of the three-phase PWM inverter is described. This inverter converts the rectified output from a wild-frequency generator to the constant-frequency (400 HZ) AC supply required by the aircraft.

The design of the three-phase PWM inverter involves two elements as shown in the block diagram figure 5.1:

1. Power circuit design.
2. Control circuit design.

The power circuit configuration of the PWM inverter is illustrated in figure 5.1. It consists of six power MOSFETs Q1 to Q6, snubber circuits, gate drive circuits, isolation circuits, isolated power supplies and blanking circuits.

The control circuit as shown in figure 5.1, consists of a sine/square wave generation circuit, filter circuit, three-phase sinusoidal wave generation circuit, triangular wave generation circuit and comparator circuits.

In the control circuit, the sine wave reference of frequency 400 HZ, from the sine/square wave generation circuit, is applied to the filter circuit to eliminate the harmonics components. The output signal of this filter is then applied to the

three-phase sinusoidal wave generation circuit to generate three-phase sinusoidal waveform signals with a phase delay of 120 degrees. In addition, the square wave signal from the sine/square wave generation circuit is applied to the triangular wave generation circuit in order to generate a triangular waveform signal of frequency of 3600 HZ. In the comparators, the three-phase sinusoidal signals are compared with the triangular waveform signal that corresponds to the desired modulation. These signals are applied to the gate of the MOSFETs.

The isolation of these signals is achieved using optical isolation circuits. These circuits have a Faraday screen between the LED and the phototransistor to prevent spurious triggering of the phototransistor by capacitive current during switching of the power circuit.

The gate drives are maintained by using gate drive circuits which are capable of providing 1.5 A of charging current. Power for both the drive and isolation circuits is provided by the isolated power supplies.

Snubber circuits are used to prevent voltage spikes and voltage oscillations across the MOSFETs during devices turn-on.

The basic working principle associated with the power and control circuitry of the PWM inverter is explained in the following paragraphs.

## 5-1 POWER CIRCUIT DESIGN

### 5-1-1 Choice of switching devices

The switching frequency and other parameters such as the input voltage, the need for a simple drive circuit and the chosen topology meant that the most suitable option was an N-channel MOSFET.

Power MOSFETs offer many advantages over conventional bipolar transistors, in both linear and switching applications [23]. These advantages include:

1. Very fast switching.
2. Freedom from secondary breakdown.
3. Voltage drive, permitting easy connection with digital systems.
4. Wide safe operating area.
5. High reverse breakdown voltage.
6. High gain at all frequencies.
7. Very limited charge effects.
8. Simple drive circuitry.

However they have a few disadvantages:

1. Limited normal current for comparatively high voltage.
2. Relatively high drain-source ON resistance.
3. High cost price.

In using MOSFETs there are several parameters one needs to look closely at, the first is ON resistance of the drain-source path ( $R_{ds-on}$ ). From the basic

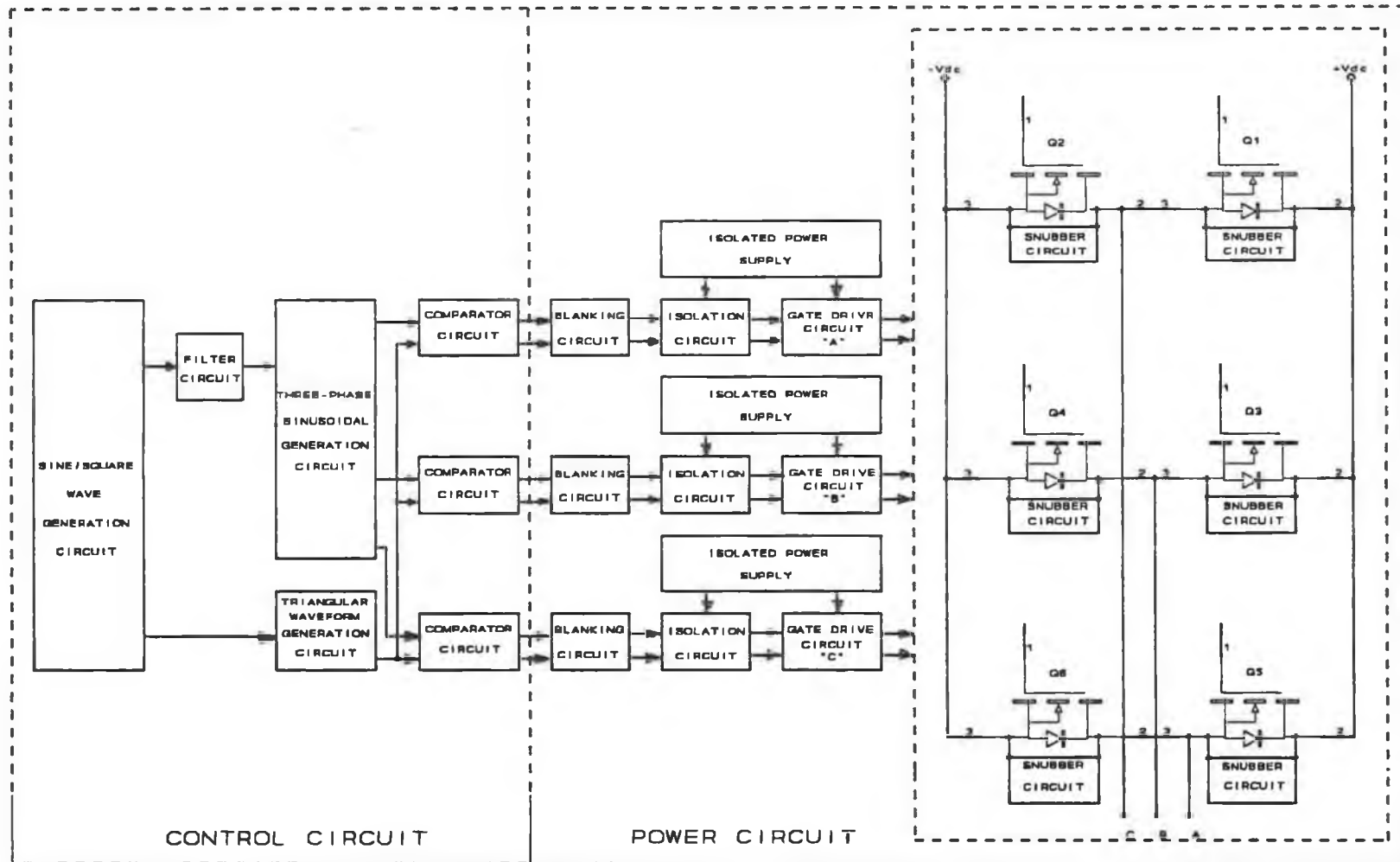


FIGURE 5.1 BLOCK DIAGRAM OF THE THREE-PHASE PWM INVERTER



theory of the device as the reverse blocking capability is increased the  $R_{ds-on}$  increases. This can lead to increased power losses in the device due to  $I^2R_{dc-on}$  relationship, this can mean a bigger heat sink is needed. Typical values of  $R_{ds-on}$  for 450 volt N-channel devices are 2-4 ohms, lower  $R_{ds-on}$  are available at much higher cost.

The next parameter that one should be aware of is the  $dv/dt$  rating of the device. There is a failure mechanism, known as latchup [24], which can lead to spurious turn ON of the device with catastrophic results. It is therefore important that one knows the intended slow rate for the switching, and also remember that the device is effectively ON, once the gate voltage reaches its threshold level. So how to avoid  $dv/dt$  problems. In many circuits,  $dv/dt$  turn-ON may be avoided. There are many ways to accomplish this [25]:

1. Reduce  $dv/dt$ .
2. Good circuit layout practice.
3. Snubbers.
4. Series drain diode.
5. Turn-on the FET during commutation.
6. Use MOSFETs with good  $dv/dt$  performance.
7. Current fed topologies.

The most obvious way to reduce  $dv/dt$  problems is to slow the switching speed. This can be accomplished easily by adding resistance in the gate of the MOSFETs.

The final parameter needing attention is the source-drain parasitic anti-parallel diode. The parasitic anti-parallel diode is inherently built in the process of fabricating any power MOSFET transistor. This diode has voltage and current ratings equal to the MOSFET, but has, in general, a slow reverse recovery. Due to the slow recovery of MOSFET inherent diodes, a temporary short may occur in several commonly used switching power circuits. The effects of the temporary short circuit are high power dissipation particularly at high switching frequencies and possible damage to the MOSFET. This should be avoided. This problem can be eliminated by effectively removing the parasitic diode from the circuit. Two solutions were recommended for this problem [25]. One requires using a center-tapped inductor in each totem pole to limit the current surge during the diode reverse recovery time as shown in figure 5.2. This arrangement requires additional free wheeling diodes around this inductor to release inductive energy when the MOSFET is cut off. The other requires the addition of schottky diode in series with each MOSFET and use a fast recovery diode as the freewheeling diode.

The purpose of the schottky diode is to prevent current from flowing through the parasitic diode. Reverse current now has to flow through the freewheeling diode. Because of the fast reverse recovery nature of freewheeling diode, the current spike during recovery is considerably reduced.

These solutions can also help to eliminate problems caused by the  $dv/dt$  ratings mentioned before.

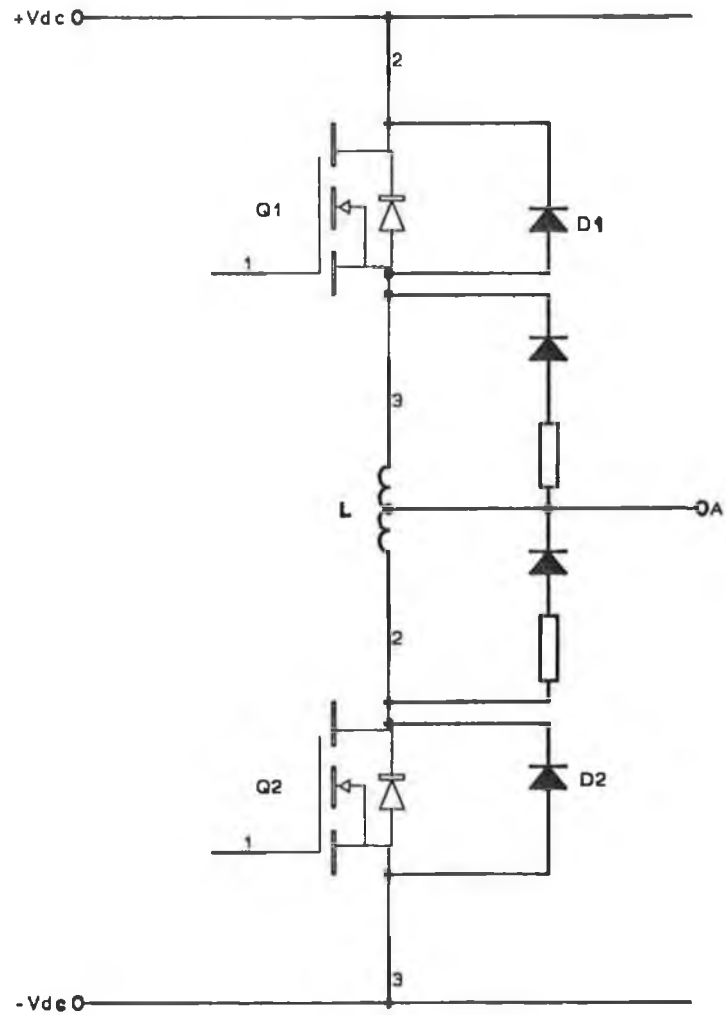


Fig. 5.2 One-phase of three-phase PWM inverter with tapped inductors to prevent shorting Q1 and Q2.

In this design, the second solution has been used as shown in figure 5.3.

Schotky diodes (10TQ045), which have the following ratings:

$I_F(\text{AV})$  10 A

$t_r(\text{max})$  50 ns

and freewheeling diodes (BYV29-500), which have the following ratings:

$I_F(\text{AV})$  9 A

$t_r(\text{max})$  50 ns

have been used in this circuit. While IRF450 MOSFETs, which have the following ratings have been used as switching devices.

$BV_{dss}$  450 Volts

$R_{ds-on}$  0.4 Ohms

$I_d$   $\pm 13$  Amps

$t_r(\text{diode})$  400 ns

For other specification see appendix (a).

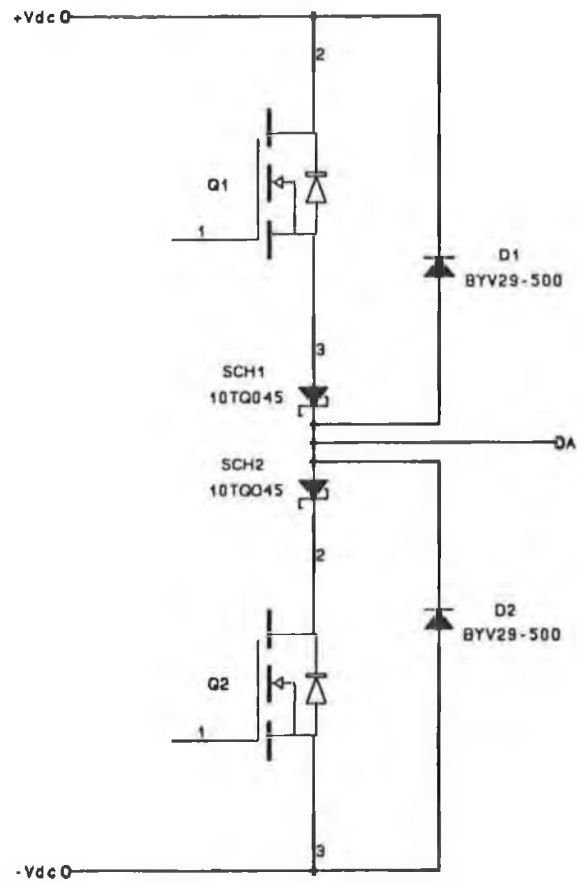


Fig. 5.3 One-phase of three-phase PWM inverter with schottky and freewheeling diodes to prevent shorting Q1 and Q2.

### 5-1-2 Heat-sink design

Semiconductor power losses are dissipated in the form of heat, which must be removed from the switching junction. The reliability and life expectancy of any power semiconductor is directly related to the maximum device junction temperature experienced [27].

In using a MOSFET, like any other semiconductor device, the junction temperature  $T_j$  must be kept below a maximum value  $T_{j,max}$ , which is generally found on the manufacturer's specification or data sheets of the device.

The average power dissipation  $P_d$  and maximum junction temperature  $T_{j,max}$ , along with the maximum ambient temperature  $T_{a,max}$  determine the design of the heat sink, according to:

$$P_d = \frac{T_{j,max} - T_{a,max}}{R_{\theta j-a}} \quad (1)$$

where

$R_{\theta j-a}$  is the total thermal resistance from the junction to the ambient air, that is:

$$R_{\theta j-a} = R_{\theta j-c} + R_{\theta c-s} + R_{\theta s-a} \quad (2)$$

where

$R_{\theta j-c}$  is the junction-to-case thermal resistance.

$R_{\theta c-s}$  is the case-to-sink thermal resistance.

$R_{\theta s-a}$  is the sink-to-ambient thermal resistance.

The junction-to-case thermal resistance  $R_{\theta_{j-c}}$  can be obtained from the data sheets, and the case-to-sink thermal resistance  $R_{\theta_{c-s}}$  depends on the thermal compound and the voltage insulator (if any) used. Knowing  $R_{\theta_{c-s}}$  and  $R_{\theta_{j-c}}$ , we can calculate the thermal resistance of the heat sink-to-ambient thermal resistance  $R_{\theta_{s-a}}$  from eq. 2.

For MOSFET (IRF450) which has the following specifications (Appendix a):

$$R_{ds-on} = 0.4 \Omega, \quad R_{\theta_{j-c}} = 0.83 \text{ }^{\circ}\text{C/W} \text{ and for } I = 15 \text{ amps.}$$

The average power dissipation is given by:

$$P_d = I^2 R_{ds-on} \times \delta \quad (3)$$

where

$I$  is the peak current ( $I = 15 \text{ A}$ ) which will apply on MOSFET.

$\delta$  is the conduction duty cycle ( $\delta = 0.5$ ) at the worst case.

$R_{ds-on}$  is the static drain-source on-state resistance ( $=0.4\Omega$ ).

by substituting the values of  $I$ ,  $\delta$ , and  $R_{ds-on}$  in the above equation, the average power dissipation was found to be;

$$P_d = (15)^2 \times 0.4 \times 0.5 = 45 \text{ W}$$

For a maximum junction temperature of  $150 \text{ }^{\circ}\text{C}$ , and assuming an ambient temperature of  $45 \text{ }^{\circ}\text{C}$ , and by applying equation 1 the required junction-to-ambient resistance was found to be;

$$R_{\theta j-a} = \frac{150 - 45}{45} = 2.33 \text{ } ^\circ\text{C/W}$$

Now using eq. 2, the thermal resistance from sink to ambient can be calculated by using equation 4;

$$R_{\theta s-a} = R_{\theta j-a} - R_{\theta j-c} - R_{\theta c-s} \quad (4)$$

where

$$R_{\theta j-c} = 0.83 \text{ } ^\circ\text{C/W} \text{ from the data sheet of IRF450.}$$

$$R_{\theta c-s} = 0.4 \text{ } ^\circ\text{C/W} \text{ from the data sheet of washer (silicon rubber).}$$

by substituting in eq. 4;

$$R_{\theta s-a} = 2.33 - 0.83 - 0.4 = 1.1 \text{ } ^\circ\text{C/W.}$$

A suitable heat-sink was selected from the catalogue.

### 5-1-3 Snubber circuit design

The transistor experiences high stresses at turn-on and turn-off when both its voltage and current are high simultaneously, thus causing a high instantaneous power dissipation. Moreover, any practical circuit has some amount of stray inductance and so a voltage spike is produced whenever, the current through it is switched off. This voltage spike can be very large and may damage the device if the stray inductance in the circuit is not minimized [26]. So it is necessary to use snubber circuits to reduce these stresses and to protect the transistors by improving their switching trajectory.

In general there are three basic types of snubber:



1. Turn-off snubber.
2. Turn-on snubber.
3. Over voltage snubber.

Because of the square safe operating area that the MOSFET has for switch-mode applications, the need for snubbers in MOSFET circuit is greatly minimized compared with other kinds of transistors. However, a small R-C-D turn-off as shown in figure 5.4 can be used to prevent voltage spikes and voltage oscillations across a MOSFET during device turn-on. The snubber must be connected directly on the component being snubbed with as short leads as possible.

#### 5-1-3-1 Choice of snubber resistor

The snubber resistance  $R_s$  should be chosen where the peak current through it is less than the reverse recovery current  $I_{rr}$  of the free-wheeling diode that is:

$$\frac{V_d}{R_s} < I_{rr} \quad (5)$$

The circuit designer usually attempts to limit  $I_{rr}$  to 0.2 output current or less, so that the forgoing eq. 5 becomes approximately:

$$\frac{V_d}{R_s} = 0.2 I_o \quad (6)$$

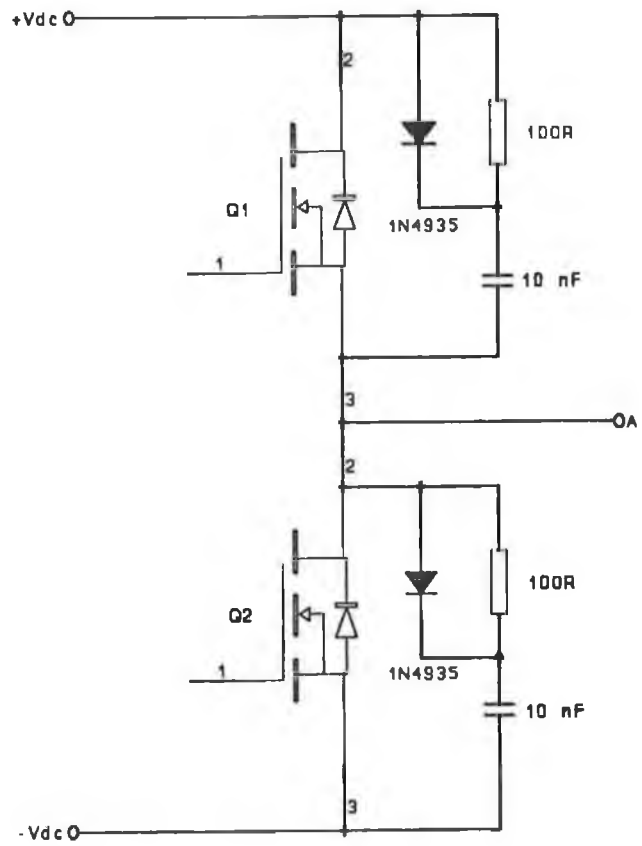


Fig. 5.4 One-phase of three-phase PWM inverter with snubber circuits.

### 5-1-3-2 Choice of snubber capacitor

The snubber capacitor should be chosen based on:

1. Keeping the turn-off switching locus within the reverse bias safe operating area.
2. Reducing the transistor losses based on its cooling considerations.
3. Keeping the sum of transistor turn-off energy dissipation and snubber resistance energy dissipation low.

We can approximately calculate  $C_s$  from the following equation [12]:

$$C_s = \frac{I_o t_{fi}}{2 V_d} \quad (7)$$

where

$t_{fi}$  is the current fall time.

$I_o$  is the output current.

$V_d$  is the input voltage.

The capacitor energy, which is dissipated in the snubber resistor, is given by:

$$W_R = \frac{C_s V_d^2}{2} \quad (8)$$

The designer must ensure that the capacitor has sufficient time to discharge down to a low voltage during the minimum on-state time of the transistor so that the turn-off snubber will be effective at the next turn-off interval.

Using the above procedures to calculate the snubber circuit parameters resulted in values of:  $C_s = 10 \text{ nF}$ ,  $R_s = 100 \text{ } \Omega$ . The RC time constant which is 1  $\mu$  Second of the snubber is then made small compared to the on time of the transistor.

The need for such a turn-off snubber increases with faster switching speeds of the MOSFETs.

The large peak current handling capability of the MOSFET and the fact its switching speed can be easily controlled by controlling the gate current eliminates the need for turn-on snubber in most cases.

#### 5-1-4 Gate drive circuit design

One of the main reasons for the choice of a MOSFET was the simplicity of the gate drive circuit. The MOSFET basically presents a capacitive load to the gate drive. Figure 5.5 shows all of the parasitic capacitances within the MOSFET. The MOSFET is a voltage driven device so the gate drive circuit must apply a voltage above the threshold voltage to produce current flow in the drain-source. To do this the drive circuit must charge the input capacitances. An approximation to the current pulse needed can be calculated as follows:

$$I = \frac{C_{gs} \times V_{gs}}{t_s} \quad (9)$$

where

$C_{gs}$  is the gate source capacitance.

$V_{gs}$  is the source voltage required.

$t_s$  is the time in which  $V_{gs}$  is to be reached.

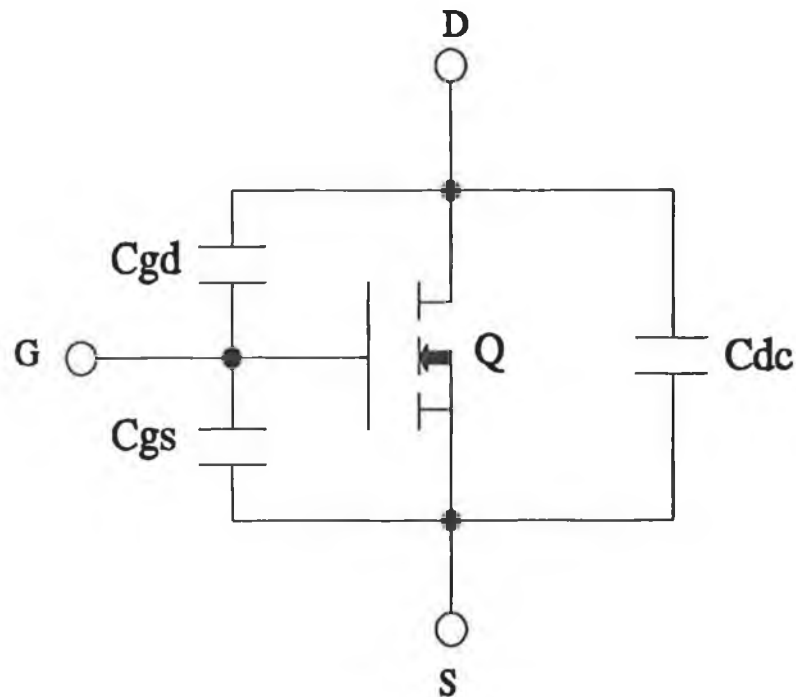


Fig. 5.5 MOSFET equivalent circuit.

The control signal to switch the MOSFET is usually supplied by a logic circuit consisting of some dedicated ICs or microprocessor, for example. The signal output stage of such logic circuits cannot drive the MOSFET gate directly because it is often not designed to provide a gate current of appropriate magnitude. Therefore a need exists for a gate drive circuit to interface the logic control signal to the gate of the MOSFET.

The gate driver must meet the following requirements:

1. Short delay time.
2. Low impedance output.
3. Capability of accepting duty cycles between 0 % and 100 %.
4. Insusceptibility to dv/dt triggering during switching.
5. Low capacitance between the two sides of the power supply.

The rate of change of  $V_{DS}$  and  $i_D$  depend on the gate current, which determines how fast the device capacitances are charged and discharged. Therefore, the circuit designer can control the MOSFET switching times by controlling the gate current supplied by the gate drive circuit.

The advantage of fast switching speed is the reduction in switching power loss due to the reduction of the crossover time, and therefore reduction of power losses. This is important in high-switching application.

To provide the fast switching speeds, the gate current required by the MOSFET can be substantial, on the order of 1.0 Ampere or more.

There are disadvantages to fast switching, including higher EMI (electromagnetic interference), increased reverse recovery current problems in the freewheeling diode, and overvoltages due to stray inductance.

Figure 5.6 is illustrated the gate drive circuit, which was designed to meet all the above requirements.

It uses a 7667 CPA MOSFET driver which has the following features:

1. It is a dual high speed driver.

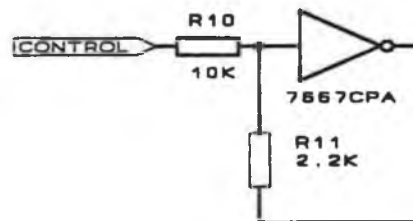
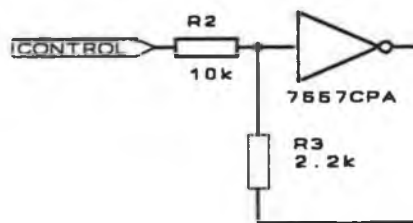
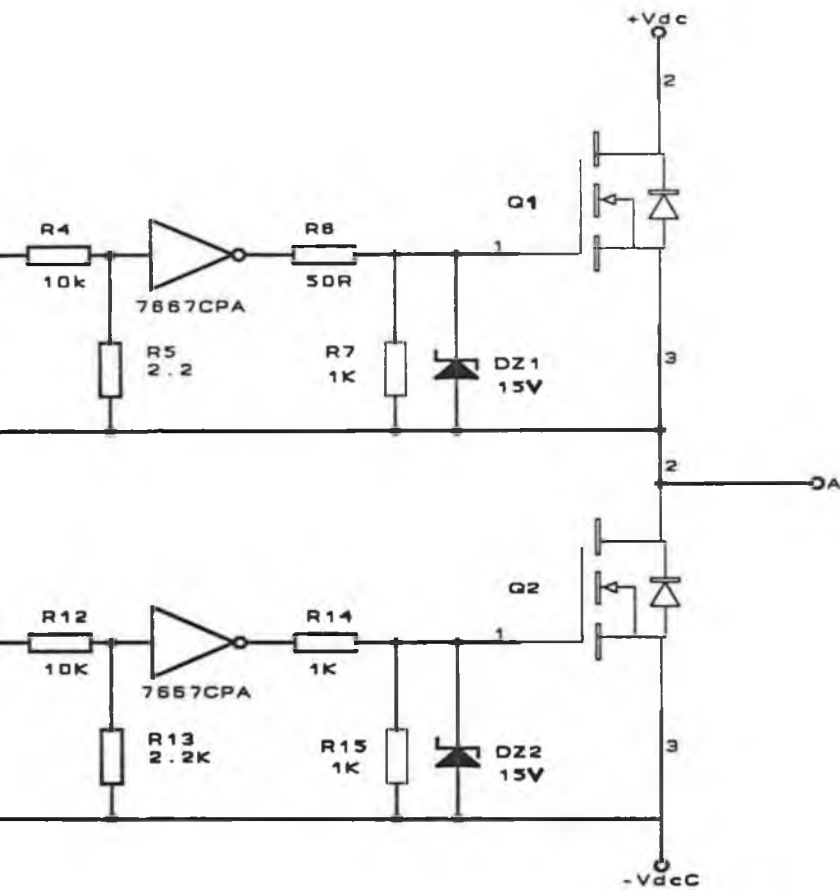


Fig. 5.6 gate



drive circuit for one-phase of PWM inverter.



2. Fast rise and fall times - 40 ns, 1000 PF load.
3. High output current 1.5 Amps.
4. It is capable of driving large capacitive loads with high slew rates and low propagation delays.
5. It can be directly driven by common pulse-width modulation i.c.s.

Resistors of values  $50 \Omega$  and  $1 \text{ k}\Omega$  for the upper and lower MOSFETs respectively were used in series with the gate of the MOSFETs, to control the rate of charging for the gate capacitances and therefore the turn-on time<sup>1</sup>.

Another important part of the gate drive is overvoltage protection. The absolute maximum voltage on the gate is specified in most cases as 20 volts, to ensure this not exceeded a zener diodes were used to clamp the gate voltage to 15 volts as shown in figure 5.6. In parallel with the zener diodes resistors were connected to ground, the purpose of this to prevent the gate voltage rising above the threshold at any time when it is not being driven. This can happen if the  $C_{gs}$  is charged via  $C_{gd}$ , this caused by the drain voltage varying. A swing of 30 volts is enough to turn the device on, this can lead to the destruction of device and circuit.

---

<sup>1</sup> The values of resistors are established experimentally

### **5-1-5 Isolation circuit design**

In three-phase inverter, the negative power rail of bridge circuit can usually be linked to the ground of the control electronics. This allows the bottom MOSFETs of the bridge to be driven either directly from the control circuit or by using isolation circuit [28]. However the potentials of the sources of the top MOSFETs swing between the positive rails of the DC supply, making it impossible for the sources of the upper MOSFETs to be linked directly to the control circuit. Therefore, there is a need for electrical isolation between the logic level control signal and the MOSFET gate drive circuit.

There are two basic ways to provide electrical isolation as following:

1. Transformer isolation.
2. Opto-coupler isolation.

#### **5-1-5-1 Transformer isolation**

Isolation between the power circuit and the control circuit may be achieved by the use of transformer coupling as shown in figure 5.7. The output impedance of the transformer secondary will depend on the reflected impedance of the primary driver circuit and on the impedance of the transformer. Therefore for fast switching the transformer must have low leakage inductance and the primary driver should have low output impedance. A series capacitor is included to block the dc component in the primary-driver output waveform.

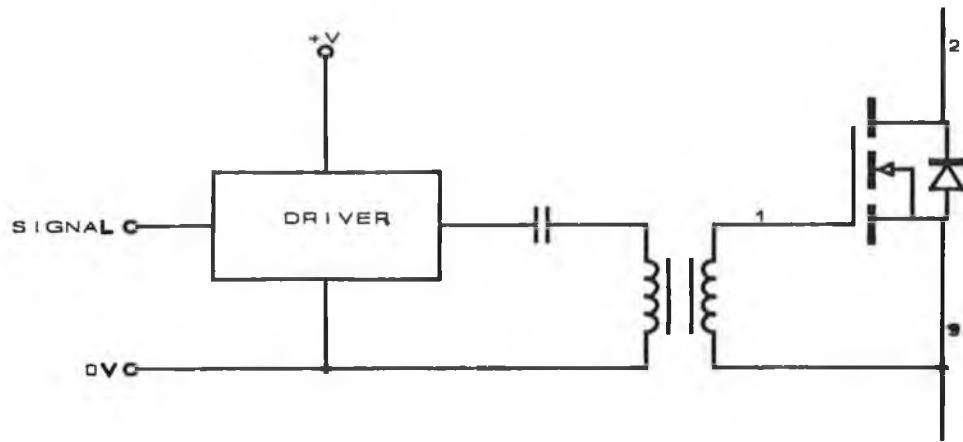


Figure 5.7 Transformer-isolated gate drive.

A major restriction on the usefulness of a transformer-coupled gate drive is that the duty cycle over which it can operate is limited. The secondary voltage waveform cannot contain a dc component. Therefore the time integral of the negative part of the waveform must equal the time integral of the positive part of the waveform.

In use transformer, we have to modulate the control signal by a high frequency oscillator output before applying it the primary of a high frequency signal transformer, since a high frequency transformer can be made quite small.

Generally, optical drives are smaller and less expensive than the transformer drives although somewhat slower [25].

### 5-1-5-2 Opto-coupler isolation

Opto-coupler is capable of switching at several MHz. It consists of a light-emitting diode and an output transistor. The capacitance between the light-emitting diode and the base of the receiving transistor within the optocoupler should be as small as possible to avoid retriggering at both turn-on and turn-off of the power MOSFET transistor due to the jump in the potential between the power transistor gate reference point and the ground of the control circuit. To reduce this problem, optocoupler with electrical shields between the LED and the receiver transistor should be used. There is a disadvantage of using an optocoupler, that it needs for an auxiliary isolated dc power supply with respect to the source of the MOSFETs.

The isolation circuit shown in figure 5.8 was designed to meet the above requirements. It uses an opto-coupler (HCPL2200) to isolate the control signal and the MOSFET gate drive circuit. The opto-coupler has a Faraday screen between the LED and the phototransistor to prevent spurious triggering of the phototransistor by capacitive currents during switching off the power circuit.

Six opto-couplers have been used for the three-phase PWM inverter. Two for each leg.

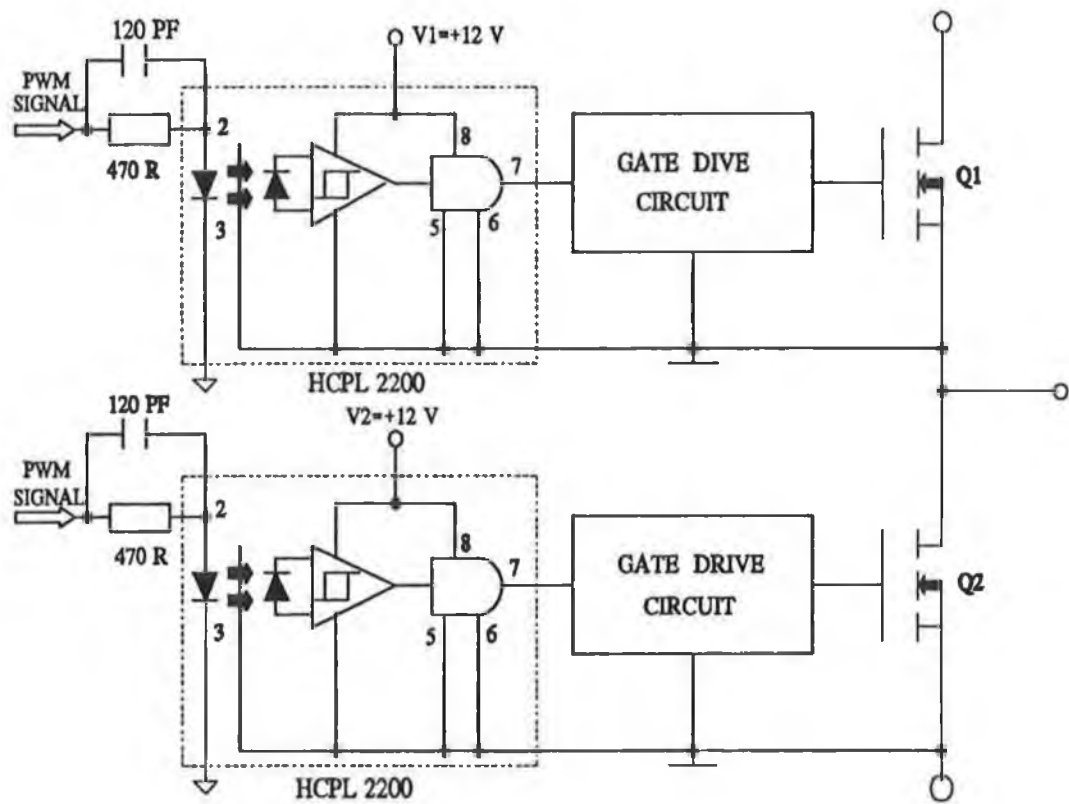


Fig. 5.8 Isolation circuit for one-phase of PWM inverter.

### **5-1-6 Isolated power supply design**

A four isolated dc power supplies are required with respect to the source terminal of the MOSFETs to provide +12V for drive and isolation circuits of three-phase PWM inverter. Three isolated power supplies for upper circuits and one for the lower circuits.

Figure 5.9 is illustrated these power circuits, which were designed to give +12 Vdc, 1A. Each power supply consists of:

1. Transformer.
2. Bridge rectifier.
3. Voltage regulator.
4. Smoothing capacitors.
5. Resistor.

The designed power supplies capable of supplying output current up to 1 Amp where the isolation and drive circuits need 100 m Amp current.

Plate 5.1 show a Photograph of the designed isolated power supply from the inside.

### **5-1-7 Blanking time circuit design**

In bridge circuits, where two MOSFETs are connected in series in one converter leg, it is important to provide a blanking time so that the turn-on control input to one MOSFET is delayed with respect to the turn-off control input of the other MOSFET in the inverter leg.

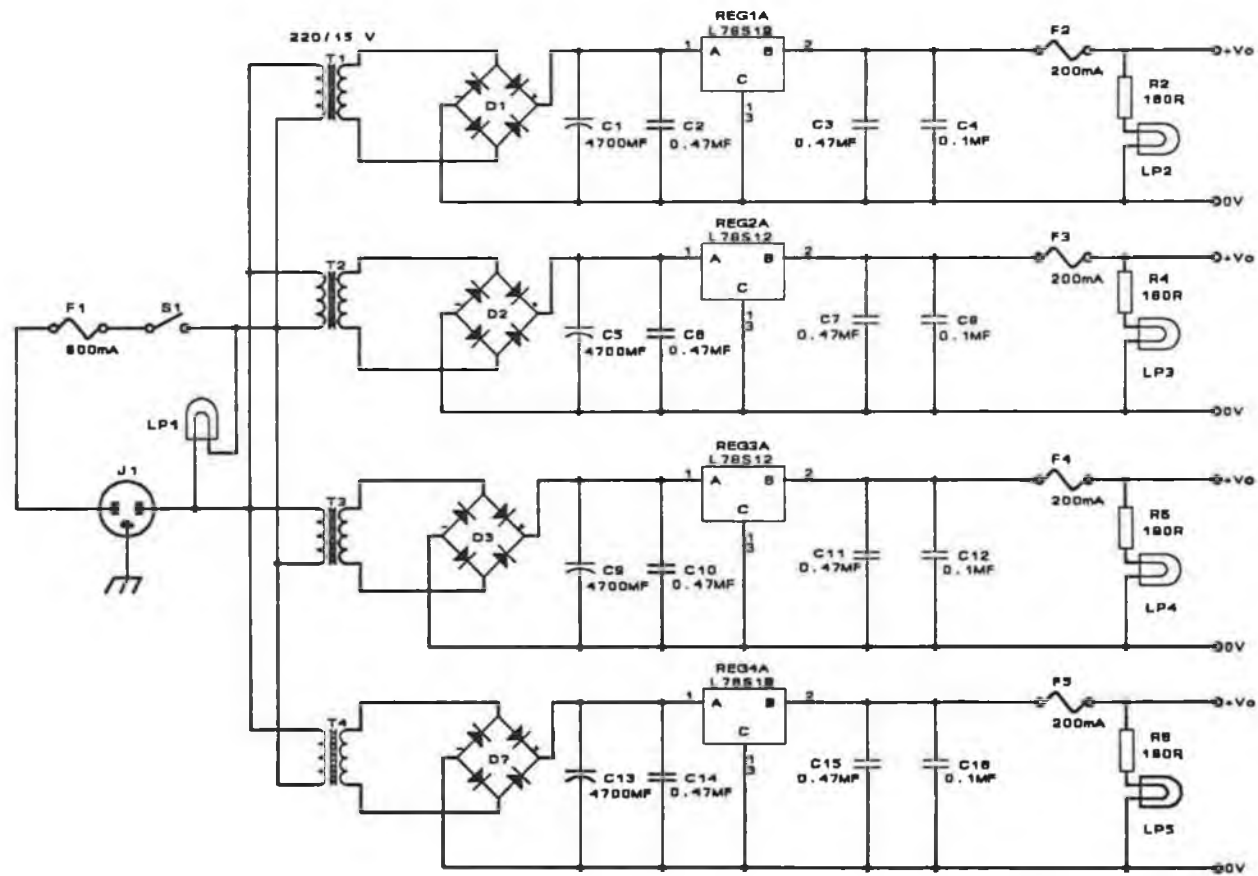


FIG. 5.9 FOUR ISOLATED POWER SUPPLIES

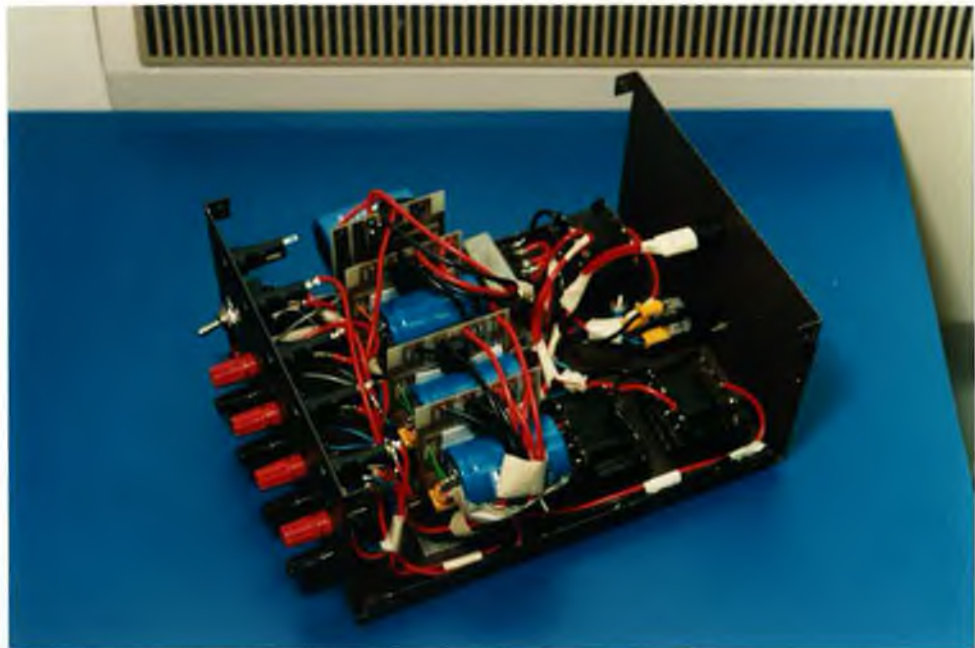


Plate 5.1 photograph of the isolated power supply (from inside).



The blanking time is chosen to be just a few microsecond under normal operation, such a conservatively chosen blanking time will cause a dead time equal to the blanking time minus the actual storage time to occur in which both the MOSFETs in the inverter leg are OFF. The effects of dead time have been described and analyzed by Evans and Close [15] and also by Murai, Watanabe, and Iwasaki [29]. Principal results in respect of harmonic performance are a reduction in the fundamental component of the inverter voltage and the addition of unwanted low order harmonics [15].

Practical solutions to minimise the unwanted effects of dead times are presented in [30]. They involve monitoring the direction of each inverter leg output current and adjusting the switching instants according to a prescribed strategy to produce an inverter output voltage waveform that is close to the ideal requirement, while maintaining switching integrity.

The blanking time in the control inputs can be introduced by means of the circuit shown in figure 5.10, where the control signal is common to both MOSFETs of the inverter leg.

When the control signal is high, the upper MOSFET should be ON and visa versa. The polarized R-C network and the schmitt triggers introduce a significant time delay [10  $\mu$ s] in the turn-on of the MOSFET and almost no time delay in turn-off of the MOSFET. The difference of these two time delays is the blanking time needed. The waveforms are shown in figure 5.11.

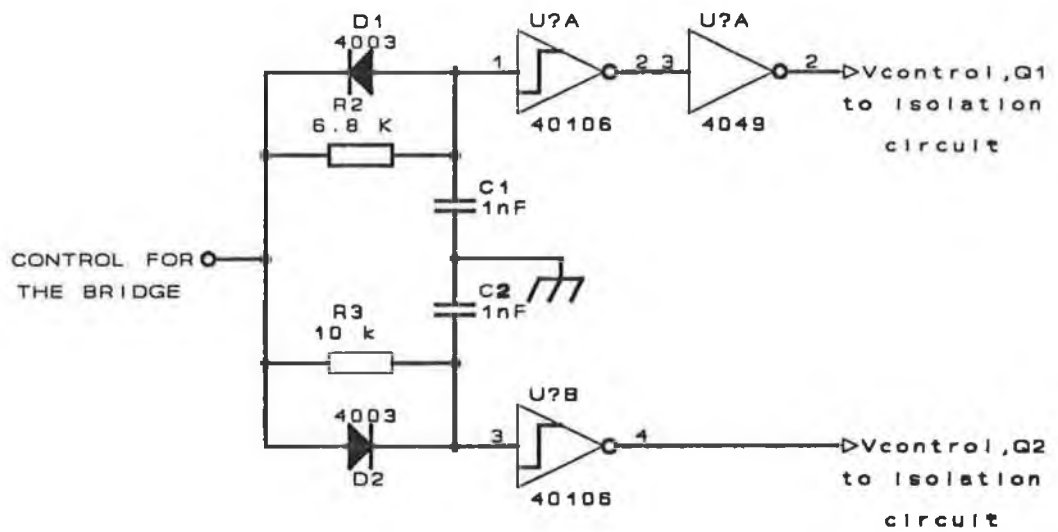


Fig. 5.10 Blanking time circuit for phase-'A' of three-phase PWM inverter.

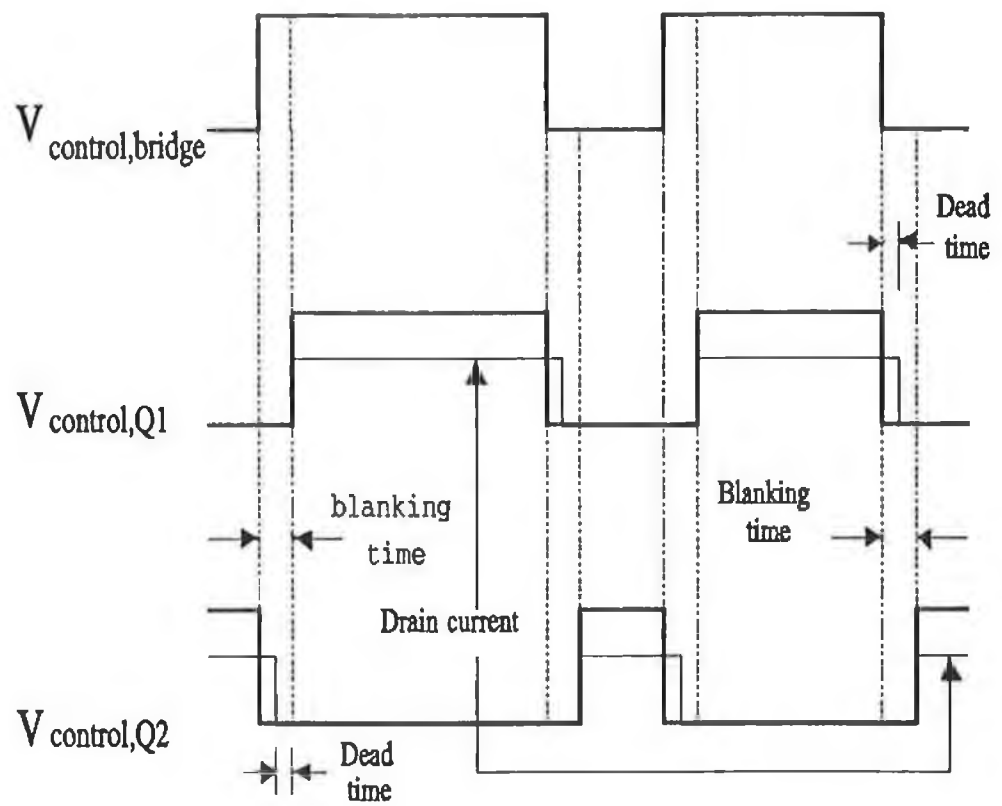


Fig. 5.11 Control signals for upper/lower inverter switches with blanking and dead times.

### **5-1-8 Breadboard construction**

Plate 5.2 shows a photograph of one-phase power circuit of PWM inverter, which contains the following:

1. Two power MOSFETs, two fast recovery diodes, and two schottky diodes.
2. Snubber circuit.
3. Gate drive circuit.
4. Isolation circuit.

All power MOSFETs, fast recovery diodes and schottky diodes are mounted on the same heat-sink with insulating material between them. This reduces the length of the power path.

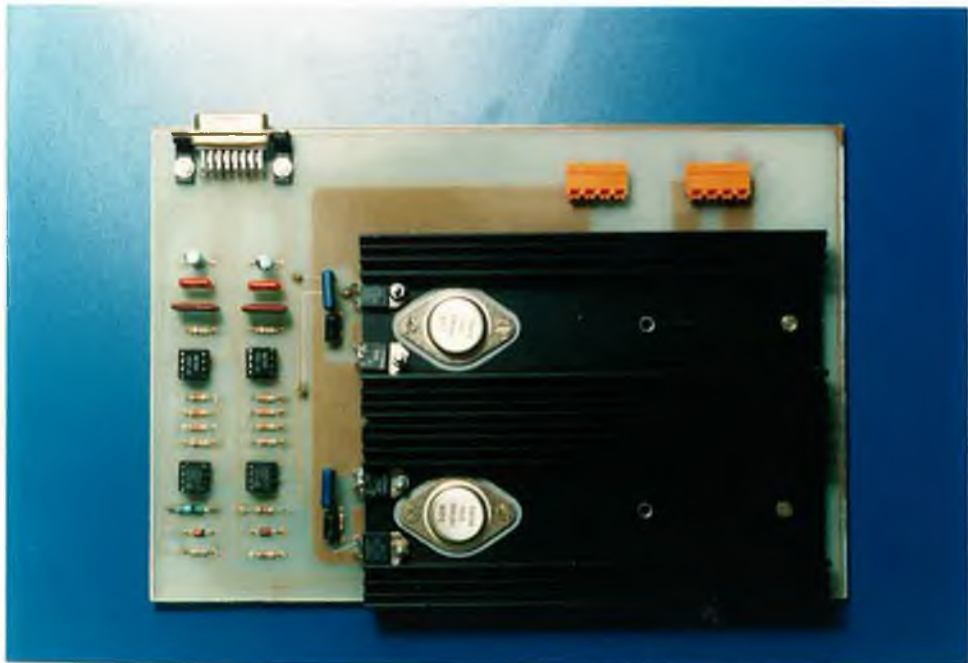


Plate 5.2 Photograph of one-phase power circuit of PWM inverter.

## 5-2 PWM CONTROL CIRCUIT DESIGN

In order to obtain balanced three-phase output voltages (400 HZ) from the three-phase PWM inverter, the MOSFET gate signals are generated by comparing the same triangular waveform signal (of fixed frequency  $f_s = 3600$  HZ) with a three sinusoidal control signals of 400 HZ and  $120^\circ$  out of phase.

In this design Natural sampled PWM has been used, because of its inherent simplicity and ease of implementation using analog techniques [31].

Figure 5.12 illustrates, in block diagram form, a very basic PWM circuit which consists of:

1. Sine and square wave generation circuit.
2. Filter circuit.
3. Three-phase sinusoidal wave generation circuit.
4. Triangular wave generation circuit.
5. Comparator circuit.

Reference 400 HZ waveform signals are generated by the sine and square wave generation circuit. The sine wave signal is applied to the filter circuit to eliminate all the harmonic components present in it. The output of the filter circuit is then applied to the three-phase sinusoidal wave generation circuit to produce a three-phase sinusoidal signals of 400 HZ, 10 V and  $120^\circ$  out of phase.

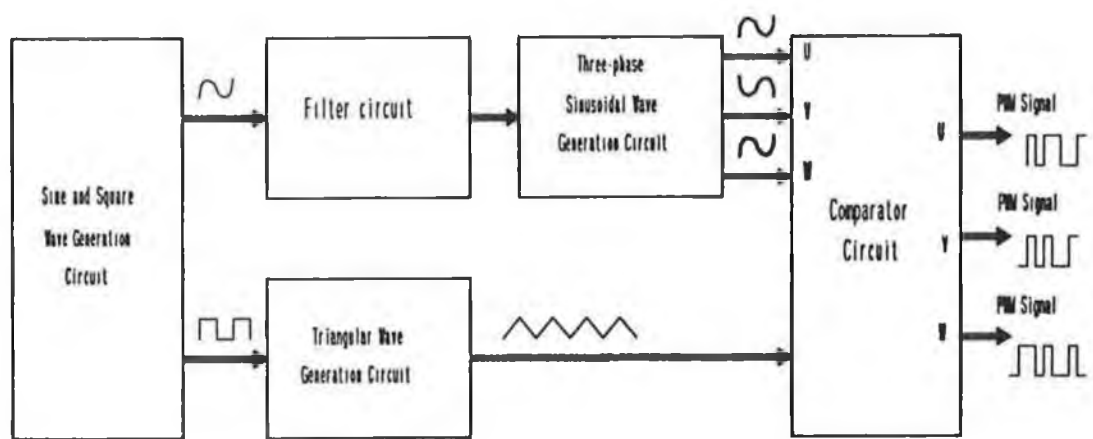


Fig. 5.12 Block circuit diagram of three-phase PWM control circuit.

However, the square waveform signal is applied to the triangular wave generation circuit to produce a synchronous triangular signal with 3600 HZ and amplitude of 10 V.

In the comparator circuit, the three-phase sinusoidal signals are compared with the synchronous triangular signal which results in the production of PWM signals. These signals causes the transistors in the inverter to turn ON or OFF.

A detailed discussions of the principle circuits of the PWM control circuits are as follow.

### 5-2-1 Sine and square waveform generation circuit

Figure 5.13 illustrates the schematic diagram and the elements arrangement for producing a sine wave signal with 400 HZ. This circuit have been using IC 8038 which is capable of producing many types of waveforms such as sine and square waveforms of high accuracy.

The frequency of this circuit can be selected externally over a range from less than 0.001 HZ to 100 KHZ and is highly stable over wide range of temperature and supply voltage. The symmetry of all waveforms can be adjusted with the external timing resistors connected to pin 4 and 5 as shown before.

The output frequency of this circuit is given by:

$$f = \frac{0.3}{R \cdot C_1} \quad \text{when } (R_A = R_B = R) \quad (10)$$

where  $R_A$  represents the connected resistor to pin 4.



$R_B$  represents the connected resistor to pin 5.

The output of this circuit are a sine wave signal with a fixed amplitude (10 V) and fixed frequency of 400 HZ at point "B" and a square wave signal with 400 HZ at point "A".

### 5-2-2 Filter circuit

The sine wave signal produced by the waveform generation circuit was had many harmonic components in it. Hence a filter circuit is required to eliminate these harmonics and so provide a pure sine wave signal.

This filter, illustrated in figure 5.14, is a cascaded arrangement of a high-pass Butterworth filter followed by a low-pass Butterworth filter. Each filter is a two-pole with a roll-off rate of 40 dB/decade.

The band-pass filter has the following specifications:

1. Bandwidth of 200 HZ.
2. Center frequency of 400 HZ.

The values of the capacitors and resistors in the circuit were calculated according to the following equations 11 and 12:

$$f_{c_1} = \frac{1}{2 \pi \sqrt{R_1 R_2 C_1 C_2}} \quad (11)$$

where  $f_{c_1}$  is the critical frequency of the high-pass filter ( $f_{c_1} = 300$  HZ).

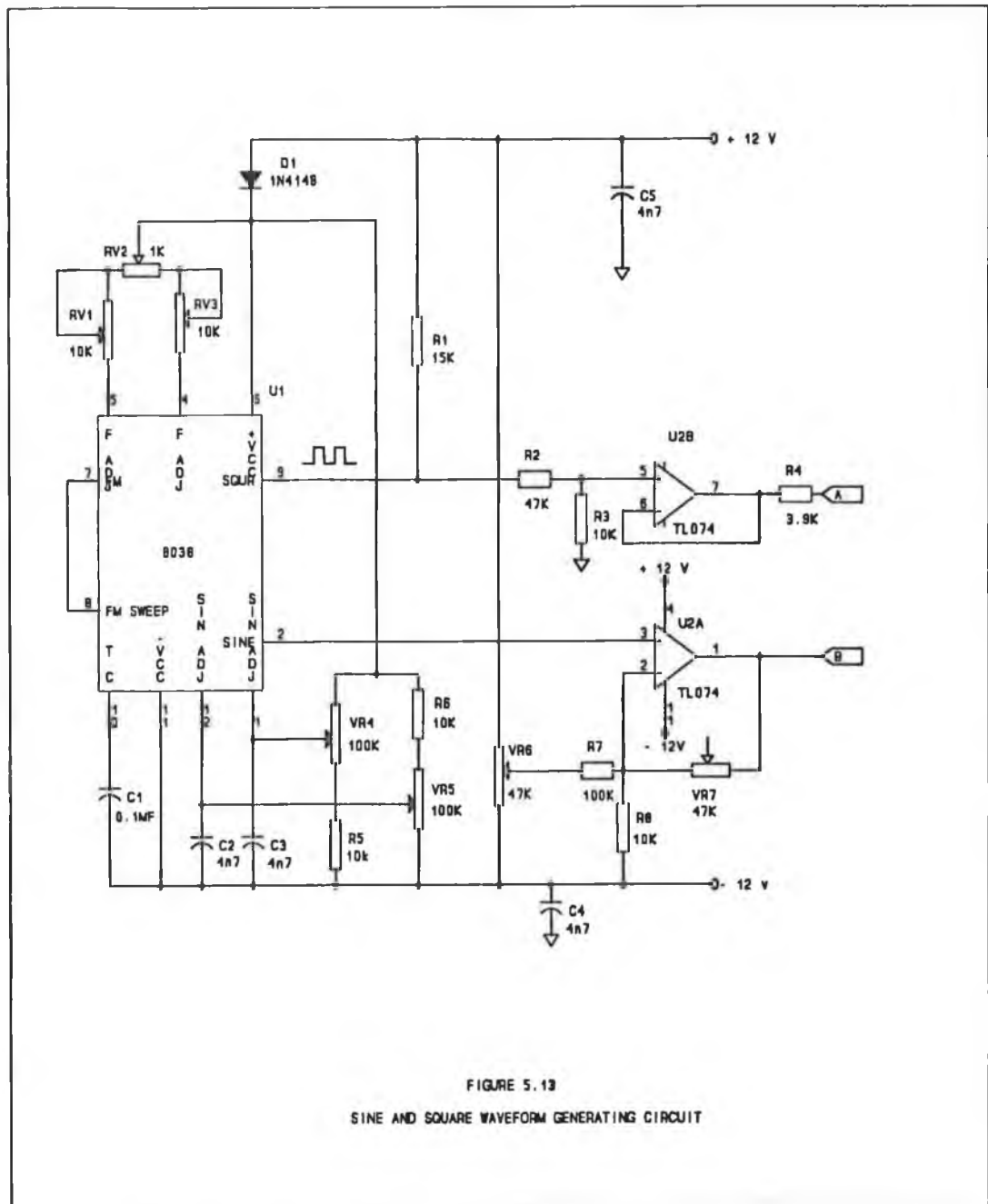


FIGURE 5.13  
SINE AND SQUARE WAVEFORM GENERATING CIRCUIT

$$R_1 = R_9 + R_{10}$$

$$R_2 = R_{11} + R_{12}$$

$$C_1 = C_6, C_2 = C_7$$

$$f_{c_2} = \frac{1}{2 \pi \sqrt{R_3 R_4 C_3 C_4}} \quad (12)$$

where  $f_{c_2}$  is the critical frequency of the low-pass filter ( $f_{c_2} = 500$  HZ).

$$R_3 = R_{13} + R_{14}$$

$$R_4 = R_{15} + R_{16}$$

$$C_3 = C_8, C_4 = C_9$$

### 5-2-3 Three-phase sinusoidal waveform generation circuit

The purpose of this circuit is to generate three-phase sinusoidal signals with 120° out of phase. These signals are compared with the triangular signal to produce the PWM signals.

Figure 5.15 illustrates the designed circuit, which contains the following sub-circuits:

1. Phase-shifter bridge (PH).
2. Inverting amplifier (U3B).
3. Summing amplifier (U3A).

Applying the reference sine wave signal ( $u_1$ ) to the phase-shifter bridge

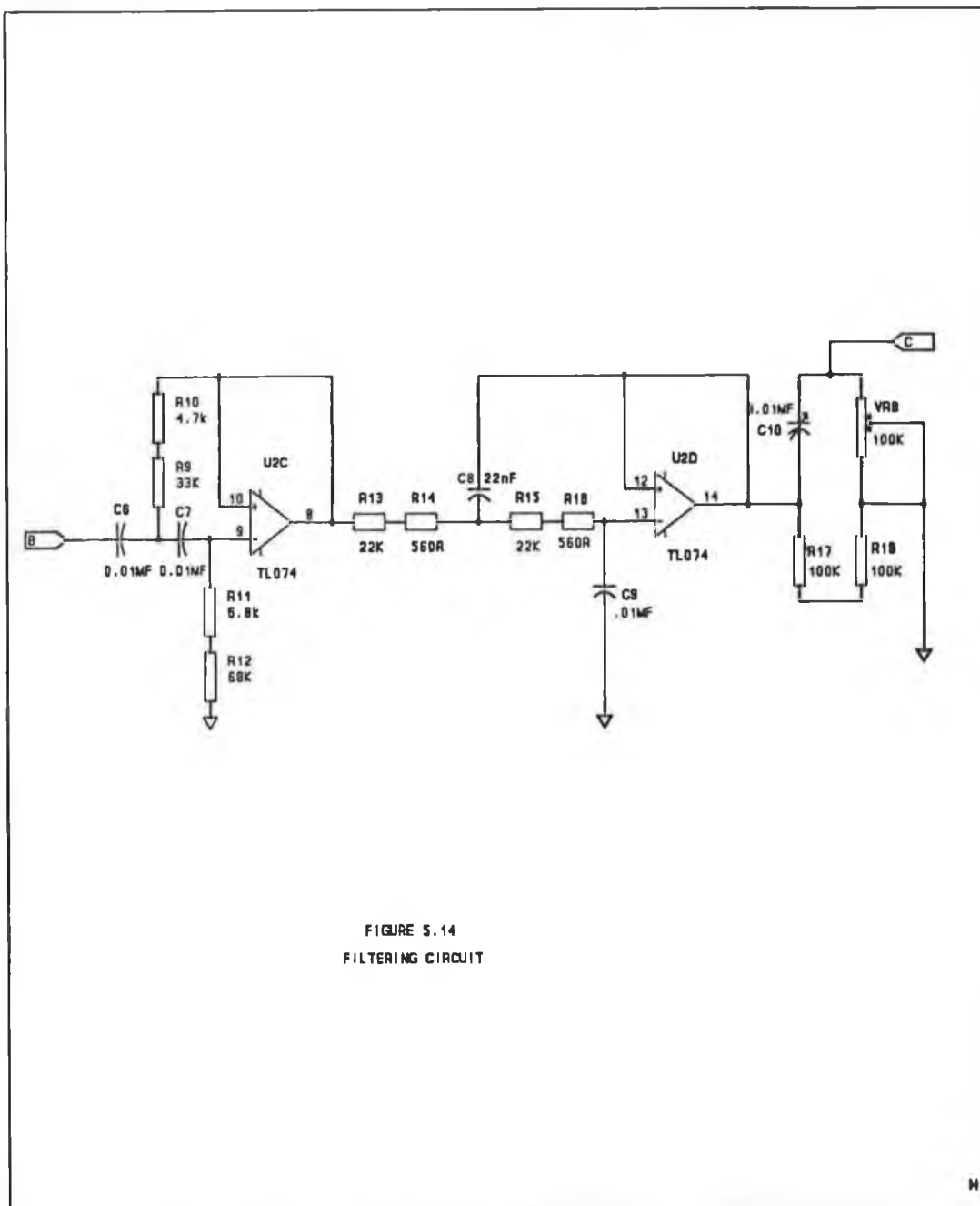


FIGURE 5.14  
FILTERING CIRCUIT

(PH) at point "A" and by manipulating the values of  $R_{v9}$  and  $C_{11}$ , a  $60^\circ$  C phase angle between the output signal ( $u_2$ ) at point "C", and the input signal  $u_1$  is obtained as shown in figure 5.16.

Using the circuit (U3B), the output signal  $u_2$  is inverted and amplified into the output signal  $u_3$  which has the same amplitude of  $u_2$  and phase angle of  $-120^\circ$  C.

The output signal ( $u_3$ ) and the output signal ( $u_4$ ) at point "D" is summed and inverted by the summing amplifier circuit (U3A). The output signal of this circuit ( $u_5$ ) has the same magnitude of  $u_3$  but with phase angle of  $+120^\circ$  C.

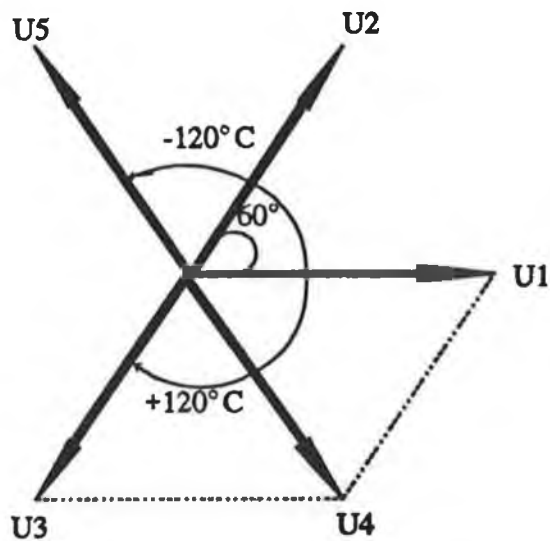


Figure 5.16 Vector diagram

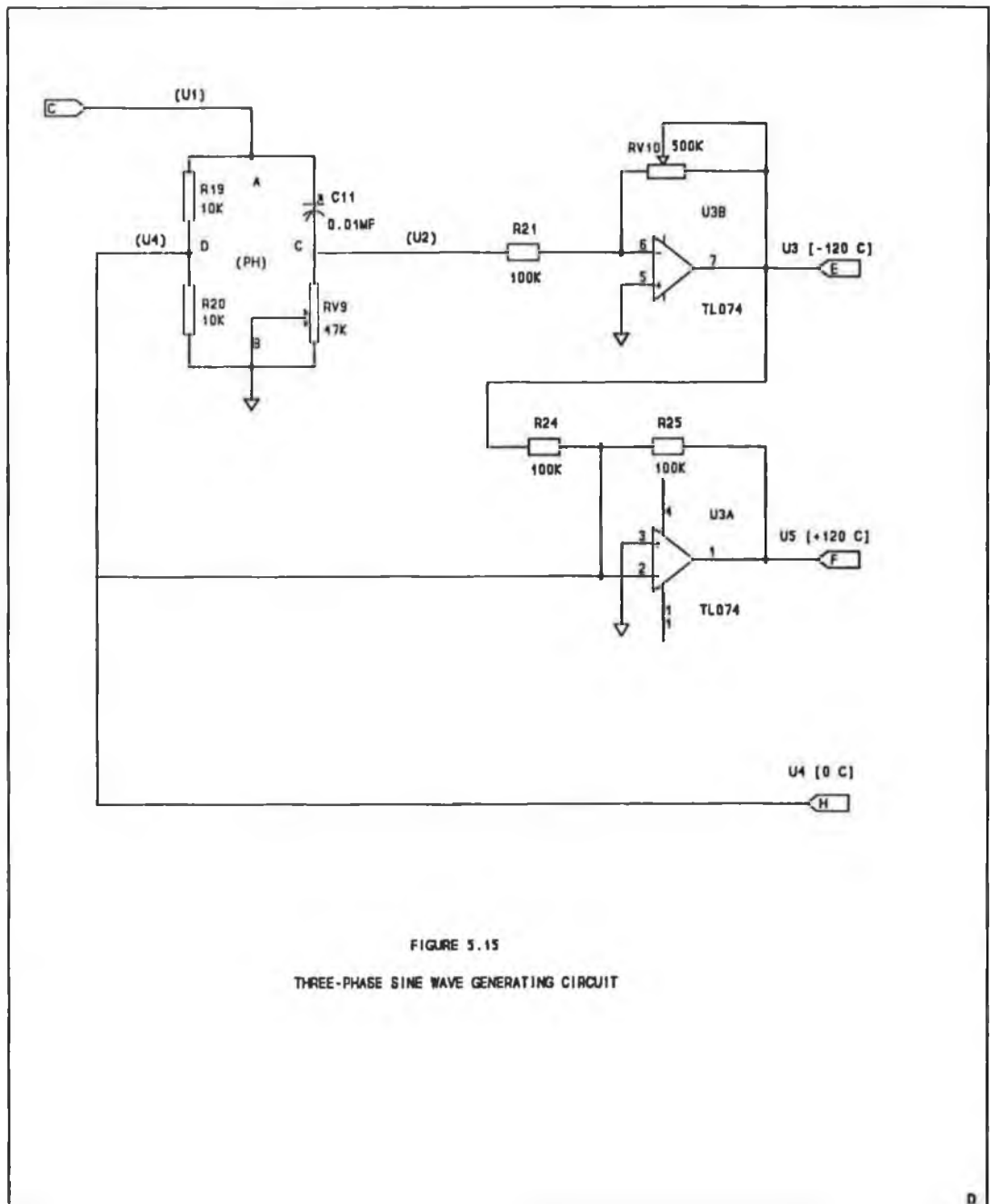


FIGURE 5.15  
THREE-PHASE SINE WAVE GENERATING CIRCUIT

Plate 5.3 shows a photograph of the actual designed PC board, which contains the following:

1. Sine and square wave generation circuit.
2. Filter circuit.
3. Three-phase sinusoidal waveform generation circuit.

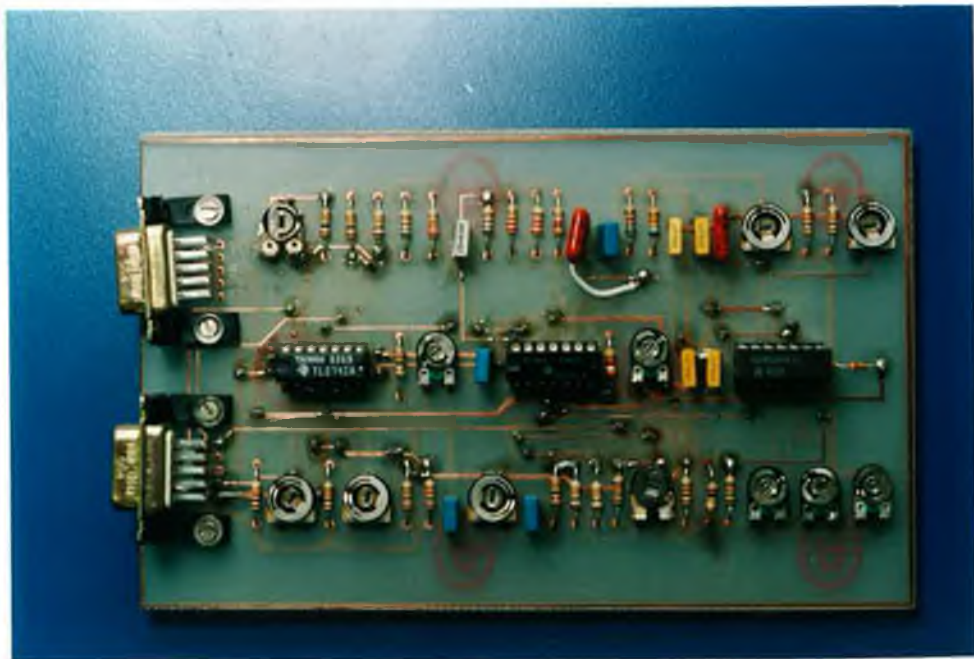


Plate 5.3 Photograph of the actual PC board of the sine and square wave, filter and three-phase sinusoidal wave generation circuits.



#### 5-2-4 Triangular waveform generation circuit

The purpose of this circuit is to generate a triangular waveform signal with a frequency of 3600 HZ, synchronized to the sine reference.

Figure 5.17 illustrates the designed circuit. It uses a Phase Locked Loop (NE 565) and a counter (14520).<sup>2</sup>

The NE 565 Phase Locked Loop (PLL) comprises a voltage-controlled oscillator (VCO) of exceptional stability and linearity, a phase comparator, an amplifier and low-pass filter. The center frequency of the PLL is determined by the free-running frequency of the VCO; this frequency can be adjusted externally with the resistor  $RV_{13}$  or the capacitor  $C_{13}$ . The VCO free-running frequency is given by:

$$f_o = \frac{1.2}{4 RV_{13} C_{13}}$$

The signal from the square wave generation circuit is feed as an input to a phase locked loop (PLL). The PLL voltage controlled oscillator (VCO) square wave output is divided in frequency by 9 (the number of output switching in one cycle of input) and feed back as square wave to the second input of the PLL phase comparator. This ensures the availability of a phase locked triangular wave output from the PLL VCO second output, with 9 times the line frequency.

---

<sup>2</sup>Another method was tried to generate a synchronizes triangular wave signal. The method use an integrator circuit to integrate the square wave signal. The result showed that, there was no good synchronizing between the triangular and sine wane signals.

The output of this circuit is an isosceles triangular of fixed amplitude (10 V) whose frequency is an integer triple multiple ( $m_s = 9$ ) of desired inverter output frequency ( $f_1 = 400$  HZ).

The reason of using the switching frequency of 9 was to eliminate the triplen harmonics in the inverter output waveform voltages.

Plate 5.4 shows a photograph of the actual PC board of the triangular wave signal generation circuit.

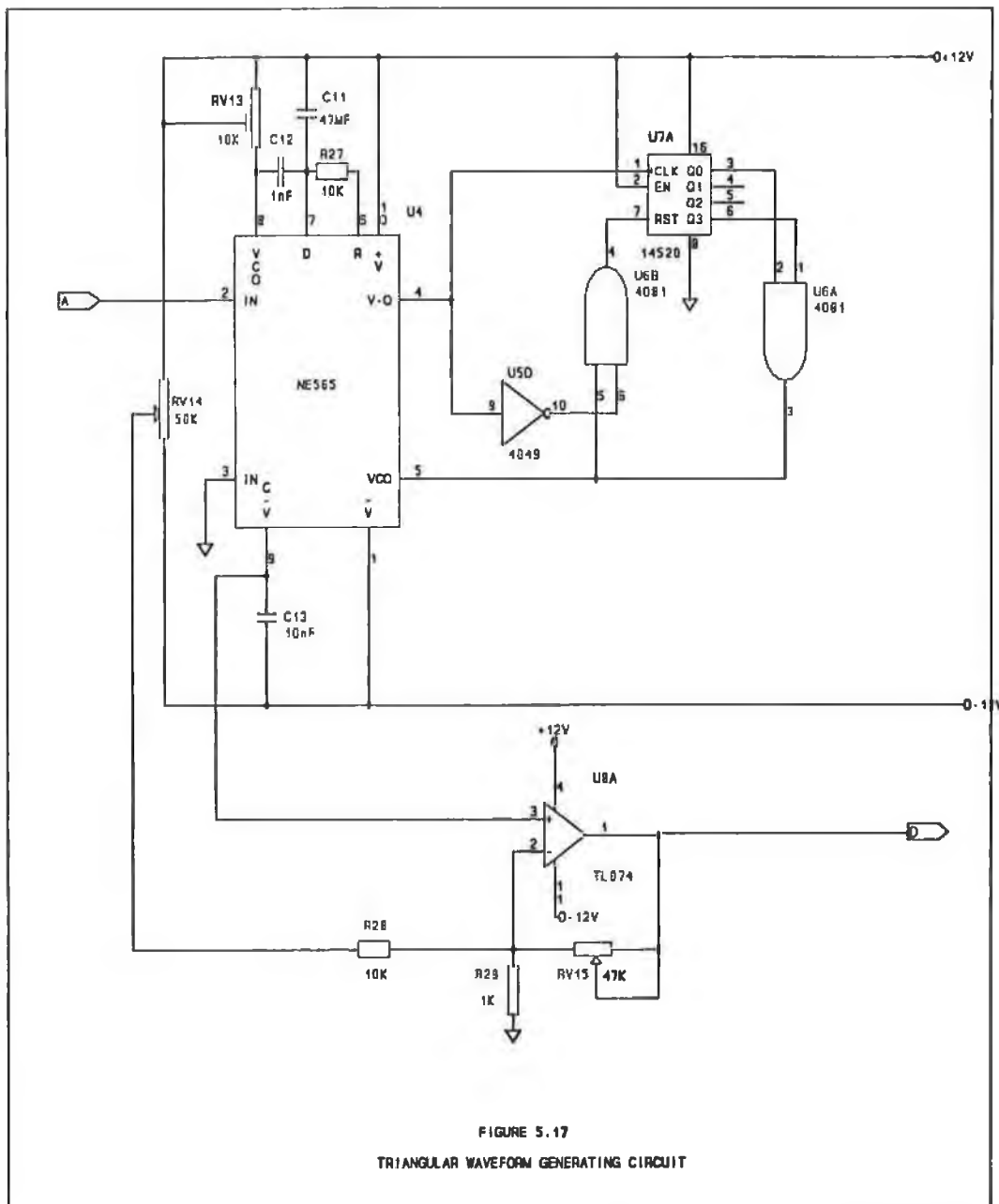


FIGURE 5.17  
TRIANGULAR WAVEFORM GENERATING CIRCUIT

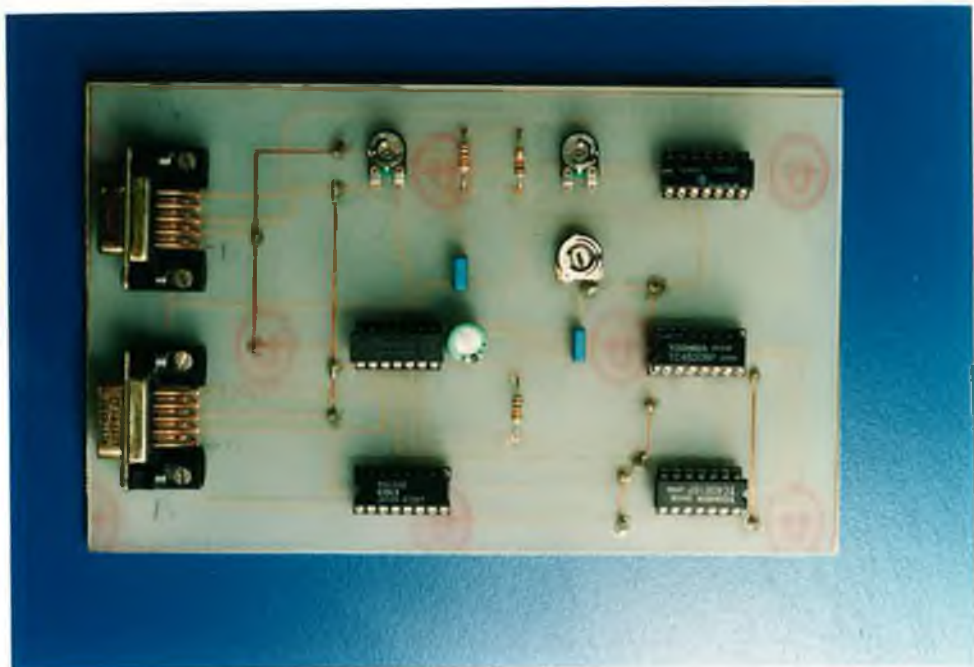


Plate 5.4 Photograph of the actual PC board of the triangular waveform generation circuit.

### 5-2-5 Comparator circuits

In order to obtain the conduction pulse pattern for each MOSFET within its  $120^\circ$  period, three comparator circuits were used. In the comparator circuits, the three sinusoidal reference signals are compared with the synchronized triangular signal.

Figure 5.18 shows one of the three comparators (LM 311) of the designed circuit.

Plate 5.5 shows a Photograph of the actual PC board of the comparator and the blanking circuit<sup>3</sup>.

Plate 5.6 shows a photograph of the power and PWM control circuits (three-phase PWM inverter) which have been assembled together in one box.

---

<sup>3</sup> Blanking circuit was described in power circuit design.

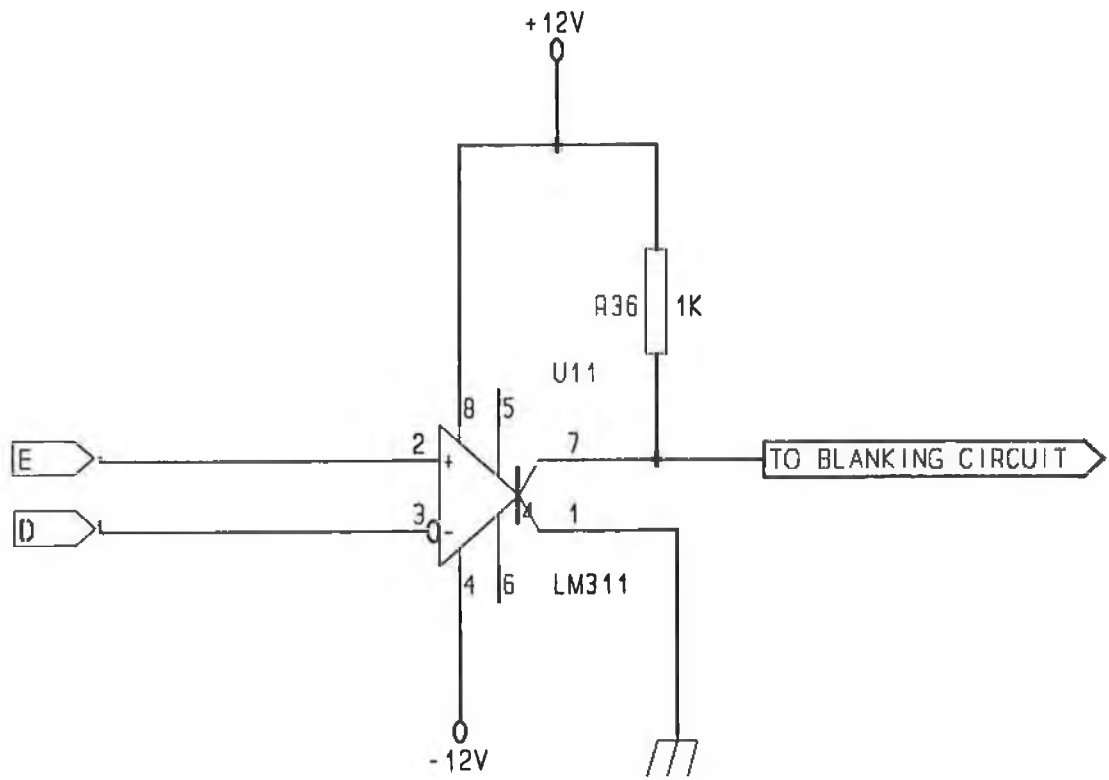
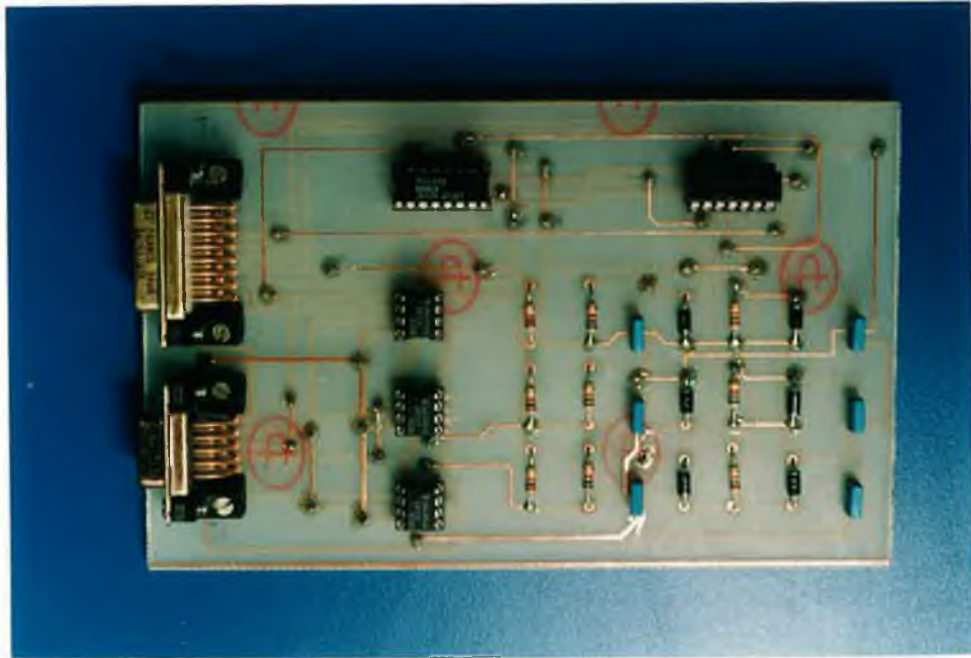


FIGURE 5.18  
COMPARATING CIRCUIT



**Plate 5.5** Photograph of the actual PC board of the comparator circuit and blanking circuit.

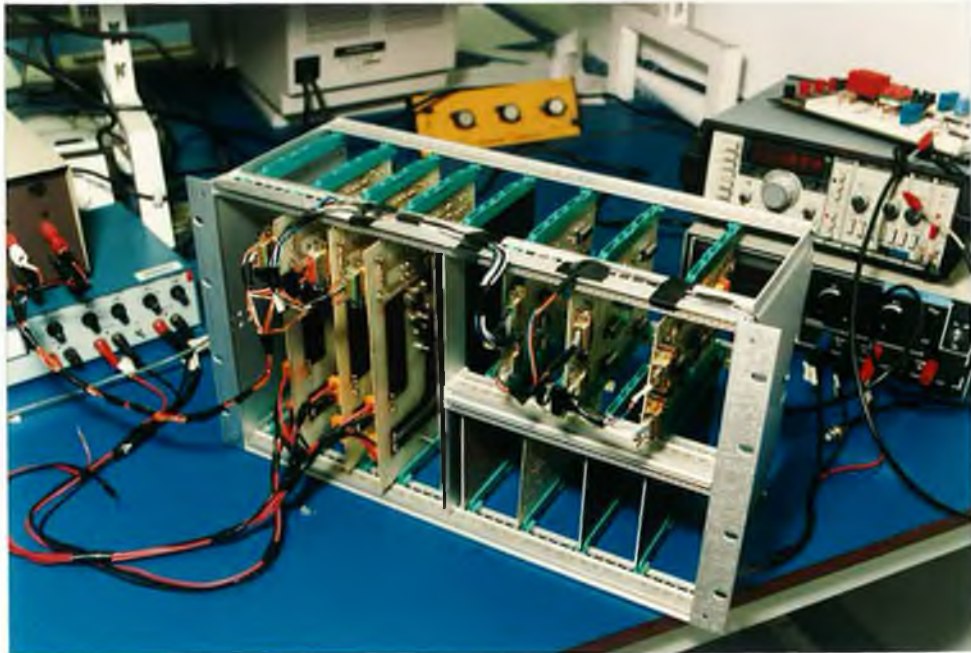


Plate 5.6 Photograph of the three-phase PWM inverter (power and control circuits together in one box).



# CHAPTER 6

## POWER HARMONIC FILTER

### 6-1 INTRODUCTION

A power-harmonic filter is needed to eliminate the harmonics in the PWM three-phase inverter outputs. Power-harmonic filters can be classified into:

1. Harmonic-voltage suppression filters.
2. Harmonic-current absorption filters.

Harmonic-voltage suppression filters are typically employed at the output of inverters for uninterruptible power supplies (UPS) and solid-state converters [32,33] to control the total harmonic distortion (THD) of the output terminal voltage.

Harmonic-current absorption filters are typically found at the input terminal of a solid-state converters where the filter absorbs the input current harmonics. By so doing, the harmonic currents are prevented from passing into the electric-supply system and producing harmonic voltages [34].

A number of filter configurations [35,36] are currently in use depending on the application; all use passive components, such as inductors and capacitors.

In this chapter, both the inverter output voltage (filter input voltage)

and the filter output voltage will be analyzed. Then, an appropriate filter design procedure for the PWM inverter will be presented. Finally, the design of the power inductor of this filter will be carefully explained in detail.

## 6-2 ANALYSIS OF THE INVERTER OUTPUT VOLTAGE (FILTER INPUT )

The inverter output voltage will contain voltage components at harmonic frequencies of  $f_s$  (3600 HZ).

The harmonic spectrum of the output voltage has the significant components as follows:

1. The fundamental frequency component.
2. A number of harmonics centred around the switching frequency  $f_s$  (3600 HZ) and its multiples.

The peak amplitude of the fundamental frequency component of the output voltage  $(V_o)_1$  is  $m_a$  times of  $V_d/2$  that is,

$$(V_o)_1 = m_a \frac{V_d}{2} \quad (m_a \leq 1.0) \quad (1)$$

The number of harmonics appear as sidebands, centred around the switching frequency and its multiples, that is, around harmonics  $m_r$ ,  $2m_r$ ,  $3m_r$  and so on [12].

The harmonic amplitudes are almost independent of  $m_r$  for all frequency modulation ratio  $m_r \geq 9$ , though  $m_r$  defines the frequencies at

which that occur. Theoretically, the frequencies at which voltage harmonics occur can be indicated as [12]:

$$f_h = (j m_f \pm K) f_1 \quad (2)$$

that is, the harmonic order  $h$  corresponds to the  $K$  th sideband of the  $j$  times the frequency-modulation ratio  $m_f$ :

$$h = j ( m_f ) \pm K \quad (3)$$

where the fundamental frequency corresponds to  $h = 1$ . For odd values of  $j$ , the harmonics exist only for even values of  $K$ . For even values of  $j$ , the harmonics exist only for odd values of  $K$ .

In table 6.1 [12], the normalized harmonics  $(V_o)_h/(V_d/2)$  are tabulated as a function of the amplitude modulation ratio  $ma$ , (assuming  $m_f \geq 9$ ). Only those with significant amplitudes up to  $j= 4$ .

h	$m_a$	0.2	0.4	0.6	0.8	1.0
1 fundamental		0.2	0.4	0.6	0.8	1.0
$m_r$		1.242	1.15	1.006	0.818	0.601
$m_r \pm 2$		0.016	0.061	0.131	0.220	0.318
$m_r \pm 4$						0.018
$2m_r \pm 1$		0.190	0.326	0.370	0.314	0.181
$2m_r \pm 3$			0.024	0.071	0.139	0.212
$2m_r \pm 5$					0.013	0.033
$3m_r$		0.335	0.123	0.083	0.171	0.113
$3m_r \pm 2$		0.044	0.139	0.203	0.176	0.062
$3m_r \pm 4$			0.012	0.047	0.104	0.157
$3m_r \pm 6$					0.016	0.044
$4m_r \pm 1$		0.163	0.157	0.008	0.105	0.068
$4m_r \pm 3$		0.012	0.070	0.132	0.115	0.009
$4m_r \pm 5$				0.034	0.084	0.119

Table 6.1 Generalized Harmonics of  $V_o$  for a Large  $m_r$ .  $V_o/V_d$  is tabulated as a function of  $m_a$ .

To get 115 V ac as output voltage of the inverter, the input voltage should be  $V_d = 326$  V (when  $m_a = 1$ ). From this assumption and from table 6.1, the rms values of the fundamental frequency voltage and some harmonics in  $V_o$  is calculated by using equation 4 [12].

$$\begin{aligned}
(V_o)_h &= \frac{1}{\sqrt{2}} \frac{V_d}{2} \left[ \frac{(V_o)_h}{\left(\frac{V_d}{2}\right)} \right] \\
&= \frac{1}{\sqrt{2}} \frac{236}{2} \left[ \frac{(V_o)_h}{\left(\frac{V_d}{2}\right)} \right] \\
&= 115.2 \left[ \frac{(V_o)_h}{\left(\frac{V_d}{2}\right)} \right]
\end{aligned}
\tag{4}$$

Figure 6.1 shows the harmonic voltages as function of frequencies.

# HARMONIC VOLTAGES

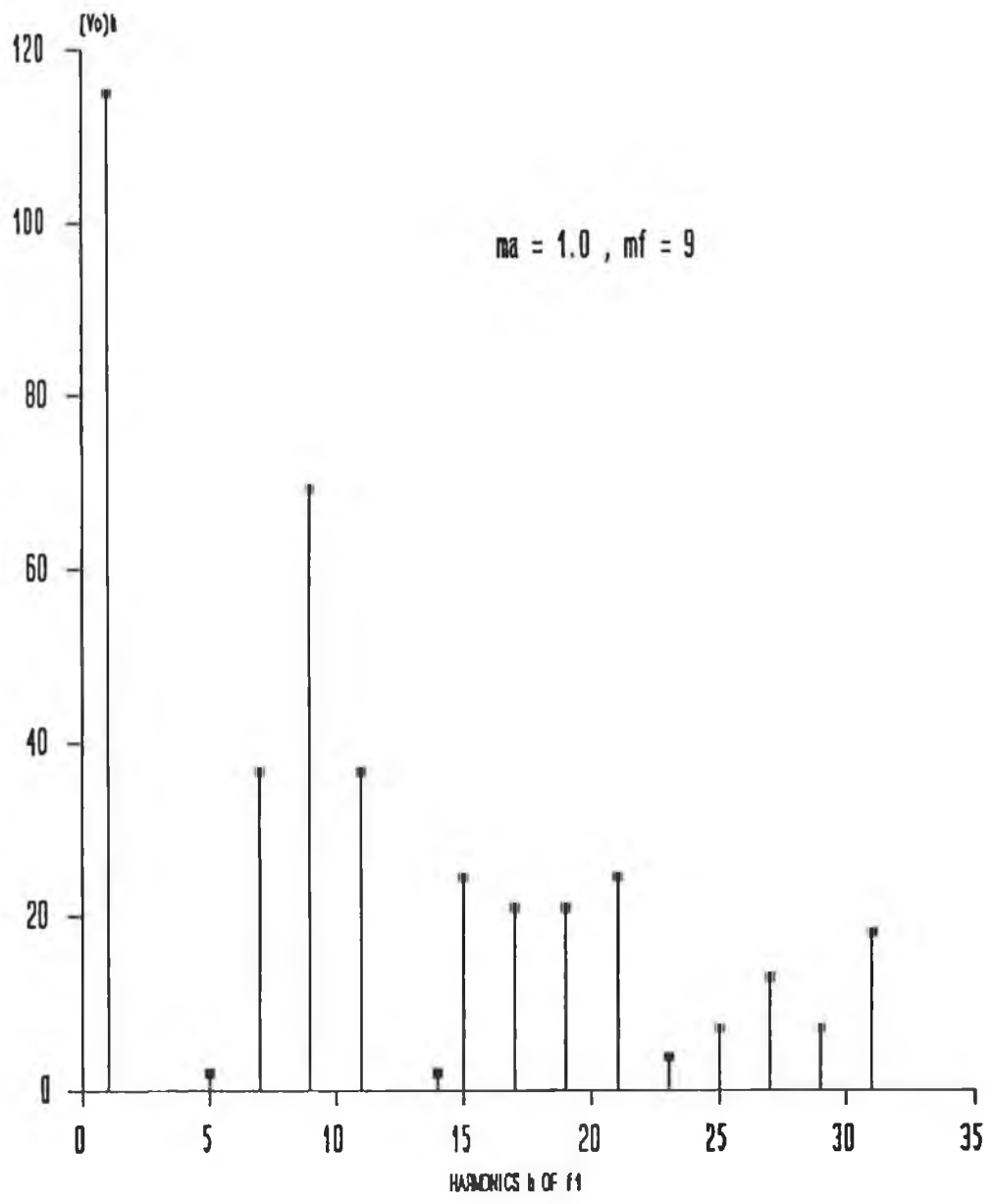


FIG. 6.1

### **6-3 ANALYSIS OF THE FILTER OUTPUT VOLTAGE**

The output voltages of the filter with cut off frequency of 1000 HZ has been calculated theoretically by using a computer program (Appendix B). Fig. 6.2, 6.3 and 6.4 show the variation of the frequency with output and input voltage of one-pole low-pass LC filter with roll off of -20 dB/dec, two-pole low-pass LC filter with roll off of -40 dB/dec and three-pole low-pass LC filter with -60 dB/dec respectively.

# FREQUENCY RESPONSE OF SINGLE LOW-PASS LC FILTER

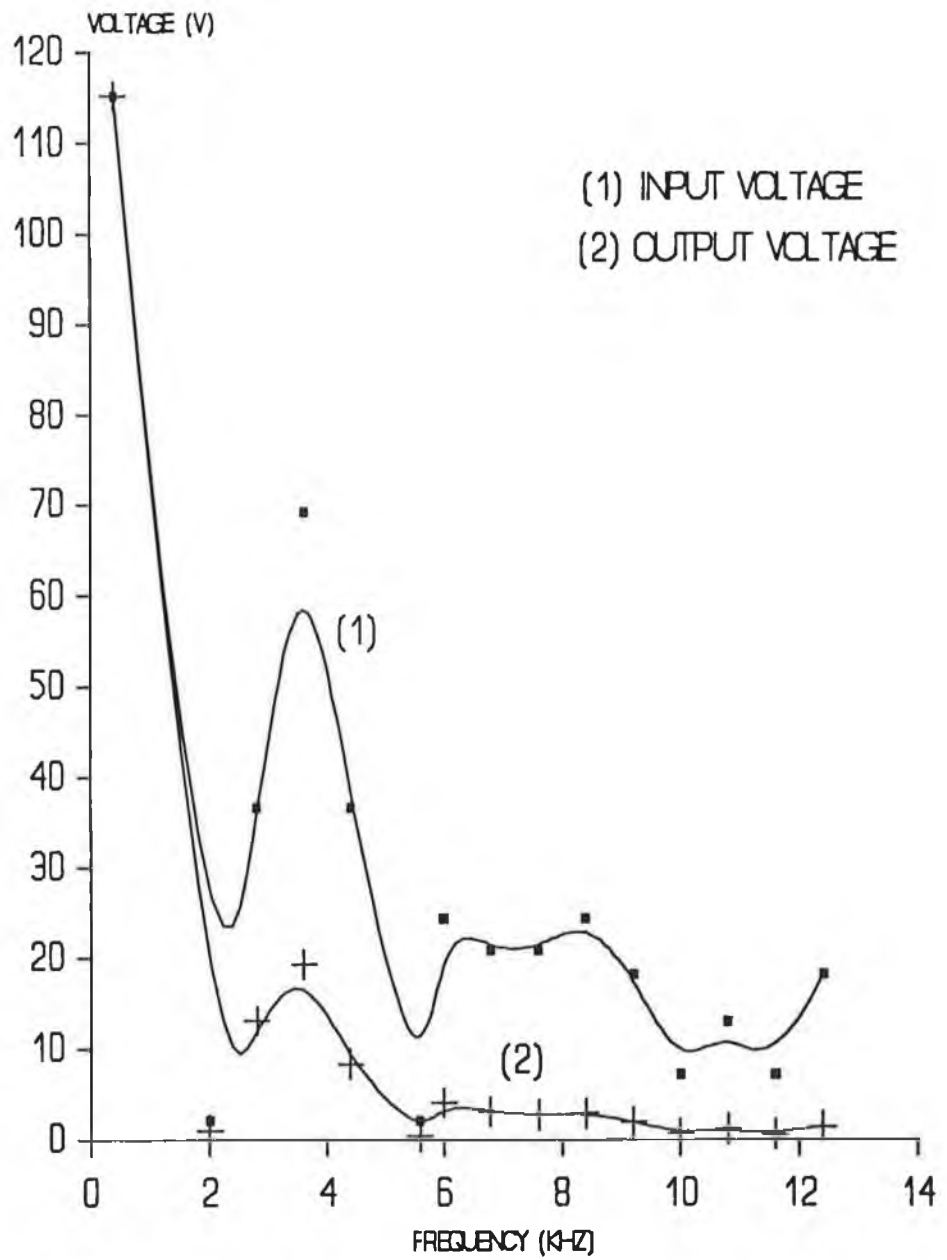


Fig. 6.2

The total harmonic distortion for this filter is 58 %.



## FREQUENCY RESPONSE OF TWO-POLE LOW-PASS LC FILTER

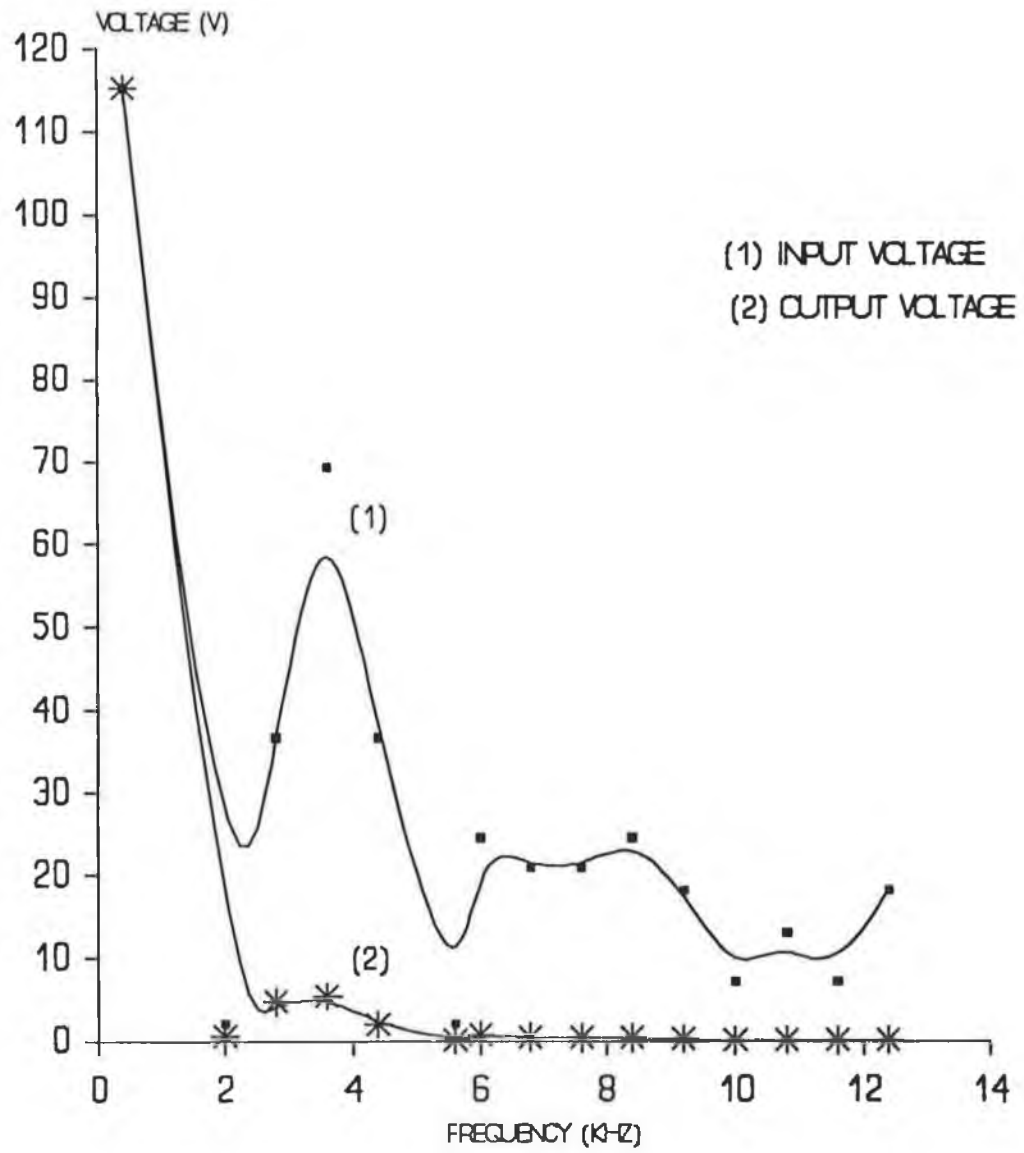


FIG. 6.3

The total harmonic distortion for this filter is 12 %.

### FREQUENCY RESPONSE OF THREE-POLE LOW-PASS LC FILTER

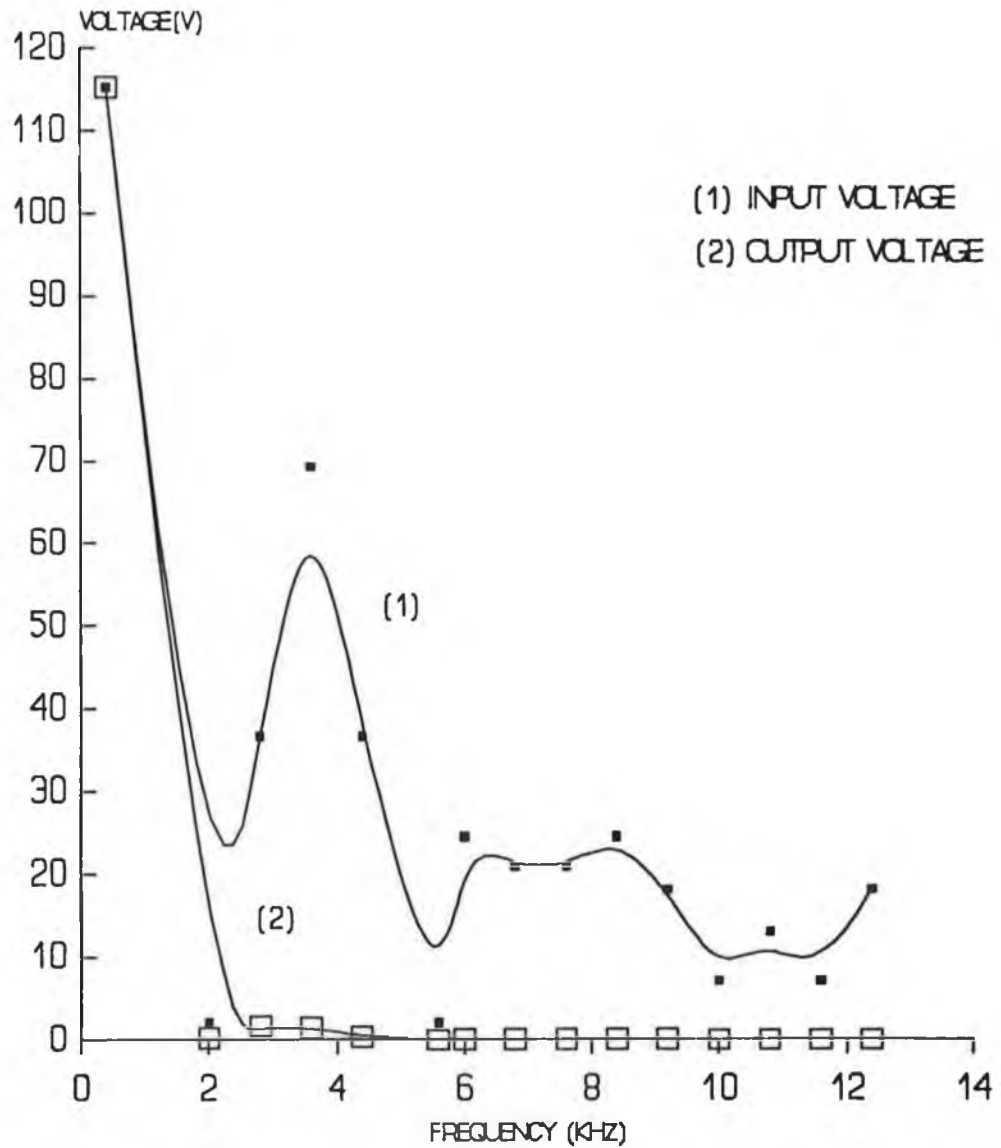


FIG. 6.4

The total harmonic distortion for this filter is 3.5 %.

## 6-4 FILTER DESIGN

To attenuate all the harmonics in the PWM inverter output voltage to an acceptable level, it is desirable to use three-pole LC filter with cutoff frequency  $f_c = 750$  Hz at the output of the inverter (one for each phase) as shown in figure 6.5.

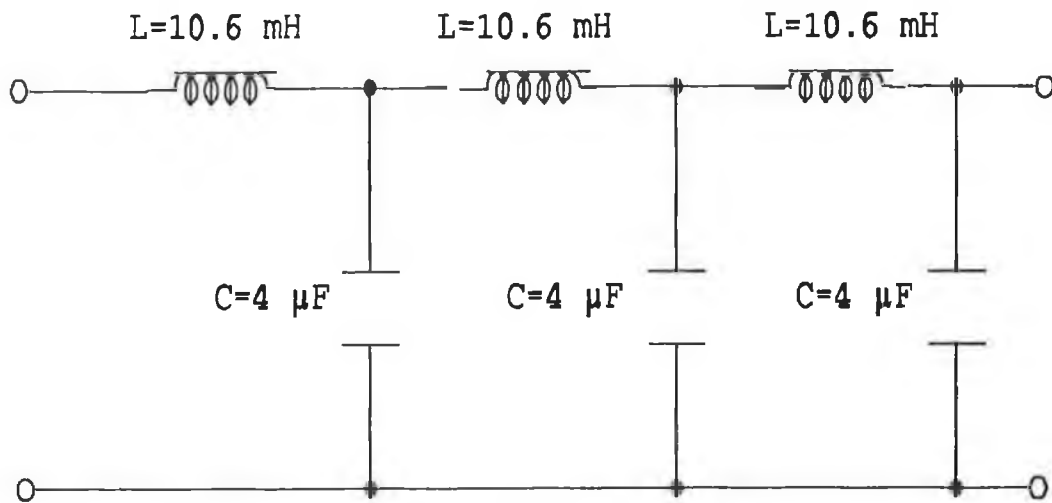


Figure 6.5 Three-pole low-pass LC filter

The filter design must satisfy the following specifications [36]:

1. The total harmonic distortion (THD) content of the filter output voltage  $V_o$  is less than five percent at rated load and no load. the THD is calculated as following:

$$THD = \left[ \sum_{\substack{n=3 \\ n=\text{odd only}}}^{\infty} \left( \frac{V_{on}}{V_{o1}} \right)^2 \right]^{1/2} \quad (5)$$

2. The output filter provides the least possible attenuation to the fundamental harmonic of the input voltage.

3. The filter must achieve the desired attenuation of harmonic components within the anticipated effects of temperature on the components, and change in the fundamental line frequency.

The cutoff frequency of this filter is determined by the values of the inductance and the capacitance of the filter when  $X_L = X_C$ , so the cutoff frequency is given as:

$$f_c = \frac{1}{2 \pi \sqrt{L C}} \quad (6)$$

#### 6-4-1 Filter capacitors

The value of C is chosen on the basis of frequency response considerations, but the type of capacitor chosen is based on voltage ripple specifications, where

$$V_{\text{ripple}} = I_{\text{ripple}} (Z_{\text{ESR}} + Z_{\text{ESL}} + Z_C) \quad (7)$$

where

ESR is the equivalent series resistance of the capacitor.

ESL is the equivalent series inductance of the capacitor.

The output ripple is not only dependent on the value of the capacitor desired, but on the ESR, ESL, and frequency characteristics of the type of capacitor chosen.

To reduce these effects, we have to use low ESR switching grade capacitors (tantalum) and parallel two capacitors of half the value. This effectively parallels the resistive and inductive equivalent elements thus halving their values. Also the power dissipated in the ESR is distributed between two capacitors thus reducing their heating and extending their lives.

#### **6-4-2 Power inductor design**

It should be borne in mind that there is a straight-forward method to design an efficient power inductor [37]. This method comprises the following steps:

1. Select the core material.
2. Select the minimum-sized magnet wire.
3. Select the minimum-sized core.
4. Determine the number of turns.

##### **6-4-2-1 Select the core material**

The core material can be selected from the hundreds of magnetic materials available.

To pick the right core material, we need to know:

- \* The required frequency  $f$ .

- \* The maximum operating temperature  $T_m$ .
- \* The core properties we need.
- \* The core geometry.

There are a variety of cores that can be used in the design of inductors, the most popular materials used in present-day high frequency switching designs are ferrite cores, iron powder cores, and molypermalloy (MPP) cores. All of these cores are good for power inductor designs [38].

Iron powder and MPP cores are generally offered in toroid forms, and they are well suited for power chokes because of the following characteristics:

1. High saturation flux density.
2. High energy storage capability.
3. Inherent air gap eliminates the need of gapping the core.
4. Wide choice of sizes.

Ferrite cores, on the other hand, have to be gapped because of their low saturation flux density, they are more temperature sensitive, and they tend to be bulkier. But ferrite cores are easier to wind especially if heavy-gauge wire is involved.

#### **6-4-2-2 Select the minimum-sized magnet wire**

The size of the magnet wire is limited by its current rating  $I_r$ , where:

$$I_r = I_{eff} + I_{dc} \quad (8)$$

Where:

$I_{\text{eff}}$  is the total effective ac.

$I_{\text{dc}}$  is the dc offset or bias.

The usual current rating for copper wire used in standard house wiring are not realistic for a power inductor. Rating based on a current density of 1000 circular mils/A causes a 20 % voltage drop per 100 ft.

Instead the current rating for industrial and military inductors are based on more practical considerations such as the maximum temperature rise. Since these ratings range typically from 5 to 20 % of the wire's fusing current, rating the inductor wire at 10 % of its fusing current is realistic. This rating applies at  $T_m$ .

At 20 C°, the fusing current for bare-copper magnet wire of diameter  $d_o$  is found by:

$$I_f = 10.244 d_o^3 \quad (9)$$

as the result, the current rating at 20 C° is:

$$I_{ro} = 0.1 I_f \quad (9)$$

Furthermore, for a required  $I_r$ , the magnet wire's minimum current rating at 20 C° must be

$$I_{ro} = I_r [1 + 0.00393 (T_m - 20)] \quad (10)$$

Current rating for copper magnet wire, based on eq. 10 are shown in appendix C along with other selected magnet-wire design data.

### 6-4-2-3 Select the minimum-sized core

The minimum-sized core can be selected by calculating  $Wa$  product of the core. The  $Wa$  product can be calculated by using the basic equation of power capability of transformer [39] as follows:

$$P = 4.55 J f W a B 10^{-8} \quad (12)$$

where:

$J$  is the current density in amperes per square inches.

$f$  is the frequency in hertz.

$W$  is the area of the core window in square inches.

$a$  is the cross-sectional area of the core in square inches.

$B$  is the flux density in gauss.

$P$  is the power in volt-ampere.

The current density can be stated in circular mils per ampere with the dimensions in inches and flux density in gauss. using  $S$  to denote this quantity, the equation (12) becomes:

$$P = \frac{f B W a}{17.26 S} \quad (13)$$

From eq. (13)  $Wa$  can be calculated as following :

$$Wa = \frac{17.26 S P}{f B} \quad (14)$$

The  $Wa$  product is usually given for each core in the catalogue.



#### 6-4-2-4 Determine the number of turns

The number of turns  $N$  of the inductor, can be determine by using the following equation:

$$N = \sqrt{\frac{l L 10^{-8}}{3.19 a \mu}} \quad (15)$$

where:

$N$  is the number of turns of the inductor.

$\mu$  is the core permeability at the appropriate flux density.

$a$  is the core cross-sectional area in square inches.

$L$  is the inductance of the inductor in henry.

$l$  is the mean magnetic path length in inches.

#### 6-4-2-5 Design calculations

The power inductor must meet the following requirements:

- The output current is 10 A at 400 HZ (according to inverter design).
- The inductance is 10.6 mH (according to eq. 6 at  $f_c = 750$ ,  $C = 4\mu\text{F}$ ).
- The rms voltage is 115 V at 3600 HZ (from measurements).
- The current density  $S$  is 400 C.M/A (according to ref. [8]).

Radiometal 48 (nickel iron alloy) is chosen for the core material because, it has very high operating flux density and high operating temperature. This material has the following specifications (Appendix D):

- The saturation flux density  $B_s$  is 16000 Gauss.
- The residual flux density  $B_r$  is 10000 Gauss.

- The initial permeability  $\mu_i$  is 8000.
- The maximum operating temperature  $T_m$  is 450 C°.

From the above requirements, the minimum-sized magnet wire, the  $W_a$  product and the number of turns of the inductor can be calculated as follows:

#### **6-4-2-5-1 The minimum-sized magnet wire calculation**

With 80 C° value of  $T_m$ , the magnet wire's minimum current rating at 20 C° can be calculated using eq. 11 as following:

$$I_{r_o} = 10 [ 1 + 00.393 ( 80 - 20 ) ]$$

$$= 12.358 \text{ A.}$$

From the data in appendix B, the thinnest wire that can accommodate  $I_{r_o}$  is AWG 15.

#### **6-4-2-5-2 The $W_a$ product calculation**

By substituting the values of  $p$ ,  $s$ ,  $f$ , and  $B$  into eq. 14 the  $W_a$  product can be calculated. Where:

$$p = V_o \times I_o = 115 \times 10 = 1150 \text{ VA.}$$

$$f = 3600 \text{ hz.}$$

$$B = B_s - B_r = 16000 - 10000 = 6000 \text{ Gauss.}$$

$$S = 400 \text{ C.M/A}$$

therefore:

$$Wa = \frac{17.26 \times 400 \times 1150}{3600 \times 6000} = 0.367 \text{ inches}^4$$

A number of values can be assigned to  $W$  and  $a$  individually so long as a proper relationship between them is maintained.

By supposing  $a = 0.25 \text{ in}^2$ , then  $W$  can be calculated as follows:

$$\begin{aligned} W &= \frac{0.367}{a} \\ &= \frac{0.367}{0.25} = 1.468 \text{ inches}^2 \end{aligned}$$

From values of  $W$  and  $a$ , the dimensions of the core can be found.

#### 6-4-2-5-2-1 Calculation of core height

From the cross-sectional area of the core  $a$ , its height is defined by the following:

$$a = H \times F \tag{16}$$

where:

$a$  is the cross-sectional area of the core.

$H$  is the height of the core.

$F$  is the differential between the outside diameter and inside diameter.

By supposing the area is square, we can write  $H = F$ , and by substituting in eq. 16 yields:

$$H = \sqrt{a} = \sqrt{0.25} = 0.5 \text{ inches} = 12.7 \text{ mm}$$

thus:  $H = 0.5 \text{ in.}$  and  $F = 0.5 \text{ in.}$

#### 6-4-2-5-2-2 Calculation of the inside diameter of the core

The inside diameter of the core can be calculated as follows:

$$W = \pi \cdot r^2 \quad (17)$$

where:

W is the case window area.

r is the radius of the window area. So  $r = I_D/2$

$I_D$  is the inside diameter.

By substituting r into eq. 17 yields:

$$W = \pi \cdot \frac{I_D^2}{4} \quad (18)$$

or

$$\begin{aligned} I_D &= \sqrt{\frac{4 \times W}{\pi}} \\ &= \sqrt{\frac{4 \times 1.468}{\pi}} \\ &= 1.36 \text{ inches} = 34.7 \text{ mm} \end{aligned}$$

#### 6-4-2-5-2-3 Calculation of the outside diameter $O_D$ of the core

The outside diameter of the core can be calculated as follows:

where:

$$O_D = I_D + 2F + 2D \quad (19)$$

$O_D$  is the outside diameter.

$I_D$  is the inside diameter.

$F = 0.5$  in.

supposing  $D = 1.02$  mm = 0.04 in.

By substituting  $I_D$ ,  $F$ , and  $D$  into eq. 19 yields:

$$O_D = 1.36 + 2 \times 0.5 + 2 \times 0.04 = 2.44 \text{ in} = 62 \text{ mm.}$$

Fig. 6.6 is illustrated the cross-sectional of this core.

#### 6-4-2-5-2-4 Calculation of the magnetic path length

The magnetic path length of the core can be calculated by means of the following eq. 20 [39]

$$l = \frac{\pi(O_D + I_D)}{2} \quad (20)$$

where:

$l$  is the main magnetic path length.

$O_D$  is the outside diameter.

$I_D$  is the inside diameter.

By substituting the values of  $O_D$  and  $I_D$  into eq. 20 yields:

$$l = \frac{\pi(2.44 + 1.36)}{2} = 5.97 \text{ inches} = 151.6 \text{ mm}$$

A search through core catalogue (Appendix E), reveals the suitable core that we can use is 8c. For this core:

$$a = 159 \text{ mm}^2.$$

$$W = 1396 \text{ mm}^2.$$

therefore:

$$Wa = 159 \times 1396 = 221968.7 \text{ mm}^4. = 0.533 \text{ in}^4.$$

which is, of course, large enough.

#### 6-4-2-5-3 Calculation of the number of turns

The number of turns of the inductor can be calculating using eq. 15 as follows [39]:

$$N = \sqrt{\frac{l \times L \times 10^8}{3.19 \times a \times \mu}}$$

where [9]:

$$l = 5.97 \text{ in.}$$

$$L = 10.6 \text{ mH.}$$

$$a = 0.25 \text{ in}^2.$$

$$\mu = 8000.$$

By substituting these values into eq. 15 yields:

$$N = \sqrt{\frac{5.97 \times 10.6 \times 10^{-3} \times 10^8}{3.19 \times 0.25 \times 8000}} = 32 \text{ turns}$$

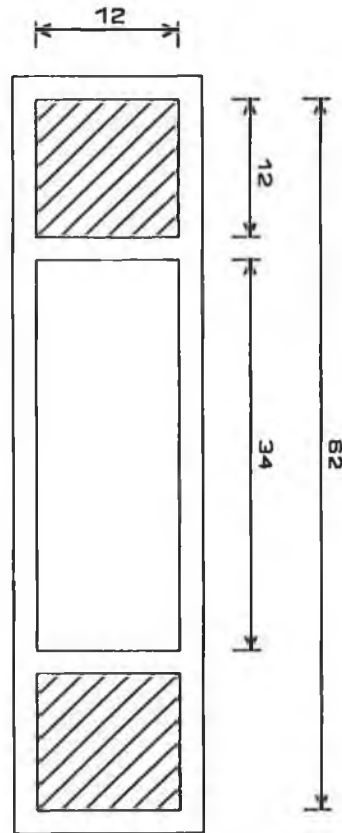


Figure 6.6 Cross-sectional of the core.

Table 6.2 shows summary of the core and inductor parameters.

Number of turns [turn]	Wxa product [inch <sup>4</sup> ]	Magnetic length [inch]	Outside diameter [inch]	Inside diameter [inch]
32	0.367	5.97	2.44	1.36

Table 6.2 Core and inductor parameters

# CHAPTER 7

## EXPERIMENTAL RESULTS AND CONCLUSION

A laboratory prototype three-phase PWM inverter and a power harmonic filter were built and tested. The inverter uses power MOSFET transistors switches, has a peak power capability of 1 KVA, and a nominal switching frequency of 3600 HZ.

### 7-1 LOW VOLTAGE TEST

A preliminary test was carried out on the inverter and filter at low voltage, in order to check the operation of the system, further test were also carried out at high voltage.

The experimental values in the subsequent figures were obtained for the case of:

- DC supply voltage  $V_d = \pm 30$  V.
- Modulation frequency  $f_1 = 400$  HZ.
- Switching frequency  $f_s = 3600$  HZ.
- Modulation ratio  $m_a = 1.0$ .
- Frequency ratio  $m_f = 9$ .



## 7-1-1 INVERTER OUTPUT

Figure 7.1 shows the output voltage of a single phase of the PWM inverter. The output voltage switches between  $\pm 30$  V and the variation in duty cycle can be seen.

Figure 7.2 shows the harmonic spectrum of the inverter output voltage at 2 dB/DIV, with significant components as follows:

1. The fundamental frequency component at 403 HZ and 30 V. This amplitude is directly proportional to the modulation ratio ( $m_a = 1.0$ ).
2. A number of harmonics centred around the switching frequency ( $f_s = 3627$  HZ) and its multiples, that is, around harmonics 3627 HZ, 7254 HZ, 10881 HZ, and so on.
3. Only odd harmonics are present, due to the odd frequency ratio chosen.
4. The total harmonic distortion (THD) is 89 %.

## 7-1-2 FILTER OUTPUT VOLTAGE

The filter output voltage is shown in figure 7.3. It has an amplitude of 30 V peak and frequency of 403 HZ. This waveform still has some higher frequency.

Figure 7.4 shows the voltage spectrum of the filter output at 2 dB/DIV. It can be seen from this figure, that most of the harmonic components have been eliminated. The total harmonic distortion (THD) is 3.5 %, which is within acceptable limit.



Fig. 7.1 Inverter output voltage (phase "A")  
20 V/div  
Timebase = 1 msec/div

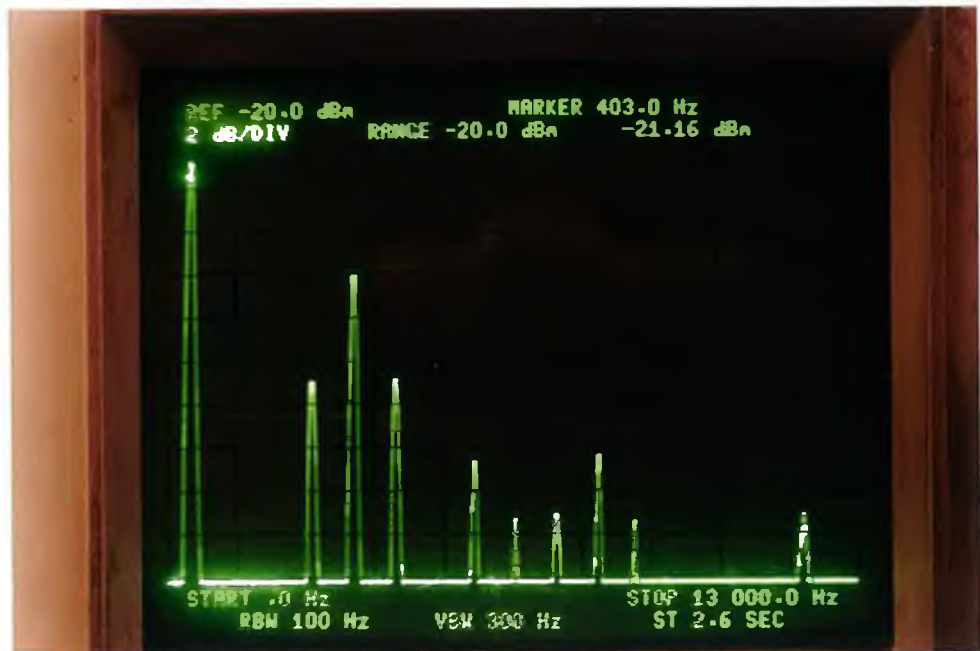


Fig. 7.2 Harmonic spectrum of the inverter output voltage at 2 dB/DIV.

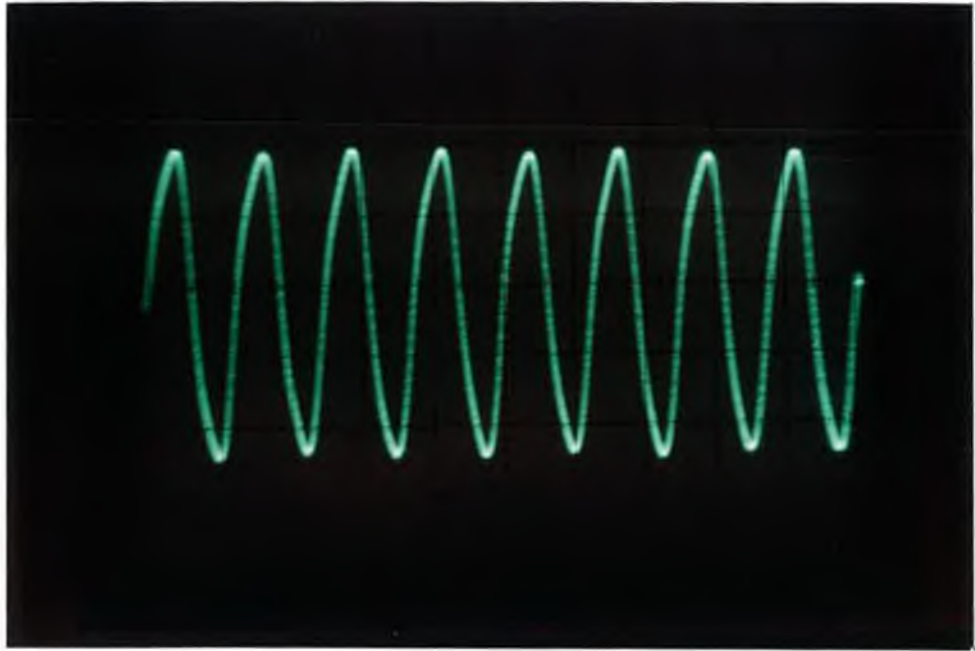


Fig. 7.3 Filter output voltage waveform of phase "A"  
20 V/div  
Timebase = 1 msec/div

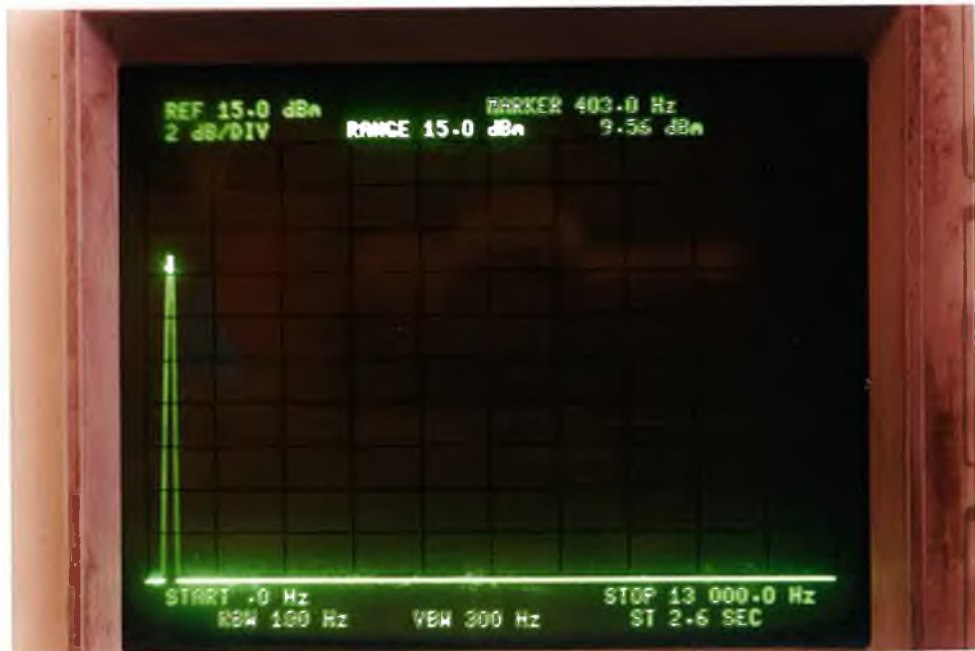


Fig. 7.4 Harmonic spectrum of the filter output voltage at 2 dB/DIV.

## 7-2 HIGH VOLTAGE TEST

To check the capability of the inverter at high voltage, an experimental test was carried out at  $\pm 120$  V. Figure 7.5 shows the output voltage of one-phase of the inverter. The filter was not tested at high voltage, because the high power filter components were not available in time for this test.

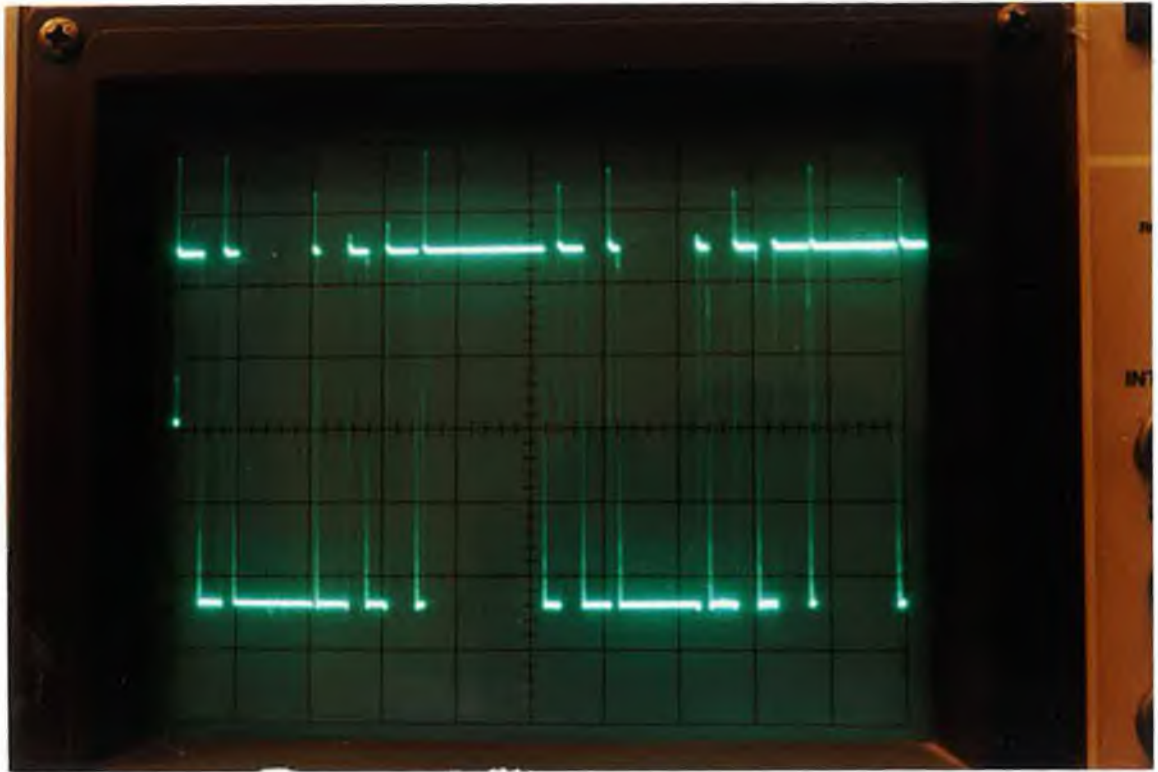


Figure 7.5 Inverter output voltage of phase "A" at 120 V.  
50 V/div  
Timebase = 1 msec/div

## 7-3 CONCLUSIONS

A DC-Link frequency converter has been shown to be a viable alternative to the constant-speed mechanical drive as a means of providing a constant frequency power supply from an aircraft generator. The ease of replacement and repair, the reduction in servicing needs, and the ability to locate the components of the electrical system throughout the aircraft all combine to bring about a considerable reduction in the maintenance time which is required.

The most important part in the DC-Link converter is the three-phase PWM inverter, which was designed and tested. The design objective of operating this inverter at constant frequency of 400 HZ, was achieved satisfactorily.

The design of the inverter was described in chapter 5. The inverter power switches used are the power MOSFETs type IRF 450 rated at 13 A and 500 V. An appropriate gate drive circuit design was developed by the author to optimize the switching speed of the MOSFET transistors. Because of the switching environment, these gate drive circuits resulted initially in voltage waveforms containing spikes. The installing of suitable capacitors between the dc level voltage and earth, was found to be a practical solution to eliminate the spikes.

Electrical isolation between the control circuit and the base drive circuits was realised by the use of opto-couplers of appropriate response speed. These were found to be practical, easy to use and provided good isolation because it has

a Farady screen between the LED and the phototransistor.

To reduce the switching power losses and to protect the MOSFETs from the high voltage spike, snubber circuits were designed and installed. The detailed information concerning this, is given in section 5-1-3 of chapter 5.

To eliminate problems of slow recovery of MOSFET diodes, schottky diodes and fast recovery diodes have been used. This also includes blanking time circuit.

The various switching techniques associated with pulse width modulation have been described. Three systems were mentioned: Natural, Regular and Optimised PWM. Natural PWM was chosen because of its simplicity. The circuits to realize this were described in section 5-2 of chapter 5.

The PWM method can move unwanted frequency components to a higher frequency region. Thus the output waveform of the PWM inverter is generally improved by using a high ratio between the carrier frequency and the output fundamental frequency.

## **7-4 RECOMMENDATIONS**

Although the Natural PWM method was maintained in this project, the



optimized PWM method may be used to generate the control signals for the inverter. In this latter method, several harmonics can be removed from the inverter output. This is made possible by developments in microprocessor technology and involve the implementation of the digital method to obtain PWM signals.

The voltage-control system is beyond the scope of this investigation. It is assumed that the voltage control regulation will be carried out by the generator control unit. However, in the case of permanent magnet generators, regulation of the dc bus with a transistor chopper, would be a preferred method. Further, investigation is needed to combine the two systems (static converter and voltage control) and so provide the complete solution for generating power in aircraft systems.

## REFERENCES

- [1]. Pallett, E. H.,: "Aircraft electrical systems". 2 Edition, Pitman, 1982.
- [2]. Bent, Ralph D. & Mckinley, James L.,: "Aircraft electricity and electronics". Third edition, McGraw-Hill Book Company, 1981.
- [3]. R.L. Gasperetti,: "Aircraft generator weight reduced by more effective cooling". Westinghouse Engineer, 1969 V. 29 PT. 3 PP. 71-75.
- [4]. R.E Corbett,: "Considerations in the selection of DC vs AC power systems for high power space applications". 18th IBCBC, 1984.
- [5]. R.Hehnen,: "AC power systems in the kilowatt range". ESTEC Power Conditioning Seminar.
- [6]. B.Mehl, G.Pierce,: "A Minimum interruption AC electric power generating system for avionics". Digital avionics systems conference, Dec. 1984.
- [7]. Kennett, R.J. (1971),: "Integrated drive generators for aircraft". Electronics and Power. In Journal of the Institution Engineers, 17 (Feb. 1971), 73-76.
- [8]. Rosswurm, M.A. (1981),: "Design considerations of DC-Link aircraft generation systems". Aircraft electrical power systems. In Proceedings of the Aerospace Congress and Exposition (Anaheim, Calif., 1981). Warrendale, Pa.: Society of Automotive Engineers, 1981, pp. 1-15.
- [9]. Yorksie, D.S., and Hyvarinen, W.E. (1981),: "The effect of critical design parameters on the selection of a VSCF system". Aircraft Electrical Power Systems. In proceedings of the Aerospace Congress and Exposition (Anaheim, Calif., 1981). Warrendale, pa.: Society of Automotive Engineers, 1981, pp. 43-50.
- [10]. R. L. Gaspereetti,: "Aircraft generator weight reduced by more effective cooling". Westinghouse Engineer, 1969, V.29 PT. 3 PP. 71-75.

- [11]. R. Krishnan. (1990),:" Modelling, Simulation, and Analysis of Variable-speed Constant Frequency Power Conversion Scheme with a Permanent Magnet Brushless dc Generator". IEEE Trans. Industrial Electronics, Vol. 37, No.4 August 1990, pp. 291-296.
- [12]. Mohan, Undeland, Robbins,: " Power Electronics; Converters, Applications, and Design". John Wiley & Sons, 1989.
- [13]. Murphy, J. M. D. and Turnbull, F. G.: "Power Electronics Control of AC Motor". Oxford; New York: Pergamen, 1988.
- [14]. Bose, B. K.: "Power Electronics and AC drives". Perntice-hall, c1986.
- [15]. Evans, P. D. and Close, P. R.: "Harmonic distortion in PWM inverter output waveforms". IEE Proc. Elect. Power. APP 1., July 1987. Vol. 134. pp. 224-232.
- [16]. Patel, H. S. and Hoft, R. G.: "Generalized Techniques of Harmonic Elimination and voltage control in thyristor inverters". PartI-Harmonic Elimination. IEEE Trans. On Industry APP1., May / June 1973, Vol. IA-9. pp.310-317.
- [17]. Katsunori Yasumasa O., Hisaichi I.:"PWM technique for power MOSFETs inverter". IEEE Trans. on Power Electronics, Vol. 3, July 1988.
- [18]. Mokrytzki, b.:"Pulse width modulated inverters for AC motor drives". IEEE Trans. Ind. and Gen. Appl. Vol IGA 3, no 6, Nov/Dec 1967.
- [19]. S.R. Bowes and M.J. Mount.:"Microprocessor control of PWM inverters". IEEE Proc., Vol. 128, Pt. B, No. 6, November 1981, pp 293-305.
- [20]. S.R. Bowes.:" New sinusoidal pulse width modulated inverter". Proc IEE, 1975, 122 (11), PP. 1279-1285.
- [21]. Casteel, J.B. and Hoft, R.G.:"Optimum PWM waveforms of a microprocessor controlled inverter". IEEE Power elec. Spec. Conf. pp. 243 - 250, 1977.

- [22]. Buja, G.S. and Indri, G.S.: "Optimal pulsewidth modulation for feeding AC motors". IEEE Trans. Ind. Appl. Vol ia-13, no 1, Jan/Feb 1977.
- [23]. Berthon, A. & Phut, PH.,: "Single phase PWM inverter with power MOSFET transistors for speed drive of electrical machines". Power Electronics and Applications. 18-18 OCT. 1985. pp. 1/159 - 162.
- [24]. Proceedings of 8th International PCI'84 Conference: Intertec Communications.
- [25]. Rudy Severns,: " Mospower applications handbook". Siliconix incorporated, 1984.
- [26]. B. R. Nair and P. C. Sen,: " Voltage clamp circuits for a power MOSFET PWM inverter". Application society IEEE - IAS - 1984 Annual meeting 30 SEP. - 4 oct. 1984 CHICAGO, IL, USA.
- [27]. B. W. Williams,: " Power electronics; devices, drivers and application". Macmillan, 1987.
- [28]. Duncan A. Grant and John Gowar,: " Power MOSFETs; Theory and Application". New York: Wiley, c1989.
- [29]. Murai, Y., Watanabe, T. and Iwasaki, H.,: " Waveform distortion and correction circuit for PWM inverters with switching lagtimes". IEEE IAS Annual meeting, Toronto Oct. 1985, pp. 436 - 441.
- [30]. R.C. Dodson, P.D. Evans, H. Tabatabaei Yazdi, and S.C. Harley,: " Compensating for dead time degradation of PWM inverter waveforms". IEEE Proc, Vol. 137, Pt. B, No. 2, March 1990.
- [31]. S.R. Bowes and M.J. Mount,: " Microprocessor control of PWM inverters". IEEE Proc., Vol. 128, Pt. B, No. 6, November 1981, pp 293-305.
- [32]. Kusko, S.M. Peeran, D. Galler,: " Nonlinear loading of static and rotating uninterruptible power supplies". International Power Electronics Conference, Tokyo,1990.

- [33]. A. Kusko, D. Galler,: " Output Impedance of PWM UPS Inverter-Feedback vs. Filters". Conf. Proc. 1990 IEEE-IBS Annual Meeting, 1990.
- [34]. A. Kusko,: " Emergency/standby power systems". McGraw-Hill Book co., New York, 1989.
- [35]. Ott, R.R.: " Filter for silicon controlled rectifier commutation and harmonic attenuation in high-power inverters". AIEE Trans. Common. & Electron., May 1963, pp. 259-262.
- [36]. Dewan, S.B., and Ziogas. P.D.: " Optimum filter design for a single-phase solid-state UPS system". IEEE Trans., 1979, IA-15, pp. 664-669.
- [37]. Walter V. Manka,: " Design power inductors step by step". Electronic Design 26, Dec. 20, 1977.
- [38]. Georgec. Chryssis,: " High-frequency switching power supplies". 2nd Edition, McGraw-Hill, 1989.
- [39]. Eric Lowdon,: " Practical transformer design handbook". 2nd Edition. Blue Rige Summit, PA, 1989.

## **Appendix (A)**

# IRF450 ■ IRF451 ■ IRF452 ■ IRF453



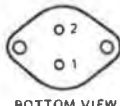
## N-Channel Enhancement Mode MOSPOWER

### APPLICATIONS

- Switching Regulators
- Converters
- Motor Drivers

### PRODUCT SUMMARY

Part Number	$V_{DS}$ Volts	$r_{DS(ON)}$ (ohms)	Package
IRF450	500	0.4	T0-204AA
IRF451	450	0.4	T0-204AA
IRF452	500	0.5	T0-204AA
IRF453	450	0.5	T0-204AA



PIN 1 - Gate  
PIN 2 - Source  
CASE - Drain

BOTTOM VIEW

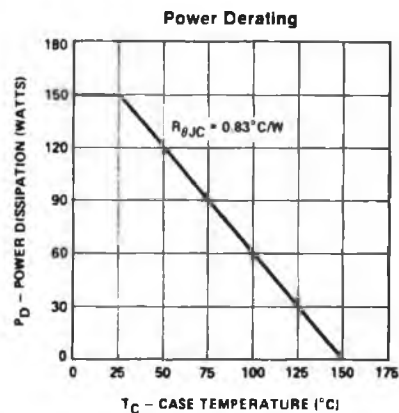
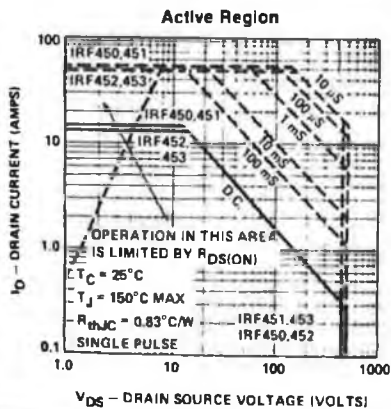
T0-204AA (T0-3)

For Additional Curves  
See Section 5: VNDC50-2

### ABSOLUTE MAXIMUM RATINGS ( $T_C = 25^\circ\text{C}$ unless otherwise noted)

Parameter	IRF450	IRF451	IRF452	IRF453	Units
$V_{DS}$ Drain-Source Voltage	500	450	500	450	V
$V_{DGR}$ Drain-Gate Voltage ( $R_{GS} = 1\text{ M}\Omega$ )	500	450	500	450	V
$I_D @ T_C = 25^\circ\text{C}$ Continuous Drain Current	$\pm 13$	$\pm 13$	$\pm 12$	$\pm 12$	A
$I_D @ T_C = 100^\circ\text{C}$ Continuous Drain Current	$\pm 8$	$\pm 8$	$\pm 7$	$\pm 7$	A
$I_{DM}$ Pulsed Drain Current <sup>1</sup>	$\pm 52$	$\pm 52$	$\pm 48$	$\pm 48$	A
$V_{GS}$ Gate-Source Voltage	$\pm 40$	$\pm 40$	$\pm 40$	$\pm 40$	V
$P_D @ T_C = 25^\circ\text{C}$ Max. Power Dissipation	150	150	150	150	W
$P_D @ T_C = 100^\circ\text{C}$ Max. Power Dissipation	60	60	60	60	W
Junction to Case Linear Derating Factor	1.2	1.2	1.2	1.2	$\text{W}^\circ\text{C}$
Junction to Ambient Linear Derating Factor	.033	.033	.033	.033	$\text{W}^\circ\text{C}$
$T_J$ Operating and Storage Temperature Range	-55 To 150	-55 To 150	-55 To 150	-55 To 150	$^\circ\text{C}$
Lead Temperature (1/16" from case for 10 secs.)	300	300	300	300	$^\circ\text{C}$

<sup>1</sup> Pulse Test: Pulsewidth  $\leq 300\mu\text{sec}$ , Duty Cycle  $\leq 2\%$



**ELECTRICAL CHARACTERISTICS (T<sub>C</sub> = 25°C unless otherwise noted)**  
**STATIC**

Parameter	Type	Min.	Typ.	Max.	Units	Test Conditions
BV <sub>DSS</sub>	Drain-Source Breakdown Voltage	IRF450,452	500		V	V <sub>GS</sub> = 0 I <sub>D</sub> = 250μA
		IRF451,453	450		V	
V <sub>GS(th)</sub>	Gate-Threshold Voltage	All	2.0	4.0	V	V <sub>DS</sub> = V <sub>GS</sub> , I <sub>D</sub> = 1 mA
I <sub>GSSF</sub>	Gate-Body Leakage Forward	All		100	nA	V <sub>GS</sub> = 20V
I <sub>GSSR</sub>	Gate-Body Leakage Reverse	All		-100	nA	V <sub>GS</sub> = -20V
I <sub>DSS</sub>	Zero Gate Voltage Drain Current	All	0.1	0.25	mA	V <sub>DS</sub> = Max. Rating, V <sub>GS</sub> = 0
		All	0.2	1.0	mA	V <sub>DS</sub> = 0.8 Max. Rating, V <sub>GS</sub> = 0 T <sub>C</sub> = 125°C
I <sub>D(on)</sub>	On-State Drain Current <sup>1</sup>	IRF450,451	13		A	V <sub>DS</sub> ≥ 2V <sub>DS(ON)</sub> , V <sub>GS</sub> = 10V
		IRF452,453	12		A	V <sub>DS</sub> ≥ 2V <sub>DS(ON)</sub> , V <sub>GS</sub> = 10V
V <sub>DS(on)</sub>	Static Drain-Source On-State Voltage <sup>1</sup>	IRF450,451	2.1	2.8	V	V <sub>GS</sub> = 10V, I <sub>D</sub> = 7.0A
		IRF452,453	2.8	3.5	V	V <sub>GS</sub> = 10V, I <sub>D</sub> = 7.0A
R <sub>DS(on)</sub>	Static Drain-Source On-State Resistance <sup>1</sup>	IRF450,451	0.3	0.4	Ω	V <sub>GS</sub> = 10V, I <sub>D</sub> = 7.0A
		IRF452,453	0.4	0.5	Ω	V <sub>GS</sub> = 10V, I <sub>D</sub> = 7.0A
R <sub>DS(on)</sub>	Static Drain-Source On-State Resistance <sup>1</sup>	IRF450,451	0.66	0.88	Ω	V <sub>GS</sub> = 10V, I <sub>D</sub> = 7.0A, T <sub>C</sub> = 125°C
		IRF452,453	0.88	1.10	Ω	V <sub>GS</sub> = 10V, I <sub>D</sub> = 7.0A, T <sub>C</sub> = 125°C

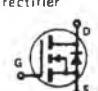
**DYNAMIC**

g <sub>fs</sub>	Forward Transconductance <sup>1</sup>	All	6.0	7.2		S (Ω)	V <sub>DS</sub> ≥ 2V <sub>DS(ON)</sub> , I <sub>D</sub> = 7.0A
C <sub>iss</sub>	Input Capacitance	All		2600	3000	pF	V <sub>GS</sub> = 0, V <sub>DS</sub> = 25V f = 1 MHz
C <sub>oss</sub>	Output Capacitance	All		280	600	pF	
C <sub>rss</sub>	Reverse Transfer Capacitance	All		40	200	pF	
t <sub>d(on)</sub>	Turn-On Delay Time	All		33	35	ns	
t <sub>r</sub>	Rise Time	All		46	50	ns	
t <sub>d(off)</sub>	Turn-Off Delay Time	All		75	150	ns	V <sub>DD</sub> = 210V, I <sub>D</sub> ≥ 7.0A R <sub>g</sub> = 5Ω, R <sub>L</sub> = 30Ω (MOSFET switching times are essentially independent of operating temperature.)
t <sub>f</sub>	Fall Time	All		31	70	ns	

**THERMAL RESISTANCE**

R <sub>thJC</sub>	Junction-to-Case	All			0.83	°C/W	
R <sub>thJA</sub>	Junction-to-Ambient	All			30	°C/W	Free Air Operation

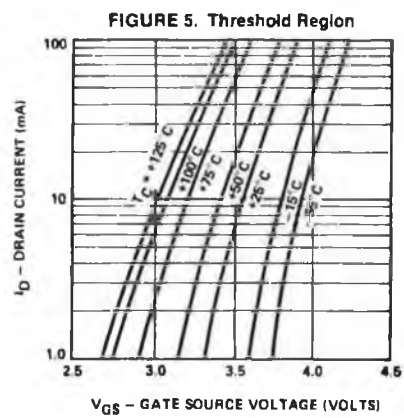
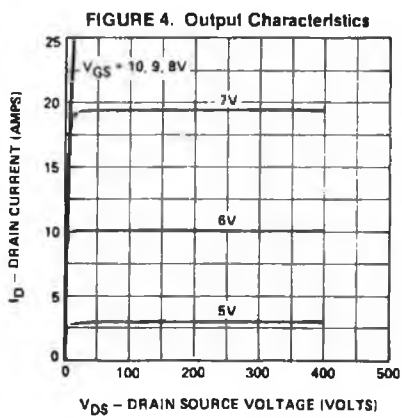
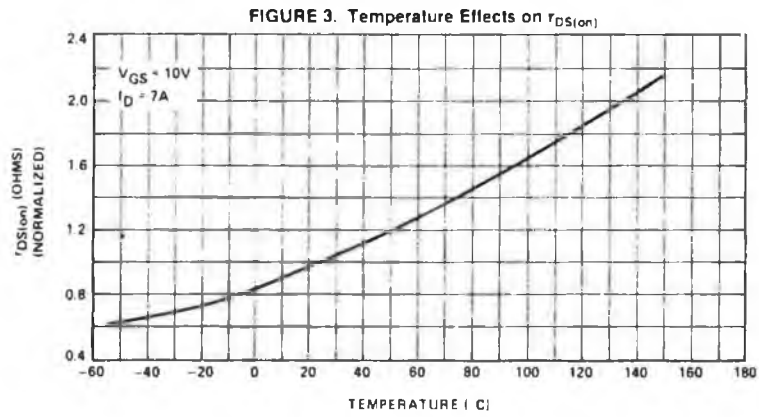
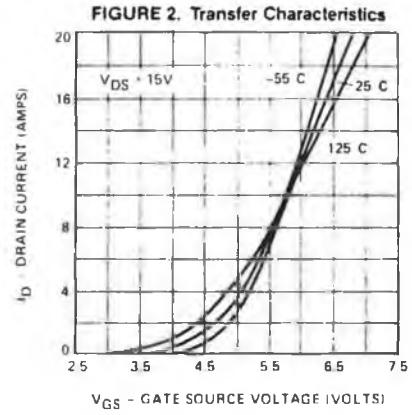
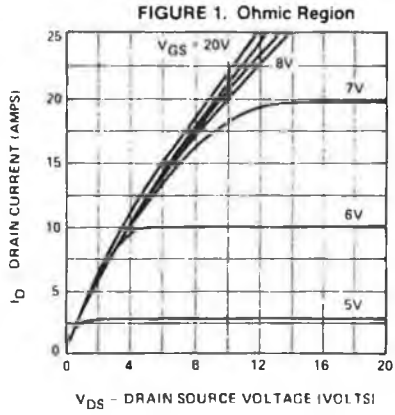
**BODY-DRAIN DIODE RATINGS AND CHARACTERISTICS**

I <sub>S</sub>	Continuous Source Current (Body Diode)	IRF450,451			-13	A	Modified MOSPOWER symbol showing the integral P-N Junction rectifier 
		IRF452,453			-12	A	
I <sub>SM</sub>	Source Current <sup>1</sup> (Body Diode)	IRF450,451			-52	A	
		IRF452,453			-48	A	
V <sub>SD</sub>	Diode Forward Voltage <sup>1</sup>	IRF450,451			-1.4	V	T <sub>C</sub> = 25°C, I <sub>S</sub> = -13A, V <sub>GS</sub> = 0
		IRF452,453			-1.3	V	T <sub>C</sub> = 25°C, I <sub>S</sub> = -12A, V <sub>GS</sub> = 0
t <sub>rr</sub>	Reverse Recovery Time	All		400		ns	T <sub>J</sub> = 150°C, I <sub>F</sub> = I <sub>S</sub> , dI <sub>F</sub> /dt = 100 A/μs

<sup>1</sup> Pulse Test: Pulse Width ≤ 300 μsec, Duty Cycle ≤ 2%



**TYPICAL PERFORMANCE CURVES (25° C unless otherwise noted)**  
**VNDC50-2**



# TYPICAL PERFORMANCE CURVES—Continued

VNDC50-2

FIGURE 6. Off-State Current

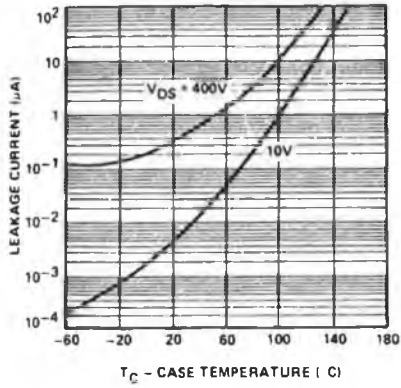


FIGURE 7. Capacitance

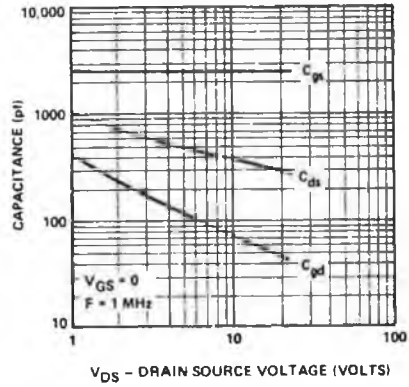


FIGURE 8. Effects on Load Conditions

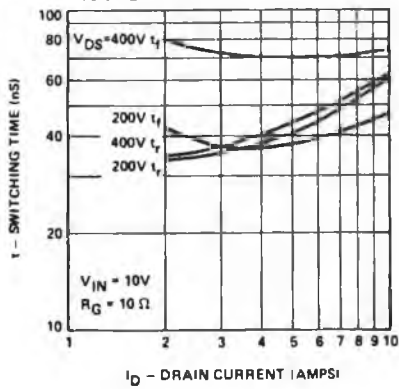


FIGURE 9. Effects of Drive Resistance

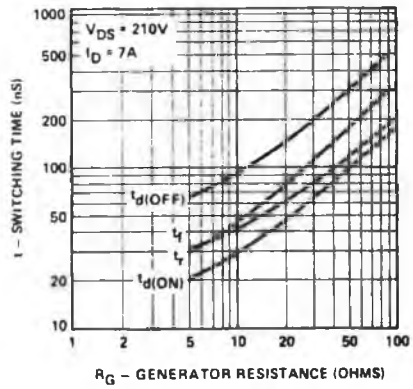
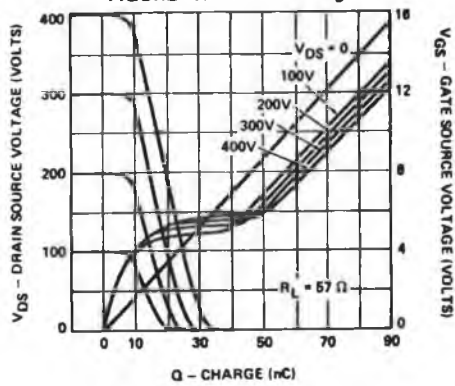


FIGURE 10. Turn-on Charge



# TRANSIENT THERMAL RESPONSE CURVES

VNDC50-2

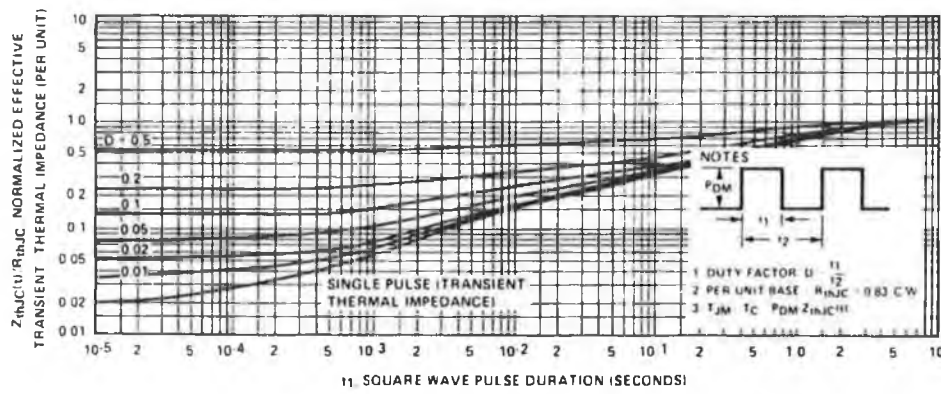


FIGURE 1. TO-3 Package



**Appendix (B)**

LIST

```
10 OPEN "r4.res" FOR OUTPUT AS #1
20 GOSUB 150
30 FC=1000
40 FOR G=-20 TO -60 STEP -20
50 READ F,VI
60 DATA 2000,2.07,2800,36.6,3600,69.2,4400,36.6,5600,2.07
70 DATA 6000,24.42,6800,20.85,7600,20.85,8400,24.42,9200,18.08
80 DATA 10000,7.14,10800,13,11600,7.14,12400,18.08
90 G1=G*(LOG(F/FC)/2.3) :Y=((G1/20)+(LOG(VI)/2.3)) :VO=10^Y
94 VOT=VOT+VO
100 PRINT #1, TAB(5),F,VI,VO,VOT
110 PRINT , TAB(9);"-----"
120 IF VI=18.08 AND F=12400 THEN 140
130 GOTO 50
140 PRINT :PRINT :GOSUB 150 :RESTORE :NEXT G :END
150 PRINT TAB(9);"*****"
160 PRINT #1, TAB(9); "F(Hz)", "Vi(volt)", "VO(volt)"
170 PRINT TAB(9);"*****"
175 PRINT , TAB(5),G
180 RETURN
190 END
0
```

F(HZ)	Vi(volt)	VO(volt)
2000	2.07	1.03504
2800	36.6	13.10925
3600	69.2	19.2862
4400	36.6	8.338012
5600	2.07	0.3692296
6000	24.42	4.076426
6800	20.85	3.070039
7600	20.85	2.746534
8400	24.42	2.910633
9200	18.08	1.96671
10000	7.14	0.7137296
10800	13	1.203955
11600	7.14	0.6151814
12400	18.08	1.458683

**Table 1**

All the above tabled result are based on a single low-pass LC filter with roll off of -20 dB/decade. The total harmonic distortion of this filter is 58 % which is greater than the required value.

F(Hz)	Vi(volt)	VO(volt)
2000	2.07	0.517117
2800	36.6	4.67646
3600	69.2	5.349571
4400	36.6	1.89185
5600	2.07	0.0658063
6000	24.42	0.6780376
6800	20.85	0.4505045
7600	20.85	0.3605632
8400	24.42	0.3456761
9200	18.08	0.2132403
10000	7.14	7.118846E-02
10800	13	0.1111795
11600	7.14	5.288695E-02
12400	18.08	0.1173033

Table 2

All the above tabled result are based on a single low-pass LC filter with roll off of  $-40$  dB/decade. The total harmonic distortion of this filter is 12 % which is greater than the required value.

F(Hz)	Vi(volt)	VO(volt)
2000	2.07	0.2583571
2800	36.6	1.668232
3600	69.2	1.483854
4400	36.6	0.4292503
5600	2.07	1.172839E-02
6000	24.42	0.1127789
6800	20.85	6.610809E-02
7600	20.85	0.0473345
8400	24.42	0.0410536
9200	18.08	2.312055E-02
10000	7.14	7.100449E-03
10800	13	1.026689E-02
11600	7.14	4.546678E-03
12400	18.08	9.43321E-03

**Table 3**

All the above tabled result are based on a single low-pass LC filter with roll off of  $-60$  dB/decade. The total harmonic distortion of this filter is 3.5 % which is less than the required value.

So this filter suitable for using in this design.



## **Appendix (C)**

# Table 2. Magnet Wire Design Data.

AWG Size	Bare Wire				Single Film					Double Film				
	Max OD	Max I	Max Tensile Strength	$\Omega/\text{ft}$	Max OD	ft/lb	$\Omega/\text{lb}$	$T_{pi}$	$T_{pi}^2$	Max OD	ft/lb	$\Omega/\text{lb}$	$T_{pi}$	$T_{pi}^2$
10	0.1024	33.6	82.4	0.00100	0.1047	31.6	0.0316	9.551	91.22	0.1061	31.5	0.0315	9.425	88.83
11	0.0912	28.2	65.3	0.00126	0.0935	39.8	0.0501	10.70	114.4	0.0948	39.7	0.0500	10.55	111.3
12	0.0812	23.7	51.8	0.00159	0.0834	50.3	0.0800	11.99	143.8	0.0847	50.0	0.0795	11.81	139.4
13	0.0724	19.9	41.2	0.00200	0.0746	63.3	0.1266	13.40	179.7	0.0757	62.9	0.1258	13.21	174.5
14	0.0644	16.7	32.6	0.00252	0.0666	79.9	0.2013	15.02	225.5	0.0682	79.3	0.1998	14.66	215.0
15	0.0574	14.1	25.9	0.00318	0.0594	101	0.3212	16.84	283.4	0.0609	100	0.3180	16.42	269.6
16	0.0511	11.8	20.5	0.00402	0.0531	127	0.5105	18.83	354.7	0.0545	126	0.5065	18.35	336.7
17	0.0455	9.94	16.3	0.00505	0.0475	159	0.8029	21.05	443.2	0.0488	158	0.7979	20.49	419.9
18	0.0405	8.35	12.9	0.00639	0.0424	201	1.284	23.58	556.2	0.0437	199	1.272	22.88	523.6
19	0.0361	7.02	10.2	0.00805	0.0379	253	2.037	26.39	696.2	0.0391	251	2.020	25.58	654.1
20	0.0322	5.92	8.14	0.0101	0.0339	318	3.212	29.50	870.2	0.0351	315	3.182	28.49	811.7
21	0.0286	4.95	6.42	0.0128	0.0303	402	5.146	33.00	1089	0.0314	397	5.082	31.85	1014
22	0.0254	4.15	5.07	0.0162	0.0270	508	8.230	37.04	1372	0.0281	503	8.149	35.59	1266
23	0.0227	3.50	4.05	0.0203	0.0243	633	12.85	41.15	1694	0.0253	625	12.69	39.53	1562
24	0.0202	2.94	3.20	0.0257	0.0217	806	20.71	46.08	2124	0.0227	794	20.41	44.05	1941
25	0.0180	2.47	2.54	0.0324	0.0194	1013	32.82	51.55	2657	0.0203	990	32.08	49.26	2427
26	0.0160	2.07	2.01	0.0410	0.0173	1282	52.56	57.80	3341	0.0182	1260	51.66	54.95	3019
27	0.0143	1.75	1.61	0.0514	0.0156	1608	82.65	64.10	4109	0.0164	1580	81.21	60.98	3718
28	0.0127	1.47	1.27	0.0653	0.0140	2033	132.8	71.43	5102	0.0147	1990	129.9	68.03	4628
29	0.0114	1.25	1.02	0.0812	0.0126	2525	205.0	79.37	6299	0.0133	2470	200.6	75.19	5653
30	0.0101	1.04	0.801	0.104	0.0112	3215	334.4	89.29	7972	0.0119	3140	326.6	84.03	7062
31	0.0090	0.874	0.636	0.131	0.0100	4065	532.5	100.0	10000	0.0108	3950	517.4	92.59	8573
32	0.0081	0.747	0.515	0.162	0.0091	5000	810.0	109.9	12076	0.0098	4880	790.6	102.0	10412
33	0.0072	0.626	0.407	0.206	0.0081	6369	1312	123.5	15242	0.0088	6170	1271.5	113.6	12913
34	0.0064	0.524	0.322	0.261	0.0072	8064	2105	138.9	19290	0.0078	7870	2054	128.2	16437
35	0.0057	0.441	0.255	0.331	0.0064	10210	3380	156.2	24414	0.0070	9940	3290	142.9	20408
36	0.0051	0.373	0.204	0.415	0.0058	12760	5295	172.4	29727	0.0063	12440	5163	158.7	25195
37	0.0046	0.319	0.166	0.512	0.0052	15800	8090	192.3	36982	0.0057	15300	7834	175.4	30779
38	0.0041	0.269	0.132	0.648	0.0047	19920	12908	212.8	45269	0.0051	19300	12506	196.1	38447
39	0.0036	0.221	0.101	0.847	0.0041	26040	22056	243.9	59488	0.0045	25100	21260	222.2	49383
40	0.0032	0.185	0.0804	1.08	0.0037	33110	35759	270.3	73046	0.0040	32200	34776	250.0	62500
41	0.0029	0.160	0.0661	1.32	0.0033	40100	52932	303.0	91827	0.0036	39500	52140	277.8	77160
42	0.0026	0.136	0.0531	1.66	0.0030	51000	84660	333.3	111111	0.0032	49800	82668	312.5	97656
43	0.023	0.113	0.0475	2.14	0.0026	65800	140.8k	384.6	147928	0.0029	63700	136.3k	344.8	118906
44	0.0021	0.0985	0.0346	2.59	0.0024	79400	205.6k	416.7	173611	0.0027	76300	197.6k	370.4	137174
45	0.00176	0.0756	0.0243	3.62	0.00205	104k	376.5k	487.8	237954	0.00230	99600	360.6k	434.8	189036
46	0.00157	0.0637	0.0194	4.54	0.00185	132k	599.3k	540.5	292184	0.00210	126k	572.0k	476.2	226757
47	0.00140	0.0536	0.0154	5.71	0.00170	162k	925.0k	588.2	346020	0.00190	153k	873.6k	526.3	277003
48	0.00124	0.0447	0.0121	7.29	0.00150	205k	1.494M	666.6	444444	0.00170	199k	1.451M	588.2	346020
49	0.00111	0.0379	0.0097	9.09	0.00130	258k	2.345M	769.2	591716	0.00150	252k	2.291M	666.6	444444
50	0.00099	0.0319	0.0077	11.4	0.00120	312k	3.557M	833.3	694444	0.00140	306k	3.488M	714.3	510204
51	0.00088	0.0267	0.0061	14.5	0.00110	416k	6.032M	909.1	826446					
52	0.00078	0.0223	0.0048	18.4	0.00100	555k	10.21M	1000	1.000M					
53	0.00070	0.0190	0.0038	22.9	0.00085	667k	15.27M	1176	1.384M					
54	0.00062	0.0158	0.0030	29.1	0.00075	859k	25.00M	1333	1.777M					
55	0.00055	0.0132	0.0024	37.0	0.00070	1.090M	40.33M	1429	2.041M					
56	0.00049	0.0111	0.0019	46.6	0.00065	1.380M	64.31M	1538	2.367M					
Units	Inches	Amperes	Pounds	$\Omega/\text{ft}$	Inches	ft/lb	$\Omega/\text{lb}$	$T_{pi}$	$T_{pi}^2$	Inches	ft/lb	$\Omega/\text{lb}$	$T_{pi}$	$T_{pi}^2$

Maximum ODs,  $\Omega/\text{ft}$  and ft/lb are taken from Materials and Processes Handbook. Maximum rated current is 10% of the fusing current at 20°C. Maximum tension is based upon a tensile strength of 10.00 PSI.  $\Omega/\text{lb}$  is derived from  $(\Omega/\text{ft}) \times (\text{ft}/\text{lb})$ .  $T_{pi} = 1/\text{Max OD}$ .  $T_{pi}^2 = 1/\text{Max OD}^2$ .

## **Appendix (D)**



## TYPICAL PROPERTIES FOR NICKEL IRON ALLOYS

Radiometal 4550	Radiometal 448	Super Radiometal	Radiometal 36	HCR	
6000	8000	11000	5000	1000	Initial Permeability d.c. $\mu_0$
40000	60000	100000	30000	100000	Maximum d.c. Permeability
1.6	1.6	1.6	1.2	1.6	Saturation Induction (Tesla)
<del>1.6</del>	<del>1.6</del>	16	12	16	(kGauss)
1.0	1.0	1.1	0.5	1.5	Remanence from saturation (Tesla)
<del>1.0</del>	<del>1.0</del>	11	5	15	(kGauss)
8	6	3	10	10	Coercivity, H <sub>c</sub> d.c. (A/m)
<del>100</del>	75	38	126	126	(mOe)
40	30	20	50	65	Hysteresis loss at B <sub>sat</sub> (J/m <sup>3</sup> cycle)
<del>450</del>	450	450	280	450	Curie Temperature (°C)
842	842	842	536	842	(°F)
8250	8250	8250	8100	8250	Density kg/m <sup>3</sup>
0.298	0.298	0.298	0.293	0.298	lb/in <sup>3</sup>
0.45	0.40	0.40	0.80	0.40	Resistivity ( $\mu\Omega$ -m)
271	241	241	481	241	(ohm-cir mil/ft)
7	8	8	2	10	Coefficient of Linear Expansion/°C ( $\times 10^6$ )
3.9	4.4	4.4	1.1	5.6	Expansion/°F ( $\times 10^6$ )
11	11	11	6.9	14	Thermal Conductivity (kcal/mh°C)
89	89	89	55.6	113	(Btu-in/ft <sup>2</sup> h°F)
0.11	0.11	0.11	0.11	0.11	Specific Heat (kcal/kg°C)
0.11	0.11	0.11	0.11	0.11	(Btu/lb°F)
250	250	275	275	275	Vickers Hardnes (HV) Hard Rolled
125	125	125	135	125	Annealed
775	775	775	971	1235	Tensile Strength Hard Rolled: (MN/m <sup>2</sup> )
112	112	112	141	179	(kpsi)
471	471	471	530	425	Tensile Strength Annealed: (MN/m <sup>2</sup> )
68	68	68	77	62	(kpsi)
167	167	167	128	167	Youngs Modulus (MN/m <sup>2</sup> ) ( $\times 10^{-3}$ )
24	24	24	19	24	(psi) ( $\times 10^{-6}$ )

SI Units  Imperial Units

## Appendix (E)

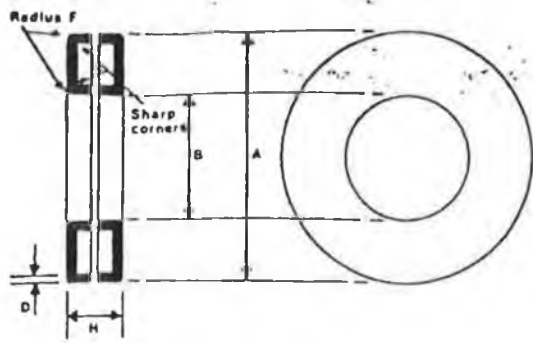


Table 8 Standard case list

	A	B	H	D	F
Core Ref.	mm ±0.13	mm ±0.13	mm ±0.10	mm ±0.13	mm ±0.13
0a	18.03	10.79	5.18	0.76	0.76
b			8.38		
1a	21.21	10.79	5.18	0.76	0.76
b			6.78		
c			8.38		
2a	24.38	12.37	6.78	0.76	0.76
b			8.38		
c			9.96		
3a	31.24	16.64	7.32	1.02	1.02
b			8.89		
c			10.46		
4a	35.99	19.81	8.89	1.02	1.02
b			10.46		
c			12.04		
5a	40.89	22.99	8.89	1.02	1.02
b			12.07		
c			15.24		
6a	50.42	29.34	7.29	1.02	1.02
b			10.46		
c			12.07		
d			15.24		
7a	59.69	35.81	7.29	1.02	1.02
b			12.07		
c			15.24		
8a	69.22	42.16	10.46	1.02	1.02
b			13.64		
c		42.16	16.81		
9a	79.25	48.51	13.64	1.02	1.02
b			16.81		
c			15.24		
10a	89.79	53.85	14.66	1.52	1.52
b			17.83		
c			22.61		
11a	112.26	66.29	16.26	1.52	1.52
b			19.43		
c			22.61		
12a	131.83	78.49	18.34	1.78	1.78
b			23.11		
c			29.46		
13a	163.58	110.24	18.34	1.78	1.78
b			23.11		
c			29.46		
14a	28.06	16.51	5.69	1.02	1.02
b			3.89		

Table 5. Standard core list

Type	Outside diameter	Inside diameter	Axial length	Magnetic length	Gross Cross-sectional area*	Weight of solid core*
	mm	mm	mm	mm	mm <sup>2</sup>	g
0a	15.9	12.7	3.17	44.9	5.0	1.99
b			6.35		10.1	3.99
1a	19.1	12.7	3.17	49.9	10.1	4.44
b			4.76		15.1	6.63
c			6.35		25.2	8.87
2a	22.2	14.3	4.76	57.4	18.9	9.55
b			6.35		25.2	12.7
c			7.94		31.5	15.9
3a	28.6	19.1	4.76	74.8	22.7	14.9
b			6.35		30.2	19.9
c			7.94		37.8	24.9
4a	33.3	22.2	6.35	81.3	44.1	27.1
b			7.94		52.9	33.9
c			9.52		60.6	40.6
5a	38.1	25.4	6.35	99.8	40.3	35.4
b			9.52		60.5	53.1
c			12.7		80.6	70.7
6a	47.6	31.8	4.76	125	37.8	41.6
b			7.94		63.0	69.3
c			9.52		75.5	83.1
d			12.7		101	111
7a	57.2	38.1	4.76	150	45.4	59.9
b			9.52		90.7	120
c			12.7		1.21	160
8a	66.7	44.5	7.94	174	88.2	136
b			11.1		123	189
c	66.7	44.5	14.3		159	245
9a	76.2	50.8	11.1	200	141	248
b			14.3		181	319
c			12.7		161	283
10a	85.7	57.2	11.1	224	159	313
b			14.3		204	402
c			19.1		272	536
11a	108	69.9	12.7	279	242	594
b			15.9		302	742
c			19.1		363	891
12a	127	82.6	14.3	329	317	918
b			19.1		423	1230
c			25.4		564	1630
13a	159	114	14.3	429	317	1200
b			19.1		423	1600
c			25.4		564	2130
14a	25.4	19.05	3.17	6.98	10.0	6.19
b			6.35		20.1	12.4

## Notes

1. Maximum outside diameter 600 mm. However, cores may be supplied up to 1 m diameter with reduced magnetic guarantees, subject to a minimum build up limitation of 5% of diameter.
2. Where cores are required with greater height they will be supplied in two or more sections.
3. Cores in 0.35 mm may be supplied with inside diameter in range 40–50 mm with reduced magnetic guarantee.

\* For actual weight and area multiply by stacking factor appropriate to strip thickness (see Table 4).

This core range has been designed for 0.15 mm strip and below. For thickness 0.025 mm and below the standard RECMF bobbin range is preferred.

Dimensional tolerances on cores larger than 600 mm by arrangement.